KU LEUVEN

FACULTY OF SCIENCE

Linking genotype to behaviour: the genetic and regulatory basis of predator-induced plasticity in *Daphnia magna*

Anton DE JONG

Thesis presented in fulfilment of the requirements for the degree of Master of Science in Biology

Promotor: Prof. S. Van Belleghem
Research group of eco-evolutionary genomics

Supervisor: PhD student A. Kiggen
Research group of eco-evolutionary genomics

Academic year 2025-2026

© Copyright by KU Leuven
Without written permission of the promotors and the authors it is forbidden to reproduce or adapt in any form or by any means any part of this publication. Requests for obtaining the right to reproduce or utilize parts of this publication should be addressed to KU Leuven, Faculteit Wetenschappen, Celestijnenlaan 200H - bus 2100, 3001 Leuven (Heverlee), Telephone +32 16 32 14 01.

A written permission of the promotor is also required to use the methods, products, schematics and programs described in this work for industrial or commercial use, and for submitting this publication in scientific contests

Acknowledgements

This thesis marks the end of my biology degree, a chapter of five years at the KU Leuven. I would like to thank the educational staff of the department of Biology for their immensely enthusiastic and passionate way of teaching and guiding throughout the years. It was fun to be surrounded by people that are so passionate and engaged by biology. It was an unforgettable journey, and I leave with friendships I hope to keep for life.

First and foremost, I would like to thank my supervisor Aaron Kiggen for his support and guidance throughout this thesis. This was a very ambitious project with many possibilities, and I greatly appreciated how open he was to ideas while still giving me enough freedom to pursue my own direction. I also want to sincerely thank him for his help in the lab with rearing the *Daphnia* and everything that came with it; without him, things would never have run so smoothly.

A special thanks goes to Prof. Steven Van Belleghem, who should serve as an example to others of how a professor ought to work. He listens genuinely and gives exceptionally valuable feedback, and his enthusiasm for results and optimism are truly infectious. I am deeply grateful to have had the opportunity to do my thesis in his lab.

I also want to thank Kristina and Silke for their company in the basement and their help with rearing the clones used in this study. More broadly, I would like to thank everyone in the lab for their useful feedback during presentations, for creating a welcoming atmosphere where I always felt comfortable asking questions.

I would further like to thank Prof. Ellen Decaestecker and Prof. Luc De Meester for evaluating this thesis.

Finally, I want to thank my friends and family for their support throughout this journey and for giving me the opportunity to study biology.

Contents

Acknowledgements ... ii
Summary ... v
Abbreviations ... vii
Introduction ... 1
Adaptive plasticity ... 1
Behavioural plasticity ... 2
Evolutionary history and its influence on behaviour ... 3
The study of Behavioural Gene Regulatory Networks (bGRNs) ... 5
Genome-wide association studies (GWAS) ... 7
Bulk RNA behavioural studies ... 9
ATAC study ... 10
Why *Daphnia* as a study organism ... 12
General aim of the thesis ... 15
Objectives & research questions ... 16
Material and methods ... 17
Clones ... 17
Culture and experimental conditions ... 18
Phenotypic assay and analysis ... 19
Quantification of behaviour ... 21
Statistics for phenotypes ... 22
RNA-seq data analysis ... 23
Data acquisition and experimental context ... 23
Quality Control and Pre-processing ... 23
Read mapping and alignment ... 23
Differential expression analysis ... 23
Functional annotation and pathway analysis ... 24
GWAS ... 24
Genotype data preparation ... 24
Phenotype preparation ... 25
Population structure ... 25
Association testing ... 26
Significance thresholds ... 26
Proportion of variance explained ... 26
Visualisation and diagnostics ... 27
Software and compute environment ... 27
BLAST ... 27
ATAC-seq ... 27

Results 28
1. Change in phototactic behaviour 28
2. Change in kinematics 30
3. GWAS 34
BLAST and missense mutations 41
RNA-seq 42
Suggestive GRN 47
Discussion: 48
1. Change in phototactic behaviour (objectives 1 and 2) 48
1.1 Validation of the experimental setup 48
1.2 Phototactic responses across population types 49
1.3 The absence of response in fish-exposed populations 49
1.4 Paradoxical upward shift in fish-naïve populations 50
2. Change in swimming kinematics (objectives 1 and 2) 51
2.1 Swimming speed and distance travelled 51
2.2 Nearest neighbour distance 52
2.3 Overall behavioural change and interclonal variation 52
3. GWAS (objective 3) 53
3.1 Sample size and statistical power 53
3.2 Population stratification and genomic inflation 53
3.3 Vertical position in the control condition 54
3.4 Vertical position under fish kairomone exposure 55
3.5 Plasticity of vertical position 55
3.6 Swimming speed plasticity 56
3.7 Overall evaluation and future directions 56
4. Differential gene expression and GRN (objective 4 & 5) 56
4.1 Overlap with kairomone-relevant signalling pathways 57
4.2 ATAC-seq chromatin accessibility 58
4.3 Putative GRN 58
Conclusion and future perspective 60
Use of generative AI 62
Bibliography 62
Addendum 1
Tables 1
Figures 13

Summary

Daphnia magna occupies a central role in aquatic food webs and faces intense predation pressure from visual hunters such as fish. Rather than relying on slow evolutionary change, organisms can respond to such pressures through phenotypic plasticity, the ability to alter behaviour or physiology within a single lifetime. Plasticity has been extensively studied in *D. magna,* yet the genetic architecture underlying it remains poorly understood. One of the best-characterized examples is diel vertical migration (DVM): in the presence of fish predation cues, *Daphnia* descend in the water column to avoid visually hunting predators, a behaviour mediated in part by light perception. DVM is an energetically costly strategy, as deeper, colder water reduces growth and reproduction, making the regulation of this behaviour critical to fitness. Although the response is heritable, the specific genes underlying it have not yet been identified.

This study investigated the behavioural changes in *D. magna* upon exposure to fish kairomones using a behavioural assay that tracked individual animals and quantified mean vertical position and locomotory behaviour. Additionally, this study examined whether the evolutionary history of each clone, more specifically their pond of origin's history of fish presence or absence and agricultural exposure, could explain observed behavioural variation. Clones originate from ponds sampled across Flanders with differences in conditions. At the meta-population level, fish kairomone exposure did not shift vertical position overall. However, fish-naïve populations paradoxically moved toward the surface upon fish kairomone exposure, the opposite of the expected predator-avoidance response, possibly reflecting the absence of plasticity in ponds with no historical fish predation. A significant reduction in swimming speed was also detected under kairomone exposure.

To explore the genetic basis of these behaviours, a genome-wide association study (GWAS) was performed on vertical position under control conditions, fish kairomone conditions, and their difference as a measure of plasticity. Baseline vertical positioning was significantly associated with an opsin-like gene. *Daphnia* possess a large opsin repertoire arising from gene duplication events, and the identified opsin may regulate depth positioning under control conditions through its capacity to absorb blue light, which penetrates deepest in the water column. No genome-wide significant associations were detected for vertical position plasticity, though suggestive findings may reach significance with increased sample size. For swimming speed plasticity, candidate genes overlapping with Rotund-like proteins were identified. These proteins are implicated in olfactory system development and may therefore mediate kairomone perception in *Daphnia.*

Differential gene expression analysis comparing control and fish kairomone-exposed *Daphnia* revealed broad metabolic suppression and changes in neurological signalling pathways. Integrating these transcriptomic data with chromatin accessibility profiles from ATAC-seq, a putative gene regulatory network (GRN) underlying the behavioural response to fish exposure was constructed. The GRN is structured around two levels of transcriptional regulation, with hub transcription factors driving downstream gene expression changes. The nodes are implicated in neurological gene regulation and developmental signalling. Together, these findings advance our understanding of the molecular mechanisms underlying the rapid behavioural response of *D. magna* in response to predation risk and highlight the value of integrating behavioural, genomic, and regulatory data to dissect the architecture of phenotypic plasticity.

Abbreviations

ATAC-seq – Assay for Transposase-Accessible Chromatin using sequencing

bGRN – behavioural GRN

CRE – cis regulatory element

DEGs – differentially expressed genes

DVM – Diel vertical migration

FK – fish kairomones

GO – gene ontology

GRN – gene regulatory network

GWAS – genome-wide association study

GxE – Genotype-by-environment interaction

MAF – minor allele frequency

NND – nearest neighbour distance

ORA – overrepresentation analysis

PCA – principal component analysis

PI – phototactic index

RNA-seq – RNA-sequencing

SNPs – single nucleotide polymorphisms

TF – transcription factor

VPC1 – vertical position control 1 (locus)

VPC2 - vertical position control 2 (locus)

Introduction

Adaptive plasticity

Organisms inhabit environments where conditions can shift faster than genetic adaptation can occur. Adaptation through genetic changes, such as indels, inversions, and mutations, can take thousands to millions of years to spread through a population. In contrast, phenotypic plasticity allows individuals to respond rapidly to environmental variation (Irschick et al., 2013). Phenotypic plasticity entails that a genotype can produce different phenotypes dependent on the interaction with the environment. It helps with the buffering of individuals against environmental variability, allowing survival in unpredictable environments, but with predictable cues, such as in the winter coat swap in snowshoe hares with reliable change in photoperiod when winter arrives (Ferreira et al., 2020).

Phenotypic plasticity is widespread throughout taxa, for instance the European Map Butterfly (*Araschnia levana*) has seasonal morphs, while genetically they stay constant (Baudach & Vilcinskas, 2021) and locusts undergo morphological and behavioural changes when shifting from solitary to gregarious phases (Panhwar & Mustafa, 2022). When the phenotypic changes cause an advantage for the fitness of the individual it is called adaptive plasticity (Shackelford & Weekes-Shackelford, 2021). This selection can work on the phenotypic trait itself but also on the reaction norm (Schlichting & Pigliucci, 1998). A reaction norm describes the change of phenotype across an environmental gradient, for example, how trait values differ between low and high temperatures for the same genotype. Because different genotypes often show varying slopes and shapes of reaction norms (GxE interactions), there is a heritable variation in plastic responses. Natural selection can favour steeper, flatter or environment-specific slopes of reaction norms depending on the fitness landscape. Consequently, plasticity itself can evolve when it contributes to differential fitness in varying environments. (Hutchings, 2011; Pigliucci, 2005; Van Tienderen & Koelewijn, 1994).

Building upon these dynamics, C.H. Waddington (1942;1953) proposed that selection can canalize an environmentally induced phenotypic trait into a fixed response regardless of the environmental stimulus. This process, where a previously plastic trait becomes constitutively expressed in future generations, is known as genetic assimilation. Similar logic was explored by Baldwin in 1896, who suggested that the ability to learn or adjust (plasticity) allows populations to survive long enough for similar traits to be reinforced through natural selection, a phenomenon often called the Baldwin effect.

Phenotypic plasticity is however not universally adaptive; it depends heavily on the reliability of the environmental cues and the organism's ability to translate these cues into appropriate phenotypic changes. When environmental signals are ambiguous or weakly correlated with actual conditions, organisms may exhibit plastic responses that do not improve fitness (Schneider, 2022; Van Kleunen & Fischer, 2005). Such responses are often described as non-adaptive plasticity, where phenotypic changes arise as a direct consequence of environmental exposure or physiological constraints, rather than as an evolved, fitness-enhancing strategy. Maladaptive plasticity can occur when organisms respond to novel stressors by co-opting genes that evolved to cope with ancestral environmental conditions, leading to phenotypic responses that are no longer beneficial in the current environment (Velotta & Cheviron, 2018). Figure 1 provides a visual overview of these plasticity types using hypothetical reaction norms.

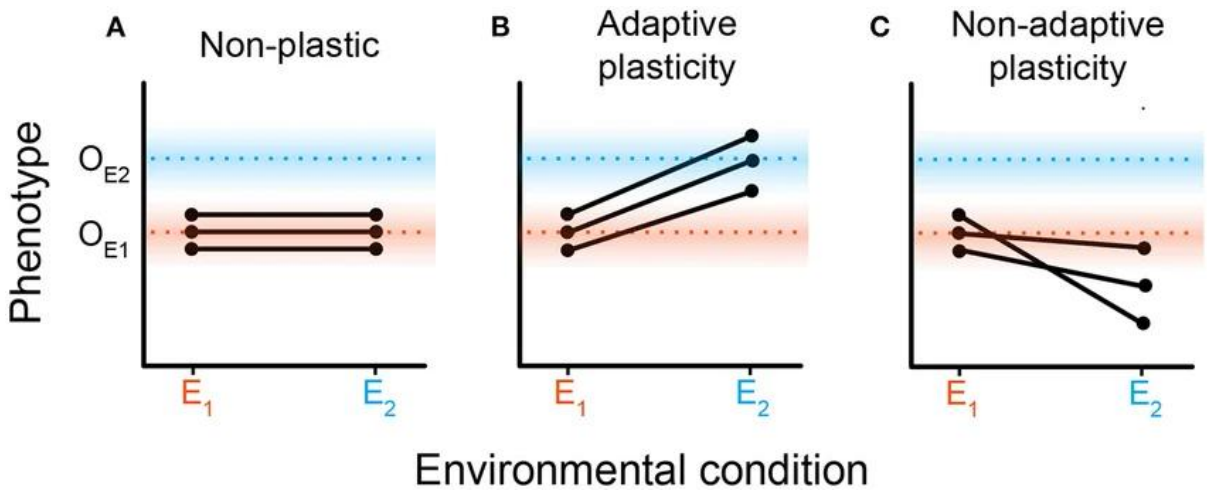


Figure 1: Graphical representation of types of plasticity using hypothetical reaction norms*. Two environmental conditions (E1 and E2) are shown on the x-axis. The y-axis indicates the phenotype expressed in each environment, with OE1 and OE2 showing the optimal phenotype in that environment. (A) Non-plastic response is characterized by a lack of change in phenotype across the two environments. (B) Adaptive plasticity is characterized by a response consistently observed in the genotype towards a new optimum. (C) Non-adaptive plasticity is characterized by an inconsistent response in the phenotype, inducing phenotypes away from the optimum. (Figure taken from Lalejini et al., 2021).*

Behavioural plasticity

Phenotypic plasticity can manifest through morphological, physiological or behavioural changes allowing organisms to adapt to environmental shifts (West-Eberhard, 1989). Among these, behavioural plasticity is the most immediate and reversible response, enabling a fast reaction to the new environment where morphological or physiological changes might be too slow or energetically costly (Gross et al., 2010; Sih et al., 2011). Consequently, behaviour plays a pivotal role in mediating the relationship between environmental variation and fitness (Ghalambor et al., 2007).

At its core, behavioural plasticity is the ability of an organism to alter its activity or response patterns in direct reaction to external stimuli, such as predation risk or social cues (Sih et al., 2004; Snell-Rood, 2013). In aquatic ecosystems, *Daphnia magna* serves as a primary model for this phenomenon, particularly through changes in its diel vertical migration (DVM), a defensive behaviour triggered by the presence of fish-secreted kairomones (De Meester, 1993). While behavioural traits are often flexible, their expression is jointly determined by the genotype and the environment, i.e. the behaviour an individual displays reflects both its genetic makeup and the conditions it currently experiences. This means plasticity itself can be heritable, and that selection can act on the responsiveness of individuals to their surroundings (Dingemanse et al., 2010; Nussey et al., 2007).

Behavioural plasticity is not a singular mechanism, but can be broadly divided into two distinct types: activational and developmental behavioural plasticity (Snell-Rood, 2013). Activational behavioural plasticity refers to the context-dependent activation of an existing underlying neural network. It represents an immediate and reversible response. DVM is a classic example of this, an individual *Daphnia* expresses different vertical positions throughout a 24-hour cycle as it encounters varying light and predation risks, seeking shelter in the bottom layer, during the day and foraging at the surface by night. In contrast, developmental behavioural plasticity occurs when genotypes follow different developmental trajectories in response to environmental cues. While DVM is primarily activational, it is associated with short term developmental changes with rapid transcriptomic (Bellot et al., 2022; Carrillo et al., 2025; Choi et al., 2023) and neurological (Graeve et al., 2021) changes, thus suggesting sustained molecular reprogramming underlying the adaptive responses.

Evolutionary history and its influence on behaviour

While behavioural plasticity allows individuals to respond rapidly to environmental cues within their lifetime, repeated exposure to consistent environmental pressures, such as fish predation, can reshape these response systems across generations. When plastic responses are repeatedly favoured, natural selection can modify the underlying reaction norms, altering their slope, sensitivity, or threshold. Thus, evolutionary history determines not only mean behavioural phenotypes but also the structure and magnitude of plasticity itself (Stoks et al., 2016; Tuomainen & Candolin, 2011; Wund et al., 2008).

Since behaviour is among the most plastic traits, behavioural shifts are often hypothesised to precede morphological evolution. Changes in behaviour can alter ecological niche use and as a consequence reshape the selective environment experienced by a population. For example, shifts in resource use can subsequently drive selection on morphological traits. Behaviour therefore does not only respond to environmental change, but can actively influence evolutionary trajectories (T. D. Price et al., 2003). Over time, repeated selection on such behavioural responses may lead to their genetic stabilisation, through genetic assimilation,

whereby an environmentally induced phenotype becomes partially or constitutively expressed (Crispo, 2007; Landry & Bernatchez, 2010; Pigliucci & Murren, 2003; Waddington, 1942, 1952). As a result, populations with different ancestral environments may exhibit distinct behavioural architecture, even when underlying sensory systems remain similar.

In the specific context of *D. magna,* populations with a prolonged exposure to fish predation tend to show a more stabilized anti-predator phototactic response (Stoks et al., 2016). This results in a more consistent response of the population toward fish predation, because predator-induced selection reduced the behavioural variance (De Meester, 1996). In contrast, populations from historically fish-free environments, that did not experience predator-induced selection, may still have a larger behavioural variance in response to fish presence (Tollrian & Harvell, 1999). Present-day differences in behavioural response to fish between these populations may therefore reflect the effects of past selection and the degree to which their underlying regulatory architecture has been 'locked in' by past selection.

To get a good representation of the behavioural variation in *Daphnia*, broad sampling across and within populations is needed. Yet most recent studies investigating behavioural plasticity work with a handful of clones. Even sophisticated approaches, such as 3D tracking system used 4 clones (Langer et al., 2019). A related limitation is that studies investigating behaviour across different *Daphnia* species use a few clones as a representation of the behaviour exhibited by the entire species (S. I. Dodson et al., 1997). A notable exception is the resurrection ecology study by Stoks et al. (2016), which evaluated 36 clones of *D. magna* clones to show how historical predation drives rapid evolution of behavioural and life-history plasticity, yet this temporal depth within a single population does not show the diversity across different ponds. Most studies investigating the behaviour of *Daphnia* exposed to fish kairomones do not take into account the predation history experienced by the source population. These two limitations make it difficult to draw broad conclusions about the extent of behavioural variation and the population-level factors shaping it.

More enigmatic still is the genetic architecture underlying behavioural plasticity. Which loci and how many contribute to variation in plastic responses, and how these are distributed across the genome. Additionally, it is unclear if the genes underlying the plasticity (i.e. reaction norms) are distinct from those underlying the baseline behaviour. Building on this, even less is known about how the genetic architecture of plasticity itself differs across ecologically distinct populations, such as those with contrasting predation histories, and how natural selection acts on this standing genetic variation. Without fully understanding the genetic basis of plasticity it is very hard to understand how rapidly populations can evolve in response to environmental change; whether plasticity is a stable long-term strategy or a translational state on the way to genetic fixation; How much of the behavioural diversity we observe across populations reflects genetic differentiation versus plastic responses to local conditions.

The study of Behavioural Gene Regulatory Networks (bGRNs)

A way to visualize genetic architecture behind a trait is through a gene regulatory network (GRN) (Fig. 2). GRNs represent a higher level of biological organization that integrates genetic and environmental inputs into a coordinated phenotypic outcome (Sinha et al., 2020). It should be emphasised, however, that a GRN is a theoretical construct based on assumptions rather than an empirical map of interactions occurring within a cell. A GRN consists of regulatory relationships among genes, often involving hundreds to thousands of components, with transcription factors (TFs) forming the core regulatory architecture through the interactions with their target genes (Barbasch et al., 2024). Rather than functioning as linear pathways, GRNs are highly interconnected systems characterized by feedback and feedforward interactions (Sinha et al., 2020). These networks can be conceptualized as nodes, representing genes or TFs, connected by regulatory edges, which may either activate or repress gene expression (Barabási & Oltvai, 2004).

Gene expression profiles can therefore be viewed as distinct network states, with each state representing a specific transcriptomic configuration of the underlying GRN (Huang, 2009). Due to their interconnected structure, GRNs can exhibit stable network states, often described as attractors in a regulatory landscape. These attractor states correspond to robust phenotypes, while transitions between them enable phenotypic change. In a sense, the structure of the GRN constrains which phenotypes are possible and how readily transitions can occur.

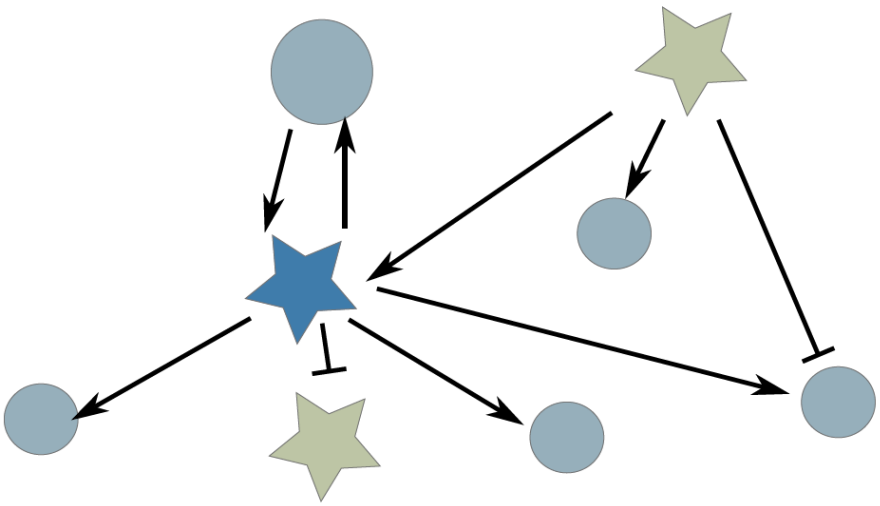


Figure 2: Schematic of a hypothetical gene regulatory network (GRN). *Nodes represent genes (circles) or transcription factors (stars), connected by directed regulatory edges. Arrowheads represent activation, flat ended bars represent repression. The blue star represents a hub node, a highly interconnected regulated that influences multiple downstream targets.*

GRNs integrate environmental cues through receptor-mediated signal transduction pathways. Environmental signals are detected by specific cellular receptors, which activate downstream signalling cascades that modulate TF activity and thereby regulate gene expression (Bravo González-Blas et al., 2023). These activated TFs bind cis-regulatory elements (CREs) of target genes, translating external signals into coordinated shifts in gene expression (Fig. 2). In this way, plastic phenotypic responses first manifest as changes in gene expression patterns, which serves as the primary interface between environmental variation and phenotypic output (Chevin et al., 2022; Swaegers & Koch, 2022).

In *Daphnia*, predator derived chemical cues (kairomones) are detected by sensory receptors located on the antennules, where olfactory neurons project to neural downstream signalling cascades (Graeve et al., 2026; Weiss, 2019). Processing the signal involves cholinergic, glutamatergic and GABAergic pathways, and further integration with environmental signals such as light, which together regulate phototactic behaviours underlying DVM (Weiss, 2019). Fish kairomone exposure changes gene expression rapidly and constitutively, yet studies in *D. magna* have typically examined expression changes under combinations of stressors rather than fish kairomones alone (Bellot et al., 2022; Carrillo et al., 2025; Choi et al., 2023; Orsini et al., 2016). Which leaves the functional annotation of differentially expressed genes specifically under fish kairomone exposure incomplete.

Critically, these studies identified gene expression changes (the nodes of the GRN), but the regulatory interactions between these genes remain largely uncharacterised (the edges connecting the nodes). Without this it is hard to go from a list of differentially expressed genes to an understanding of how environmental cues are processed through a GRN into a behavioural response (Huang, 2009; Sinha et al., 2020).

Thus, to move towards understanding the regulatory architecture behind behavioural plasticity, genotype, gene expression and phenotype must be studied together in multiple individuals and environments. Recent advances in genomic technologies now make such integrative approaches possible. RNA-seq identifies the differentially expressed genes, the nodes of the GRN, while ATAC-seq reveals open chromatin regions, including cis-regulatory elements where TFs can bind. Which thus provides empirical evidence for the regulatory edges connecting the nodes. Linking these molecular layers to phenotypic variation across natural populations with contrasting predation histories, through a genome-wide association study (GWAS), allows the genetic variants underlying both baseline and plastic responses to be identified. This multi-omics approach offers a unique opportunity to uncover the bGRN, linking environmentally induced changes in gene expression to the regulatory interactions that coordinate them and the genomic variation that shapes them.

In honeybees (*Apis mellifera*) similar approaches of integrating gene expression patterns and chromatin accessibility data to construct a GRN have been used. Where changes in specific TFs within the GRN are indicative of an individual bee's specific behaviour (Jones et al., 2020). Within the bee, the behaviour between different castes is very different despite sharing the same genotype and is environmentally determined. So, it is expected that a similar workflow could work in *Daphnia* to produce a suggestive GRN, because *Daphnia*'s behaviour upon fish kairomone exposure tends to differ.

Genome-wide association studies (GWAS)

Genome-wide association studies (GWAS) provide a powerful framework for dissecting the genetic basis of complex traits by testing statistical associations between genome-wide polymorphisms and phenotypic variation across natural populations. In contrast to classical quantitative trait locus (QTL) mapping, which relies on controlled crosses and is limited by the recombination events within mapping populations, GWAS exploits historical recombination in natural populations to achieve higher mapping resolution and to capture standing genetic variation in natural populations (Korte & Farlow, 2013). This makes GWAS particularly well suited for investigating ecologically relevant traits shaped by natural selection in heterogenous environments.

The interpretability and resolution of GWAS fundamentally depend on patterns of linkage disequilibrium (LD), defined as the non-random association of alleles at different loci (Slatkin, 2008). LD reflects the combined effects of recombination, mutation, genetic drift, selection, and demographic history. Since recombination breaks down associations between loci over time, LD typically decays with increasing physical distance between sites (Slatkin, 2008). As a result, loci identified in GWAS represent genomic regions statistically associated with phenotypic variation, but not necessarily the causal variants themselves, which may lie nearby within the same LD block.

In *Daphnia*, population genomic analyses indicate a relatively homogeneous recombinational landscape, with LD decay patterns deviating from simple equilibrium expectations (Lynch et al., 2022). This means that when a variant is significantly associated with a trait in GWAS, the association signal is confined to a narrow genomic region, allowing for relatively fine-scale localisation of candidate loci. However, the partially clonal reproductive system of *Daphnia* can locally extend LD, potentially inflating the LD detection window (Balloux et al., 2003). The clones used in this study are sampled across Flanders (see further), which helps with the resolution, because LD structure is expected to differ across populations, introducing LD backgrounds that can further narrow association signals.

GWAS can be extended beyond identifying loci associated with mean trait values in specific environments to detecting loci underlying phenotypic plasticity itself, by specifically modifying the genotype-by-environment interaction (GxE). Such interactions arise when the effect of a genetic variant on a trait differs across environments. Incorporating GxE into GWAS, for instance as the reaction norm slope as the phenotypic trait, allows identification of loci contributing to the variation in plastic response. This approach has been applied in *Drosophila melanogaster*, where a GxE GWAS on thermal plasticity in body size successfully identified candidate loci underlying the plastic response (Lafuente et al., 2018).

Diel vertical migration (DVM) is precisely such a response, its expression depends on the interaction between predator cue presence and change in light intensity (Ringelberg, 1999). Which means that genetic variation may underlie both the baseline response to light and the magnitude of predator-induced behavioural shifts. A caveat is that behavioural traits such as DVM is expected to exhibit polygenic characteristics, with quantitative genetic theory predicting that complex traits are typically influenced by numerous loci of small to moderate effect (Des Marais et al., 2013).

Despite the polygenic nature of behavioural traits, several lines of evidence suggest that GWAS should still be capable of identifying loci contributing to variation in predator-induced behaviour in *Daphnia* and thus uncover important nodes of the underlying GRN.

Using dormant egg banks to reconstruct temporal changes, Cousyn et al. (2001) for instance demonstrated pronounced genetic differentiation in predator-induced phototactic behaviour across periods of contrasting fish predations, while neutral genetic markers showed minimal divergence (Cousyn et al., 2001). This contrast between behavioural differentiation and neutral genomic divergence provides strong evidence that predator-mediated behavioural responses are shaped by natural selection acting on standing genetic variation. These findings show that predator-mediated behavioural plasticity can thus evolve rapidly and independently of genome-wide neutral divergence and suggest that the underlying genetic architecture is sufficiently strong and repeatable to be detectable using genome-wide approaches. In addition, despite the predicted polygenic architecture, predator-induced phototaxis and DVM often show moderate to high heritability in natural populations (Cousyn et al., 2001), indicating that a substantial fraction of behavioural variation is genetically determined rather than purely environmental. This is particularly important for GWAS, as the power to detect genotype-phenotype associations depends on the presence of heritable variation across individuals (Korte & Farlow, 2013). From an evolutionary perspective, spatially heterogenous predation regimes such as the presence or absence of fish create divergent selective environments that may promote local adaptation. Under migration-selection balance, alleles that increase in fitness in specific environments can be maintained despite gene flow (Slatkin, 2008).

In polygenic traits such as DVM, adaptive divergence is therefore expected to involve coordinated allele frequency shifts across many loci, potentially alongside a smaller number of loci with larger effects. GWAS therefore provides a means to detect genomic regions contributing to adaptive divergence in ecologically relevant behavioural traits.

Together, the presence of strong selection, measurable heritability, and spatially variable predation pressure makes DVM in *D. magna* a promising system for GWAS aimed at identifying the loci underlying behavioural plasticity. However while indicative, loci identified through GWAS do not directly reveal functional causality, but instead represent candidate regions associated with phenotypic variation. To understand how these loci influence phenotype, they must be interpreted in the context of regulatory and transcriptional processes.

Bulk RNA behavioural studies

A way to identify nodes in a GRN is bulk RNA-sequencing (RNA-seq). It quantifies the level of gene expression across the whole transcriptome by measuring transcript abundance across tissue, organs, or whole organisms at a given moment in time (Wang et al., 2009). Whereas GWAS identifies genomic loci associated with phenotypic variation and ATAC-seq characterises regulatory accessibility, RNA-seq provides a functional view of transcriptional activity under specific environmental or behavioural conditions. In this way, RNA-seq captures the molecular responses that link genotype and regulatory state to the expressed phenotype (Hitzemann et al., 2013).

In behavioural ecology, RNA-seq has become an important tool for identifying transcriptional responses to environmental stimuli such as predation cues, temperature shifts, and social interactions (Choi et al., 2023; Robinson et al., 2005). By comparing expression profiles across conditions, differentially expressed genes (DEGs) can be identified, revealing candidate pathways and molecular processes involved in behavioural responses. Behaviour is typically regulated through changes in gene expression rather than presence or absence of specific genes, transcriptomic data are particularly useful for investigating the mechanisms underlying behavioural plasticity (Bendesky & Bargmann, 2011; Robinson et al., 2005). Although RNA-seq does not directly establish causality, it provides a powerful means of identifying the molecular pathways associated with environmentally induced phenotypic shifts.

Critically, while bulk RNA-seq reveals which genes are differentially expressed, it cannot reveal why those differences occur. Or in other words, what upstream regulatory regions and TFs might drive them. In this way, previous studies using RNA-seq in *Daphnia* have been able to identify differences in transcriptional responses but have not been able to connect expression changes to their underlying regulatory architecture (Weiss, 2019).

Nevertheless, this method remains a robust framework for investigating sustained phenotypic responses, where differential gene expression is hypothesized to induce changes in neural sensitivity, physiology, or behavioural state (Sinha et al., 2020; Traniello et al., 2023). In *D. magna,* predator-induced behaviours such as DVM are likely maintained through transcriptional responses to fish kairomones, making RNA-seq a suitable approach for identification of genes and pathways involved in this process. An additional advantage of working with *Daphnia* is that clonal lineages can be maintained in the laboratory. The transcriptomic analyses benefit from the reduced background genetic variation, allowing clearer separation of environmental and genetic effects on gene expression (Ebert, 2022).

ATAC study

While GWAS can identify loci statistically associated with phenotypic variation, they do not directly reveal how these loci might influence gene regulation, in particular the regulatory edges in the GRN. This is important because many variants associated with complex traits are located in non-coding regions of the genome, where they are more likely to affect TF binding, enhancer activity, or chromatin state than protein-coding sequence itself (Gusev et al., 2018; Maurano et al., 2012). The Assay for Transposase-Accessible Chromatin using sequencing (ATAC-seq) provides a high-resolution method for identifying open chromatin regions across the whole genome (Buenrostro et al., 2013). By using the ability of hyperactive Tn5 transposase to simultaneously cut and insert sequencing adapters into nucleosome-depleted regions of DNA, ATAC-seq identifies “open” genomic regions that are accessible to TFs and transcription itself (Buenrostro et al., 2015). These regions typically correspond to promoters, enhancers and insulators, which together define the regulatory landscape controlling when and where genes are expressed (Corces et al., 2017).

Just like the phenotype chromatin accessibility is not static but can change in response to environmental conditions. Genomic regions may shift between a condensed, transcriptionally inactive state and a more open, accessible state through mechanisms such as histone modification, nucleosome repositioning, and DNA-methylation (Herrel et al., 2020). Chromatin-based regulation is increasingly recognized as an important component of phenotypic plasticity because these modifications can alter the transcription without modifying the underlying DNA sequence (Beldade et al., 2011; Herman & Sultan, 2011).

Besides quantifying differential chromatin accessibility, ATAC-seq data can also be used to identify the TFs likely responsible for observed regulatory changes. Open chromatin regions represent areas where TFs can bind, scanning these regions for TF binding motifs allows for identification of possible binding regulators. Tools such as HOMER (Heinz et al., 2010) perform this by searching within accessible regions for sequence motifs that match a curated TF binding database. When these motifs are near differentially expressed genes, it directly links specific downstream transcriptional changes to their upstream molecular drivers.

In this way, ATAC-seq provides a direct window into how environmental cues can reshape the regulatory landscape. This makes the technique particularly relevant for studying plastic responses, where environmentally induced shifts in phenotype are expected to arise through changes in regulatory state.

The relationship between chromatin accessibility and behavioural change has been demonstrated in Japanese quail (*Coturnix japonica*), where a study examined the photoperiod-induced seasonal reproductive activation in males. Through the combination of ATAC-seq with RNA-seq and DAP-seq across four timepoints. DAP-seq is a high-throughput genomic technique used to map where TFs bind to DNA. These methods were used to map chromatin accessibility changes that drive the hormonal and behavioural transition from reproductive inactivity to activity in response to long-day photoperiods (Chang et al., 2024). This shows that environmental cues can induce chromatin remodelling, which results in transcriptional change and ultimately behavioural change.

In *D. magna*, ATAC-seq provides an opportunity to investigate whether exposure to fish kairomones alters chromatin accessibility in genomic regions associated with behavioural plasticity. In the context of predator-induced DVM, ATAC-seq can identify regulatory elements that become more or less accessible following fish exposure, thereby highlighting candidate cis-regulatory regions involved in the behavioural response. Motif enrichment analyses can further be used to identify TFs likely to bind these accessible regions.

When combined with RNA-seq, ATAC-seq can identify candidate regulatory interactions underlying predator-induced gene expression changes. Accessible regions associated with differentially expressed genes can be analysed for enriched TF binding motifs, revealing TFs that may regulate these genes. By linking differentially expressed TFs to accessible motif-containing regions near their putative target genes, RNA-seq and ATAC-seq together enable the inference of candidate edges within behavioural GRNs.

ATAC-seq can also be integrated with GWAS results to investigate whether loci associated with variation in predator-induced DVM overlap with accessible regulatory regions. Such overlap would provide evidence that naturally occurring genetic variation influences behavioural plasticity through effects on gene regulation. Through GWAS, genomic regions associated with behavioural variation can be identified; ATAC-seq can determine whether these regions are accessible to the transcriptional machinery, while RNA-seq reveals whether genes within these regions are differentially expressed in response to fish kairomones. Together, these approaches allow a layered and mutually informative interpretation of behavioural variation, linking genetic variation, chromatin accessibility, and transcriptional output.

The key advance of this framework lies in the integration of GWAS, RNA-seq, and ATAC-seq into a coherent multi-omics approach. Although each of these methods has previously been applied independently, they are rarely combined within a single study of behaviour. By integrating these complementary datasets, the analysis moves beyond describing patterns of differential gene expression towards identifying the molecular mechanisms that generate behavioural phenotypes.

Together, RNA-seq, ATAC-seq, and GWAS enable the reconstruction of candidate bGRNs. In these networks, genes and TFs represent nodes, whereas regulatory interactions constitute the edges connecting them. While RNA-seq and GWAS can identify candidate nodes, regulatory interactions can be inferred from TF binding motifs detected in accessible chromatin regions using tools such as HOMER (Heinz et al., 2010). Consequently, ATAC-seq provides a valuable means of investigating the regulatory architecture underlying behavioural plasticity.

Importantly, ATAC-seq has already been successfully applied in *D. magna* (Grunau et al., 2021), demonstrating the feasibility of chromatin accessibility profiling in this emerging model system. Furthermore, recent functional genomic studies have shown that fish kairomones, including bile salts such as 5α-cyprinol sulfate, induce widespread changes in metabolic and neural gene expression in *Daphnia* (Choi et al., 2023; Hahn & von Elert, 2022). Together, these advances establish a strong foundation for applying an integrated multi-omics framework to predator-induced behavioural plasticity. To the best of our knowledge, such an approach has not yet been used to investigate predator-induced behaviour in *Daphnia* or comparable invertebrate systems, highlighting its potential to reveal the regulatory mechanisms linking genotype to behavioural phenotype.

Why *Daphnia* as a study organism

The freshwater cladoceran *Daphnia magna* is a widely used model organism in ecology and evolutionary biology because it combines strong ecological relevance with strong capability of experimental repeatability. Species of the genus *Daphnia* are key grazers in freshwater food webs, linking primary production to higher trophic levels by transferring energy from phytoplankton to invertebrate and vertebrate consumers such as insect larvae and planktivorous fish (Muñoz et al., 2016; Stoks et al., 2016). As a consequence, predator-induced changes in *Daphnia* behaviour or life history can have cascading effects on community structure, trophic interactions, and nutrient cycling. With the consumption of primarily phytoplankton they prevent algal blooms, maintain water clarity and nutrient cycling. This ecological centrality has made *Daphnia* a classical system for studying predator-prey interactions, phenotypic plasticity and rapid evolution (Cousyn et al., 2001; De Meester, 1993).

An important advantage of *D. magna* is its cyclical parthenogenetic life cycle, which allows the establishment of genetically identical clonal lineages. Under favourable conditions, individuals reproduce asexually, enabling the same genotype to be replicated across different environmental treatments, whereas environmental stress induces sexual reproduction and the formation of dormant resting eggs enclosed in ephippia (Ebert, 2022). This clonal structure is especially valuable for GRN research because it allows regulatory responses to be studied independently of background genetic variation. Identical genotypes can be exposed to different predator or light environments, making it possible to isolate environmentally induced shifts in gene expression and chromatin state, while reducing noise caused by standing genetic differences.

The production of resting eggs also enables resurrection ecology, a unique feature of *Daphnia* that is particularly relevant for understanding the evolution of behavioural regulatory networks. Dormant eggs preserved in lake sediments can be hatched decades after they were produced, allowing historical and contemporary genotypes to be compared directly (Decaestecker et al., 2007; Ebert, 2022). Through the ease of resurrecting ecology, it is possible to compare contemporary clones drawn from ponds that differ in their long-term predation history. For example, populations that have experienced sustained fish predation pressure versus those that have evolved in fish-free environments. Since clonal reproduction preserves genotypic identity, phenotypic and regulatory differences between such lineages can be attributed to divergent evolutionary histories, rather than variation arising during development (Ebert, 2022). In the context of bGRN, this approach offers the possibility of comparing not only behavioural phenotypes across populations, but also the regulatory systems that generate them. Allowing examination of how natural selection under contrasting predation regimes may have reshaped cue responsiveness, chromatin accessibility, and network dynamics. While these evolutionary differences can be studied across populations, understanding how they are expressed behaviourally requires a controlled and ecologically relevant environmental stimulus.

In natural systems, one of the most important environmental cues driving behavioural plasticity in *Daphnia* is the presence of predators. Fish kairomones represent a particularly reliable and ecologically relevant cue for inducing DVM in *D. magna*. The active compounds have been identified as bile salts, most notably 5α-cyprinol sulfate, which are continuously excreted by fish into the water column (Hahn & von Elert, 2022). These chemical signals are highly specific to vertebrate predators and are present whenever fish are active, providing a temporally and spatially reliable indicator of predation risk. *Daphnia* perceives these kairomones through specialised chemosensory structures on the antennules, where sensory neurons project into the deutocerebrum (Weiss, 2019).

The downstream processing involves cholinergic, glutamatergic and GABAergic pathways, and behavioural responses such as DVM emerge through integration of predator perception with light-dependent pathways (Weiss, 2019). Since fish kairomones are consistently produced as metabolic by-products rather than as warning signals, they cannot be suppressed by the predator, making them an honest and environmentally stable cue. This reliability likely underlies the strong and consistent DVM responses observed across *Daphnia* populations and makes kairomone-mediated DVM an ideal system in which to study the genetic and regulatory basis of predator-induced behavioural plasticity.

Experimental studies have demonstrated that exposure to these fish kairomones induces consistent changes in *Daphnia* movement behaviour. For example, Langer et al. (2019) showed that daphnids exhibit reduced swimming speed and shift in vertical position when exposed to predator cues. In contrast, movement parameters such as turning behaviour and horizontal directionality remained largely unchanged, suggesting that predator-induced responses are not random but involve specific behavioural adjustments. Interestingly, individuals also altered their spatial distribution with increased nearest neighbour distances, indicating changes in aggregate behaviour that may influence predator detection risk (Pijanowska & Kowalczewski, 1997). Such coordinated modifications in movement patterns highlight that anti-predator behaviour in *Daphnia* is structured and regulated, rather than random.

Yet a critical limitation of existing work is its narrow sampling of clonal diversity. The majority of studies characterizing behavioural plasticity use a handful of clones, typically five or less, often coming from a single population or laboratory stock. As a result, the degree to which these responses differ across clones with different evolutionary histories remains largely unchecked. Mapping variation across a broad panel of clones is the necessary step toward understanding evolutionary and genetic architecture of anti-predator behaviour in *Daphnia*.

Understanding this variation ultimately requires tools that can connect behavioural differences to their underlying genetic and regulatory mechanisms. Fortunately, recent advances in genomic resources now make such integrative approaches feasible. The availability of genome assemblies, transcriptomic resources, and comparative genomic data has elevated the genus to a genomics empowered ecological model system (Ebert, 2022; Orsini et al., 2016). In particular, the high-quality genome assembly of *Daphnia magna* provides a strong foundation for integrative analyses (Lee et al., 2019). These resources make it possible to combine population genomics, transcriptomics an chromatin accessibility assays to investigate the molecular architecture of plastic traits.

Following these advancements, another major advantage of *Daphnia* as a model for studying bGRNs is its 'ecoresponsive' genome. Comparative and functional genomic studies have shown that *Daphnia* exhibits pronounced transcriptional sensitivity to ecological stressors, with large suites of genes responding to environmental challenges such as predation, hypoxia, and pollutants (Ebert, 2022; Orsini et al., 2016; Yuan et al., 2020). This makes *Daphnia* especially suitable for studying how environmental "input" signals are translated into coordinated changes in gene expression and ultimately in behavioural 'output' phenotypes (Colbourne et al., 2011; Sinha et al., 2020). Since behavioural plasticity is initiated through environmentally induced changes in gene regulation, such a system provides a direct opportunity to investigate how bGRNs are activated, modulated, and potentially rewired under different ecological conditions. However, despite extensive research, the regulatory architecture underlying these transcriptional responses remains poorly characterized.

For instance, it is poorly understood which genomic regions act as condition-sensitive regulatory elements, how chromatin accessibility changes in response to ecological signals, and which TFs or upstream regulators are responsible for the behavioural change upon fish kairomone exposure. Moreover, while differential gene expression in response to fish exposure has been studied, the causal link between differential gene expression, regulatory variation, chromatin accessibility and behavioural phenotype is rarely established. Addressing this requires an integrated framework which simultaneously resolves genetic, regulatory and transcriptional dimensions of behavioural plasticity.

General aim of the thesis

This thesis investigates the genetic and regulatory basis of predator-induced behavioural plasticity in *D. magna*, with a focus on DVM. By integrating GWAS, ATAC-seq and RNA-seq, the study links behavioural variation to genetic variants, chromatin accessibility and gene expression. GWAS identifies loci associated with variation in DVM, while ATAC-seq and RNA-seq provide insight into the regulatory and transcriptional mechanisms underlying the trait. Together, these approaches aim to identify candidate genes and regulatory elements involved in DVM.

Objectives & research questions

1. **What is the behavioural variation between *Daphnia* clones under different predation conditions?**

Predator-induced behavioural shifts in *Daphnia* have previously been characterized in studies comparing only few clones (Bellot et al., 2022; Carrillo et al., 2025; S. I. Dodson et al., 1997; Langer et al., 2019). By conducting behavioural assays across 100 clones under both control and kairomone-exposed conditions, this thesis aims to provide a substantially more comprehensive picture of the magnitude and variance of behavioural responses to predatory stress.

2. **How does evolutionary history shape behavioural phenotypes across populations with contrasting predation regimes?**

By integrating pond-level metadata into the statistical analysis, it is possible to test whether the historical presence or absence of fish predation has a significant effect on the observed phototactic behaviour. This objective directly addresses whether evolutionary history shapes the magnitude of DVM responses across populations with contrasting predation regimes.

3. **What genomic variants are associated with predator-induced behavioural phenotypes in *Daphnia*?**

Using a genome-wide association study (GWAS) across 100 genotypes from 20 ponds, this objective aims to identify candidate loci showing a non-random association with phototaxis and swimming speed phenotypes, including genotype-by-environment interaction effects, thereby pinpointing genomic regions potentially subject to natural selection.

4. **What transcriptomic changes occur in *Daphnia* exposed to fish kairomones?**

By using publicly available RNA-seq data from an existing study (Carrillo et al., 2025), this objective aims to identify condition-dependent changes in gene expression between control and kairomone-exposed individuals. Differentially express genes will point to the molecular pathways activated during predator induced DVM.

5. **What is the putative bGRN underlying DVM?**

By integrating GWAS candidate loci with chromatin accessible data from ATAC-seq and differentially expressed genes from publicly available RNA-seq dataset (Carrillo et al., 2025), this objective aims to try to identify the underlying regulatory architecture behind DVM. This way it provides a putative foundation for the broader behavioural GRN. Although the complete construction of the full GRN was not achievable within the scope of this study, the multi-omics approach identified putative regulatory intersections and candidate nodes within this network.

Material and methods

Clones

For the pilot study a total of 3 clones were used, P_{132},96, P_{132},85 and C1242. These clones were derived by a crossing experiment of Luc De Meester and differ in both their origin and phototactic behaviour.

P_{132},85 originates from a fish pond with low and variable predation pressure. It exhibits a strong plastic response: strongly positive phototaxis in the absence of fish, shifting to strongly negative phototaxis under kairomone exposure (De Meester, 1993; De Meester & Cousyn, 1997; Kieu et al. 2001). P_{132},96 also originates from a fish pond with low and variable predation pressure, but displays negative phototaxis under both conditions (De Meester, 1993; Decaestecker et al., 2002). C1242 originates from a fishless pond and shows positive phototaxis under both conditions, though its response is less pronounced (slightly less phototactic) under kairomone exposure (De Meester, 1991; Kieu et al., 2001).

The clones used for the GWAS experiment were sourced from 20 ponds across Flanders and collected 20 clonal lines per pond, resulting in a total of 400 clones (Fig. 3). Due to time constraints on the laboratory work, 100 of these clones were selected for the GWAS, 5 clones per pond. Sampling sites are shown in Figure 3, categorised based on agricultural land use and fish presence: A_F (5 ponds), NA_F (7 ponds), A_NF (5 ponds), and NA_NF (3 ponds). Fish presence was based on physical surveys and updated using eDNA data.

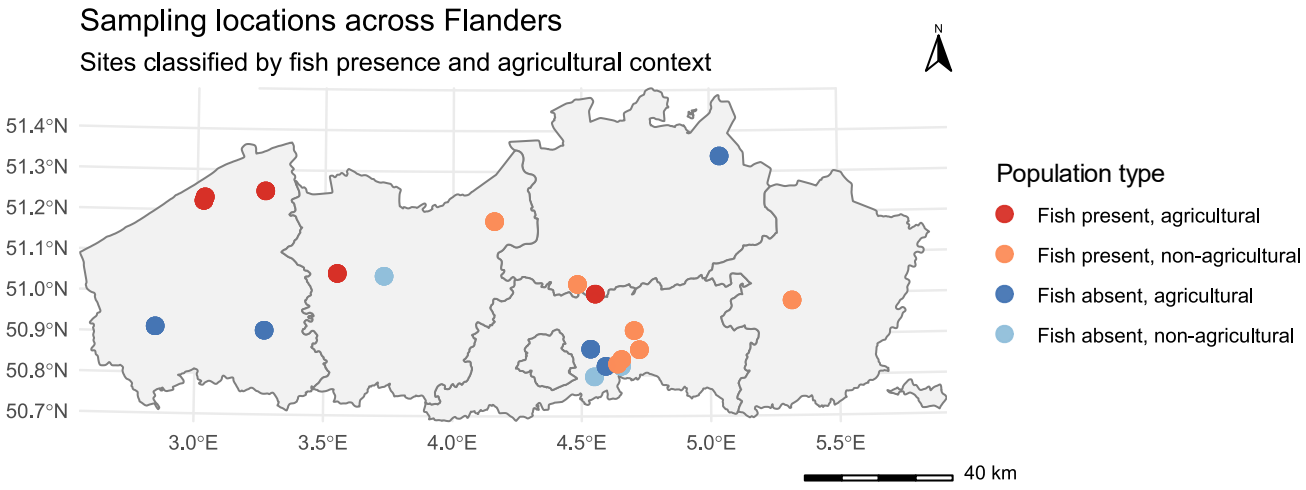


Figure 3: Map of Flanders showing the 20 sampling sites, colour-coded by population type according to fish presence and agricultural exposure. A scale bar and north arrow are provided for reference.

Culture and experimental conditions

The animals were maintained under standardised conditions between experiments at a temperature of 20 ± 1 °C and a photoperiod of 14 h light and 10 h dark (14:10 L:D). *Daphnia* were fed the unicellular green alga *Acutodesmus obliquus*. Feeding quantities depended on jar volume and developmental stage. Adult *Daphnia* housed in 210 mL jars received 3 feeding units, while neonates kept in 500 mL jars also received 3 units initially; after five days, the ration for neonates was increased to 5 units. Feeding frequency further varied throughout the week: animals received 5 units on Mondays, Wednesdays, and Fridays, and 3 units on Tuesdays and Thursdays. During weekends, all animals received 3 units.

The culture medium was refreshed on Mondays, Wednesdays, and Fridays, and additionally during weekends when animals were ready for experimental use (see requirements in the following section). During medium renewal, approximately 50–67% of the water column was replaced with dechlorinated tap water. Tap water was filtered using an Oasis filter and allowed to stand for at least 12 h prior to use. At each refreshment, *Daphnia* were transferred to clean jars while retaining approximately one-third to one-half of the original culture medium to minimise handling stress.

For the exposure phase of the experiment (see details below), a fish-conditioned medium was introduced. This medium was obtained from an aquarium containing three-spined-sticklebacks (*Gasterosteus aculeatus*) at a density of 0.6 fish L^{-1}. The fish-conditioned water was filtered through a membrane filter with a pore size of 0.45 µm and subsequently diluted to a final concentration of 0.1 fish L^{-1}. This diluted fish medium replaced the dechlorinated tap water and simulated conditions of high fish predation risk for the *Daphnia*, exposing the experimental animals to fish kairomones, mimicking fish predation (Cousyn et al., 2001; De Meester et al., 1999; Weiss, 2019).

Culturing of the GWAS clonal lines involved a few minor practical complications. During the pilot phase, clones experienced suspected fungal infection, which was treated by adding dried hay. Despite this, pilot clone behavioural results remained consistent with previous findings. For the main GWAS experiment, straw was routinely added to the cultures, especially during the neonate stage, as a precautionary measure. For two clonal lines (39 and 56), one of three replicates was replaced by a duplicate due to insufficient offspring production. Sporadic male production, a known stress response in *Daphnia* (Ebert, 2022), was occasionally observed; affected cultures were maintained using only females and phenotyping was postponed by one generation. Two clonal lines (29 and 50) were absent from the final dataset, possibly due to human error, resulting in a final sample size of 98 rather than 100 clonal lines (excluding the three pilot clones). Phenotyping was conducted in two batches (November-December and February-March), laboratory conditions remained constant and recording date was included as a non-significant random effect in all analyses.

Phenotypic assay and analysis

We performed a phenotypic assay on approximately 100 clones across three replicates and two conditions (fish kairomone exposure and control), yielding around 600 jars in total.

To minimise maternal effects, maternal females were obtained from the second brood of each of the 100 GWAS clone cultures and reared under standardised conditions (as described above) (Fig. 4). Experimental neonates were taken from the second brood of these females. Maternal females were kept in 210 mL jars at maximum density of 3 individuals per jar. When they had enough brood (>24 neonates), 12 neonates were transferred to 500mL jars containing dechlorinated tap water, this was done twice (once for each condition). After five days, the medium in the fish-exposure condition was replaced with fish-kairomone-containing medium (as described above). Animals were considered ready for phenotypic assay once they carried a full brood pouch and had completed their first clutch, which typically occurred nine to ten days after neonate isolation.

Before the *Daphnia* were ready for phenotyping, they were transferred to fresh 500mL jars containing dechlorinated tap water and acclimated for a minimum of 1.5 hours. This transfer applied to both conditions: for fish-exposed animals the kairomone-containing medium was replaced by kairomone-free water at this stage, while for the control animals, fresh water replaced the existing kairomone-free medium.

The phenotypic assay was conducted in a setup consisting of a top-mounted light shining down onto a rectangular arena (25 x 13.8 x 3.1 cm, H x L x W; 1070 mL; Fig. S1) in which 6-7 *Daphnia* were placed. Prior to recording, animals underwent a 5-minute dark acclimatisation, followed by a 5-minute light acclimatisation period. This was followed by 5 minutes of recordings, these were captured as 5 consecutive 1-minute recordings, serving as technical replicates. Recordings were conducted between 11:00 and 18:00h, to avoid confounding diurnal effects. In total, 630 jars were processed over 53 days.

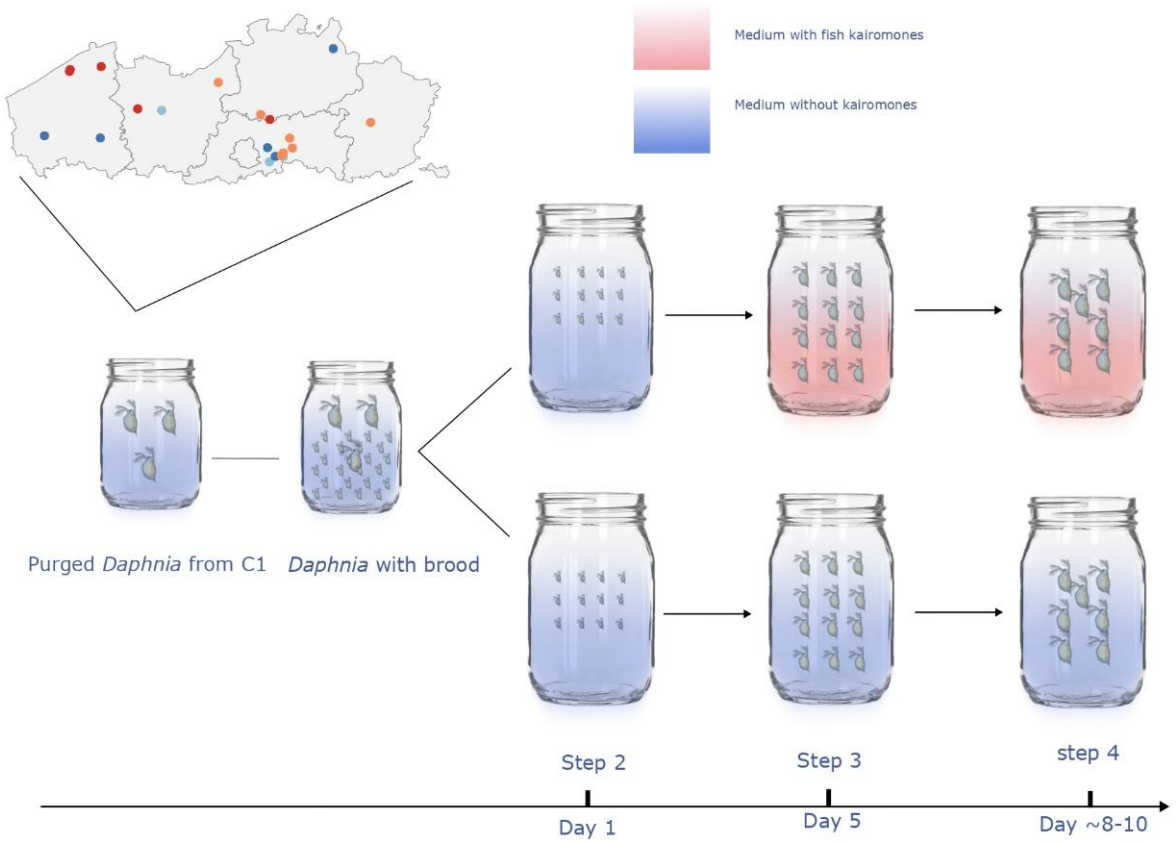


Figure 4:Schematic overview of the rearing workflow applied to each clone prior to phenotyping. The workflow was performed on 5 clones per pond (20 ponds; 100 clones total), three replicates per condition (fish – no-fish), resulting in 600 experimental jars total. A map of sampling sites is shown in the top left corner. The purged mothers were kept in jars of 210ml until their second brood, which had to be around 24 neonates, these were then split up into two jars of 500ml each containing 12 neonates (Step 2). The medium was replaced on day five in the fish exposed group by a medium containing fish kairomones (Step 3). Around day 8-10 they were mature and had their first brood, which was the sign that they were ready to be phenotyped (step 4).

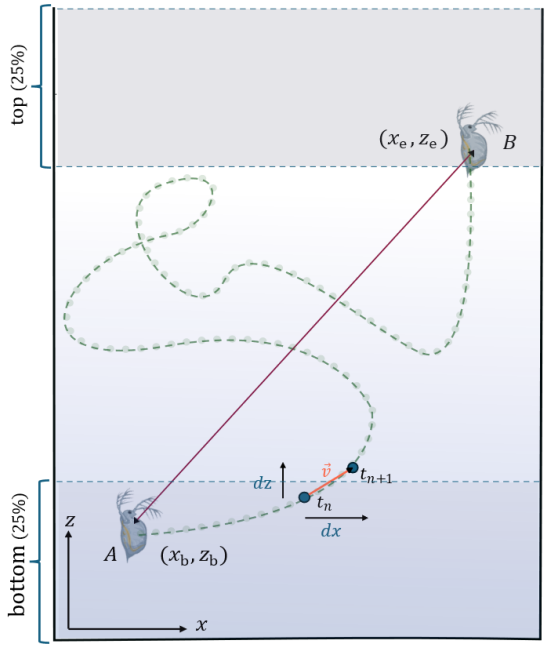
Video recordings were made using an in-house MATLAB script (A. Kiggen, unpublished) ran on MATLBAB (version R2023a). Tracking and data extraction were subsequently performed using an in-house Python-based pipeline (A. Kiggen, unpublished) (Python v3.14), which tracked each *Daphnia* individually and extracted data along X and Z axes, corresponding to the horizontal and vertical dimensions of the arena, respectively. Each recording yielded trajectories across 60 seconds at 30 frames per second, equating to approximately 1800 frames tracked per individual.

While providing a solid basis of the general positional information, the tracking setup was subject to recurring technical artefacts that inflated kinetic parameters. Two problems were particularly common: brief camera dropouts resulting in loss of frames, and label jumping errors in which the tracker briefly assigned wrong coordinates to an individual, producing false displacements and inflating total distance travelled.

To address this, a cleaning script was written to process all per-frame tracking files and remove movement artefacts prior to analysis (available at github.com/Anton03dj/Thesis-2025-2026). Frame-to-frame displacement was calculated from successive X/Z coordinates, and frames were excluded under three criteria. Firstly, frames were excluded when they showed an implausible displacement between two successive frames, suggesting a glitch. Secondly, single frames with an excessive displacement compared to previous and later frames, suggesting a missed frame or label swap. Lastly, frames exceeding the 99.9th percentile of an individual's displacement distribution. After exclusion of these frames, a 5-frame rolling mean was applied to smooth the remaining displacement vectors and reduce noise. This script was tested and modified on the pilot study data, testing different ranges for the rolling mean and exclusion criteria.

Quantification of behaviour

To quantify movement behaviour from the two-dimensional (x-z axis) tracking data, several locomotor parameters were calculated per individual and averaged across the seven individuals recorded per trial (Fig. 5). This included average vertical and horizontal position, instantaneous speed, net displacement, total distance travelled, path straightness, turning angle between successive displacements, and direction expressed as continuous angle and categorized into eight 45° sectors for categorical analysis.



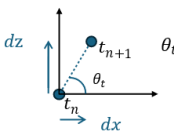
Phenotype	Formula
Displacement	$dz = z_{t+1} - z_t$ $dx = x_{t+1} - x_t$
Speed	$v = \sqrt{\left(\frac{dx}{dt}\right)^2 + \left(\frac{dz}{dt}\right)^2}$
Net displacement	$\lvert AB\rvert = \sqrt{(x_e - x_b)^2 + (y_e - y_b)^2}$
Distance travelled	$D_{total} = \sum_{t=1}^{N-1} \sqrt{(x_{t+1} - x_t)^2 + (z_{t+1} - z_t)^2}$
Average position	$\bar{z} = \frac{1}{N}\sum_{i=1}^{N} z_i \qquad \bar{x} = \frac{1}{N}\sum_{i=1}^{N} x_i$
Phototactic index	$PI = \frac{N_{top} - N_{bottom}}{N_{total}}$
Direction	$\theta_t = \text{atan2}(dx, dz)$ 

Figure 5: Schematic overview of the movement variables per individual extracted from two-dimensional tracking data. Right is a table listing the phenotypes with their accompanying formula.

To quantify vertical distribution relative to the light source, a phototactic index (PI) was calculated, following the formula described in De Meester, (1993) and used throughout different studies (Cousyn et al., 2001; De Meester et al., 1999; Stoks et al., 2016). The arena was divided into vertical zones, and the PI was defined as:

$$PI = \frac{N_{top} - N_{bottom}}{N_{total}}$$

Where N_{top} and N_{bottom} are the mean numbers of individuals present in the upper and lower 25% of the arena, respectively, calculated across the 1-minute recording period, and N_{total} is the total number of tracked individuals (n=7). The index ranges from -1 to +1, where positive values indicate surface aggregation (positive phototaxis), negative values indicate bottom aggregation (negative phototaxis), and values near zero indicate no vertical preference. Aggregation behaviour was additionally characterised through nearest neighbour distance (NND). The conversion of distances in pixels (px) to millimetres (mm) was done using ImageJ (version 1.54p), 1 cm is equivalent to 72.9 pixels, so 1 mm is 7.29 pixels.

Statistics for phenotypes

All statistical analysis of behavioural phenotypes were performed using R (v4.5.2) in Rstudio (v 2026.01.0). Model family selection was based on AIC, with the lowest-AIC model selected as most appropriate for each response. When models had an AIC value of less than 2 difference, the most parsimonious model was selected. All models included the condition (fish – no-fish) and population type (A_F, NA_F, A_NF, NA_NF), and their interaction as fixed effects, and recording date and clone nested within pond of origin as random effects. Fixed effects were tested using ANOVA type III (package car v3.1.5), appropriate for the unbalanced design which was arising from an unequal number of clones in the population types.

Mean vertical position and phototactic index are bounded responses, vertical position was scaled to the open interval (0,1), and phototactic index was rescaled from (-1,1) to (0,1). They were therefore modelled using a generalised linear mixed model (GLMM) with beta distribution and logit link function, fitted with the glmmTMB package (v1.1.14). Swimming speed and distance travelled were modelled using linear mixed models (LMMs) with a Gaussian distribution, fitted with lme4 (v2.0.1), as residuals showed a normalised distribution. Swimming speed was additionally modelled with prior fish exposure as a fixed variable replacing the population type as the grouping factor. Nearest neighbour distance followed a right-skewed, strictly positive distribution and was modelled using a GLMM with gamma distribution and log link function (glmmTMB). Post-hoc pairwise comparisons (no-fish vs fish within and between groups) were performed using the emmeans package (v2.0.2).

RNA-seq data analysis

Data acquisition and experimental context

The transcriptomic data originated from a study investigating the effects of scopolamine and fish kairomones on the induction of DVM in *D. magna* (Carrillo et al., 2025). In that study 15-day-old *Daphnia* were exposed to fish kairomones for 24h before RNA was extracted from whole individuals. The authors used clone P_{132},85, a highly plastic genotype that was also used in the pilot study. Raw sequencing reads were retrieved from the NCBI Sequence Read Archive (SRA; id: PRJEB81116).

Quality Control and Pre-processing

Initial assessment of raw sequence quality was performed using FastQC (v0.12.1). This was a way to double check the quality, because the trimming of the adaptor content was performed before the reads were made available on SRA. So the quality seen after was performing FastQC was sufficient to go further with the analysis.

Read mapping and alignment

Processed reads were aligned to the *D. magna* reference genome (UOB_LRV0_1; PRJNA777104; Chaturvedi et al., 2023), using HISAT2 (v2.1.0) (D. Kim et al., 2019). To ensure compatibility with downstream transcript assembly and quantification, the –dta (downstream transcriptome assembly) flag was used.

The resulting SAM files were converted to BAM format, sorted and indexed using Samtools (H. Li et al., 2009) (v1.22.1). Alignment quality was monitored by extracting the overall alignment rate for each sample, only samples with high mapping efficiency were retained for further analysis. To create the read counts needed for further analysis, featureCounts (v2.1.1) (Liao et al., 2014) was used, it mapped around between 63 and 68% of the reads.

Differential expression analysis

Read counts were quantified and normalized using DESeq2 (v 1.50.2) (Love et al., 2014) package in R (v4.5.2). Differential expression was modelled to compare kairomone exposed vs control non-kairomone exposed *Daphnia*. Genes were considered significantly differentially expressed (DEGs) if they met a threshold of an adjusted p-value (Padj) <0.05 and an absolute log2 fold change (|L2FC|) >1. Significant genes were visualized using volcano plots (via EnhancedVolcano v1.28.2) and heatmaps of scaled normalized counts (via pheatmap v1.0.13). Overlaps between clone-specific responses were assessed using Venn diagrams.

Functional annotation and pathway analysis

To interpret the biological significance of the DEGs, functional enrichment was performed using ClusterProfiler (v4.18.4) (Yu et al., 2012). Gene ontology (GO) and KEGG pathway annotations were made using eggNOG v7 (Hernández-Plaza et al., 2026) and Fantasia, providing functional assignments based on orthology and learning based GO-prediction (with Fantasia). KEGG pathway annotations were obtained from EggNOG-mapper, linking GO terms to a specific biological pathways. Both overrepresentation analysis (ORA) and gene set enrichment analysis (GSEA) were conducted to identify significantly enriched pathways. ORA was used to find GO terms overrepresented against the GO terms of the genomic background, while GSEA assessed coordinated expression shifts across the entire ranked gene list.

Results were visualized using dotplots, enrichment maps (emapplot), and gene-concept networks (cnetplot) from the enrichplot (v1.30.5) (Yu G. 2026) package. Enrichment maps display GO terms as nodes connected by edges weighted by gene set overlap, making identification of functionally related genes easier. Gene-concept networks link enriched pathways to their contributing genes, it is coloured based on the Log2FC, to highlight hub genes driving pathway enrichment.

GWAS

Genotype data preparation

The genotype dataset was derived from whole-genome sequencing alignments of 400 *D. magna* clones (Kourtidis, A., unpublished). The full dataset was subset to include only the clonal lines used in the experiments described in this thesis. Additionally, whole-genome sequences generated of the pilot study clones were incorporated into the dataset. Sample subsetting was done using BCFtools (v1.15).

Genotype-level filtering was applied using BCFtools (H. Li & Barrett, 2011), with the following threshold: a minimum genotype quality (GQ) score of 20, a minimum read depth of 8x, and a maximum read depth of 200x per genotype (to flag duplicated regions). At the variant level, a maximum missingness threshold of 25% was applied, and only biallelic SNPs were retained. Variant-level filtering was performed using PLINK (v2.0.0) (Chen et al., 2019), with flags --allow-extra-chr and --allow-no-sex to accommodate the scaffold-based *D. magna* genome assembly.

Phenotype preparation

Phenotypes for GWAS were derived from the tracking metrics described above. Analyses were performed separately for the control condition, the fish kairomone condition, and the difference between both conditions, referred to as the plastic response.

For the vertical position, the primary phenotype was the mean vertical position per clone, calculated across the three replicate samples. In addition to this continuous measure, alternative phenotype encodings were tested, including ordinal ranking scores based on relative vertical position within the water column and z-score normalised categorized groupings.

Plasticity phenotypes were based on the difference in mean vertical position between control and fish-exposed conditions within each clone. Both difference and the absolute value of the difference, together with z-score normalised categories. Additional analyses focused on clones showing the strongest responses, including extremes-only subsets and comparisons of the top and bottom 30% responders.

For swimming speed, several phenotypes encodings were considered, including mean speed, scaled mean speed, ranked categorical groupings, and z-score normalised categories.

All phenotypes were derived from the tracking data described above. For vertical position, four phenotype encodings were considered for each condition separately (control and fish kairomone-exposed): mean vertical position (continuous), arena segment score (ordinal, -5 to 5), and z-score normalised categorical score (-3 to 3). For plasticity, five encodings were tested: the mean difference between conditions (continuous), the absolute mean difference, a z-score normalised categorical score (-3 to 3), an extremes-only subset (largest absolute differences), and a top/bottom 30% subset. For swimming speed, four encodings were considered for each condition and their difference: mean speed (continuous), scaled mean speed, a ranked grouping score (FK: 0.9 to 2.1 in increments of 0.2; control 1.0 to 2.8 in increments of 0.3), and a z-score normalised categorical score (-3 to 3).

Population structure

To assess population structure a centred kinship matrix was made from all SNPs passing quality filters using GEMMA (Zhou & Stephens, 2012), and used as a random effect in the association model to account for genetic relatedness among samples. Principal component analysis (PCA) was additionally performed in PLINK (v2.0.0), and the first four PCs were retained as fixed-effect covariates in the linear mixed model to control for residual population stratification not captured by the kinship matrix. No prior population or family groupings were assumed during either analysis. GEMMA fits a univariate linear mixed model:

$$y = W\alpha + x\beta + u + \epsilon; u \sim MVN_n\,(0, \lambda\tau^{-1}K), \epsilon \sim MVN_n(0, \tau^{-1}I_n)$$

Where:

- y is the phenotype vector
- $W\alpha$ represents the fixed covariates (PC1-4)
- $x\beta$ is the effect of an individual SNP
- u is the polygenic random effect, with K the centred kinship matrix
- ϵ is the residual error
- MVN_n denotes the n-dimensional multivariate normal distribution

The three pilot clones were very much outliers in the population PCA plot (**Figs.** S7-8), so they were excluded from the eventual plot depicted below (Manhattan plot; **Fig.** 13A,B). The kinship matrix and PCA were made on 98 individuals instead of 101, to salvage the problem of genetic outliers.

Association testing

Association testing was performed using GEMMA (Zhou & Stephens, 2012), applying a univariate linear mixed model (LMM) with the Wald test (-lmm4). The centred kinship matrix was included as a random effect to account for genetic relatedness and population structure, and the first four principal components were included as fixed-effect covariates to further control for population stratification. Since *D. magna* has a non-standard, scaffold-based genome assembly, PLINK was run with flags permitting non-standard chromosome identifiers and samples lacking sex assignments (--allow-extra-chr --allow-no-sex). A total of 1,457,196 SNPs were available prior to filtering, after applying variant-level quality filters, 1,073,027 SNPs were retained and used in the association analysis.

Significance thresholds

A SNP was considered statistically significant if its p-value fell below the Bonferroni-corrected threshold ($0.05/n$, where n is the number of SNPs tested; threshold=4.68x10^{-8}). We applied this threshold rather than the conventional genome-wide significance threshold of 5x10^{-8}, which was derived empirically for human GWAS and assumes a level of linkage disequilibrium that has not yet been characterized in *D. magna.* Given the relatively small sample size of this study, we additionally examined SNPs surpassing a suggestive threshold of 1x10^{-8}.

Proportion of variance explained

The proportion of phenotypic variance explained by each lead SNP was estimated as $R^2 = (2\ x\ MAF\ x\ (1 - MAF)\ x\ \beta^2/V_p$, where MAF is the minor allele frequency, B is the GEMMA-derived effect size, and V_p is the total phenotypic variance (based on formula $V_p = V_g + V_e$) (Falconer, 1996) extracted from the GEMMA log file.

Visualisation and diagnostics

For visualisation R (v4.5.2) was used with packages ggplot2 (v4.0.2), dplyr (v1.2.0), scales (v1.4.0) and ggrepel (0.9.8) to create Manhattan plots and QQ plots for each phenotype considered in the analysis.

Software and compute environment

GEMMA (v0.98.5), PLINK (v2.0.0), BCFtools (v1.18), R (v4.5.2) for visualization. The VSC (Vlaamse Supercomputer Centrum) was used for running the scripts.

BLAST

To see the biological relevance of the significant and suggestive SNPs the protein sequences near or containing the SNP were isolated from public dataset (NCBI, ref. UOB_LRV0_1). These protein sequences were then aligned to the RefSeq data base using, more specifically, the subset of Arthropoda (taxid 6656).

ATAC-seq

To characterize the regulatory landscape of the *D. magna* genome, ATAC-seq data from lab clones in control condition (*Aaronkiggen/Daphnia-ATAC-Pipeline*, n.d.). Briefly, raw reads were trimmed, aligned and shifted to account for Tn5 insertion bias, followed by peak calling using MACS2 (v2.2.7.1). To generate a robust consensus peak set, peaks across biological replicates were merged into single genomic intervals. Consensus peaks were subsequently assigned to three distance-based regulatory tiers relative to the start and end of a gene; promoter (0-2kb), proximal (2-5kb), and distal (5-20kb). HOMER (v4.11) was then used to find statistical motif enrichment by comparing a foreground (peaks near DEGs) against a background (peaks near non-DEGs) and using a non-redundant motif database combining JASPAR 2026 and CIS-BP. To provide regulatory context for GWAS candidate loci, GWAS-associated SNPS were intersected with the consensus ATAC-seq peak set using bedtools intersect, identifying variants residing within open chromatin regions. The resulting TF-target edge and node tables were imported into Cytoscape (v3.10.4) (Shannon et al., 2003) for network visualization. To generate a putative GRN, the network was filtered on hub TFs that were themselves differentially expressed, with target genes downstream from these hubs containing TF-binding motifs and differential expression under kairomone exposure.

Results

To address the objectives outlined in the introduction, the results are presented in three parts. First, behavioural responses to fish kairomone exposure are characterised across population types based on tracking data. This focusses on phototaxis, swimming kinematics, and nearest neighbour distance. Second, GWAS results are presented for phenotypes capturing constitutive differences in phototactic behaviour as well as kairomone-induced plasticity in swimming behaviour, with candidate loci discussed in relation to underlying molecular mechanisms. Third, RNA-seq data are used to identify differentially expressed genes upon fish kairomone exposure, from which a putative GRN underlying the anti-predator response in *D. magna* is proposed.

1. Change in phototactic behaviour

1.1 Mean vertical position

For the analyses of phototactic behaviour the three pilot clones (C1242, P_{132},85, P_{132},96) are included in the models used and the effect plots described below. The phototactic behaviour of these clones is well documented and serves as a proof of concept for the experimental setup. As culturing conditions for these clones were suboptimal, they were excluded from all other behavioural analyses to avoid confounding effects on swimming kinematics and nearest neighbour distance. In the models they were assigned to their own population type, that way the three clones are considered as individual population types. The pilot clones had 5 replicates per condition instead of the 3 replicates considered for the GWAS clones.

Mean vertical position in the full dataset, containing the 98 GWAS clones and the three pilot clones, differed between fish kairomone (FK)-exposed and control conditions across population types, with the direction and magnitude of response varying considerably by group (Table 1; Fig. 6). The *Daphnia* from the non-agricultural fishless ponds (NA_NF) showed a significant increase in vertical position when FK-exposed ($p<0.01$, Table S1). A similar, non-significant, trend can be seen in the agricultural fishless type (A_NF). While the population types with previous exposure to fish, A_F and NA_F, did not significantly alter their vertical position. The pilot clone P_{132},85 significantly altered its vertical position ($p<0.05$, Table S1), with a decrease under FK-exposure. Clones C1242 and P_{132},96 did not alter their vertical position significantly (Table S1), however a slight decrease can be seen in C1242. Population type and its interaction with condition were both significant predictors of vertical position (Table 1). Between groups Bonferroni post-hoc comparison showed that the response from the NA_NF type is significantly different from NA_F ($p = 0.045$; Table S2), while all the other population types were not significantly different from each other (Table S2), except when compared to constitutively negative clone P_{132},96 (Table S2). Per-pond distributions of vertical position and fish kairomone effect sizes are provided in Supplementary Figures S3 and S4.

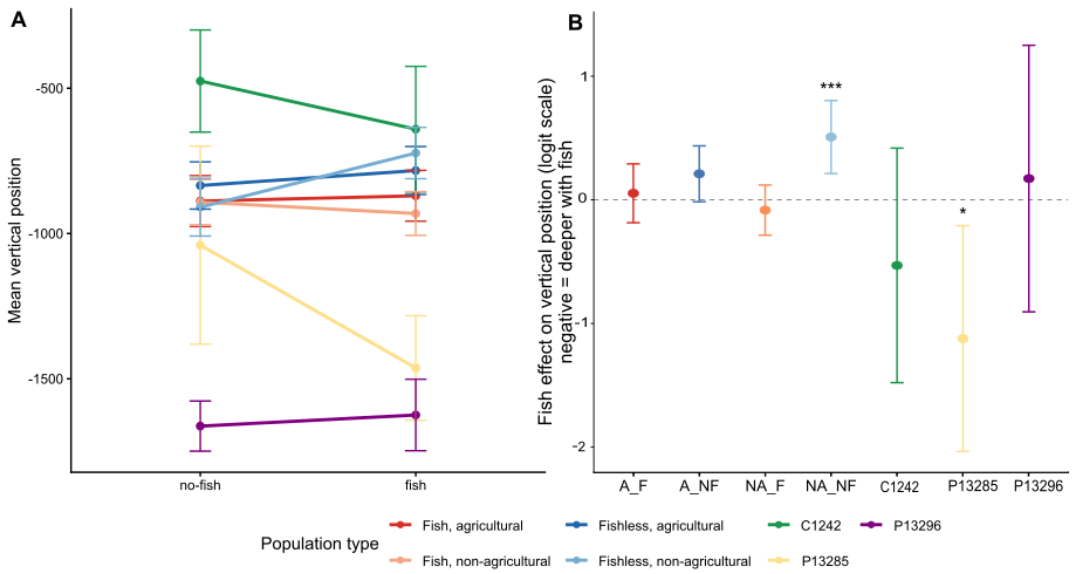


*Figure 6: Logit-transformed vertical position in response to fish kairomone exposure across population types and pilot study clones. (A) Reaction norm plot of estimated marginal means under fish and no-fish conditions for four GWAS population types (fish exposed agricultural, A_F; fish-exposed non-agricultural, NA_F; fishless agricultural, A_NF; fishless non-agricultural, NA_NF) and three pilot study clones (C1242, P_{132},85, P_{132},96). Error bars represent 95% confidence intervals. Positive values indicate position more toward surface, negative more toward the bottom of the arena. (B) Fish kairomone effect sizes (fish - no-fish) per group from post-hoc pairwise comparisons (Table S1). The dashed line indicates no difference from the no-fish baseline. Significance codes: *** p < 0.001, * p < 0.05.*

***Table** 1: Results of ANOVA type III performed on the model fitted on the vertical position phenotype*

Fixed effect	X^2	Df	p
Condition	0.19	1	0.663
Population type	13.65	6	**0.034***
Condition x population type	20.14	6	**0.003****

1.2 Phototactic index

Phototactic index (PI; Fig. 5) responses to fish kairomones exposure varied across population types, with no consistent directional shift shared by all groups (**Table** 2; **Fig.** 7), showing a near similar pattern as mean vertical position (**Fig.** 6). Populations which experienced prior fish exposure (A_F, NA_F) showed a non-significant change in their phototactic index upon FK-exposure. Fishless populations showed an increase in PI under fish kairomone exposure, reaching significance in the fishless population with no agricultural exposure ($p<0.01$) and a slight positive shift in the agricultural fishless population type. The pilot clones showed behaviour relatively consistent with assumptions, C1242 remained positively phototactic, with a slight decrease, non-significant, in phototactic index upon FK-exposure. The plastic clone P_{132},85 showed a significant alteration in its phototactic index, with a significant decrease in FK-exposed condition ($p<0.05$). P_{132},96 retained a stable negative PI with no significant change.

Population type and its interaction with condition were both significant predictors of PI (Table 2). Between population types Bonferroni post-hoc comparison showed no significant difference in response to fish kairomones, except when compared to the constitutively negative clone P_{132},96 in both fish exposed and control condition (Table S6). Per-pond distributions of phototactic index and fish kairomone effect sizes are provided in Supplementary Figures S6 and S7.

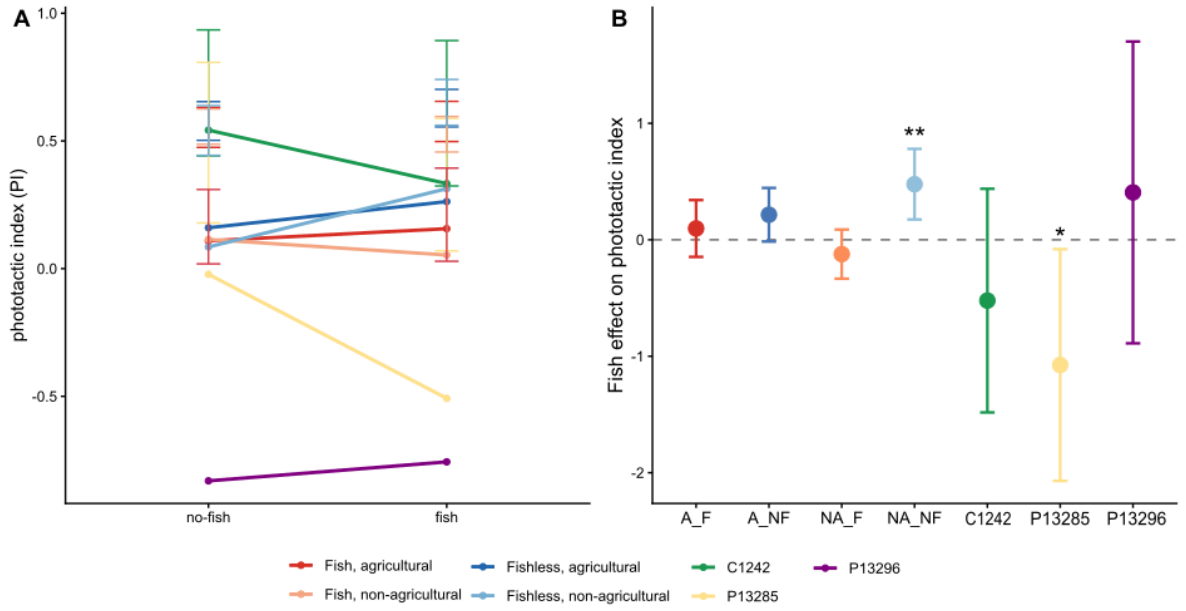


*Figure 7: Phototactic index change in response to fish kairomone exposure across population types and pilot study clones. (A) Reaction norm plot of estimated marginal means under no-fish and fish condition for four GWAS population types (A_F, NA_F, A_NF, NA_NF) and three pilot study clones (C1242, P_{132},85, P_{132},96). Error bars represent 95% confidence intervals. (B) Fish kairomone effect sizes (fish – no-fish) per group form post-hoc pairwise comparisons (Table S4). Dashed line shows indicates no difference from the no-fish baseline. Significance codes: ** p < 0.01, * p < 0.05.*

Table 2: Results of ANOVA type III analysis performed on the model fitted on phototactic index (PI)

Fixed effect	X^2	Df	p
Condition	0.61	1	0.436
Population type	13.25	6	**0.039***
Condition x population type	18.41	6	**0.005****

2. Change in kinematics

2.1 Swimming speed and distance travelled

Within the kinematics analyses, the pilot clones were excluded because during culturing they experienced suboptimal condition possibly affecting their locomotory behaviour. **Swimming speed** (Fig. 5) was expected to decrease in response to fish kairomone exposure, consistent with findings by Langer et al (2019). Neither condition nor population type alone significantly predicted swimming speed, but their interaction was significant (Table 3).

Indicating that the direction of the kairomone effect on speed depended on population type. Fish-naïve population types (A_NF, NA_NF) showed a negative slope in the reaction norm plot (Fig. 8A), indicating reduced speed under FK-exposure, whereas the fish-exposed population types (A_F, NA_F) showed a positive slope, indicating increased speed. Post-hoc pairwise comparisons revealed that only the fish-naïve non-agricultural populations (NA_NF) showed a statistically significant decrease in speed under fish kairomone exposure ($p<0.05$; Fig. 8B). Between types post hoc comparison showed a non-significant difference between population types (Table S8).

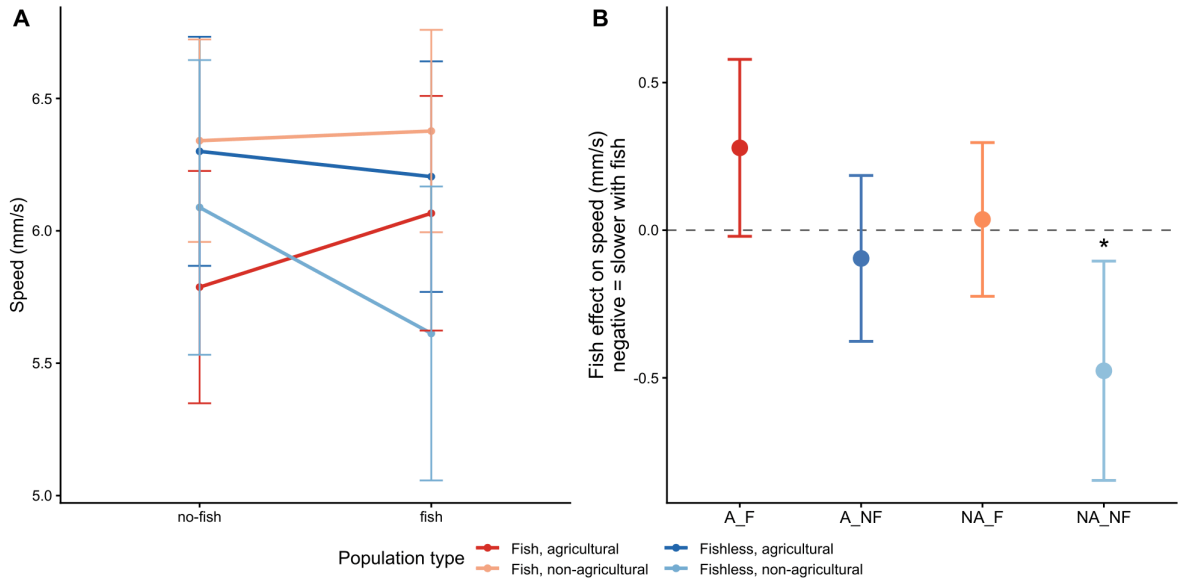


*Figure 8: Swimming speed (mm/s) in response to fish kairomone exposure across four population types (A_F, A_NF, NA_F, NA_NF). (A) Reaction norm plot of estimated marginal means under no-fish and fish conditions. Error bars represent 95% confidence intervals. (B) Fish kairomone effect sizes (fish – no-fish) from post-hoc pairwise comparisons (Table S8), negative values indicate slower swimming under fish kairomone exposure, the dashed line indicates no difference from the no-fish baseline. Significance codes: * p < 0.05.*

***Table** 3: Results of ANOVA type III performed on the model fitted on the swimming speed*

Fixed effect	X^2	Df	p
Condition	3.25	1	0.072
Population type	4.77	3	0.189
Condition x population type	9.83	3	**0.020***

When populations were regrouped into two types, population with and without prior fish exposure a more consistent pattern emerged (Table 4; Fig. 9). *Daphnia* from ponds with no prior fish exposure, were significantly slower under fish kairomone exposure ($p<0.01$), while those from ponds with prior fish exposure showed a non-significant increase in speed. Both groups were significantly different in their response to fish kairomones ($p = 0.027$; Table S10).

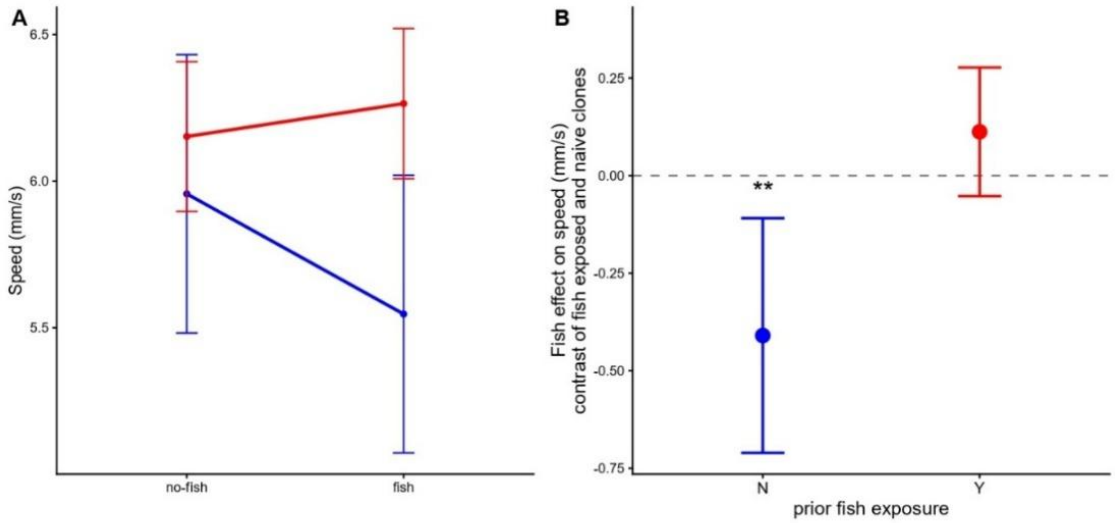


*Figure 9: Swimming speed (mm/s) in Daphnia with (Y, red) and without (N, blue) prior fish exposure. (A) Reaction norm plot of estimated marginal means under no-fish and fish conditions. Error bars represent 95% confidence intervals. (B) Fish kairomone effect sizes (fish – no-fish) per group from post hoc pairwise comparisons (Table S10). Negative values indicate slower swimming under fish-kairomone exposure, the dashed line indicates no difference from baseline. Significance codes: **p<0.01.*

***Table** 4: Results of ANOVA type III on model of prior fish exposure*

Fixed effect	X^2	Df	p
Condition	6.55	1	**0.010***
Prior fish exposure	0.17	1	0.677
Condition x population type	7.61	1	**0.006****

Distance travelled (D_{total}; Fig. 5) was expected to decrease alongside the decrease in speed, because they are expected to covary. Similar to swimming speed condition and population type were non-significant in the prediction of distance travelled, but their interaction was (Table 5). Both fish-naïve population showed a negative slope in the reaction norm plot (Fig. 10A) indicating a lower distance travelled. Whereas both the fish-exposed population types (A_F, NA_F) showed a positive slope, indicating an increase in distance travelled. Post-hoc pairwise comparison showed that only the NA_NF group showed a significant difference in distance travelled (p<0.01; Fig. 10B). Between population types Bonferroni post-hoc comparison revealed no significant difference in response to fish kairomones or control condition (Table S13).

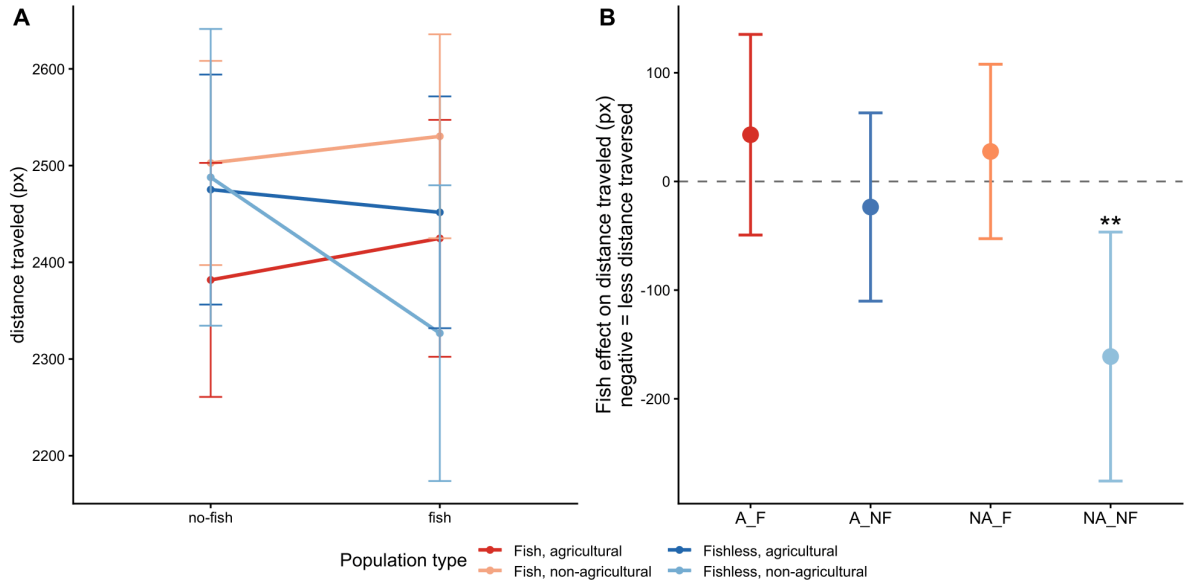


*Figure 10: Distance travelled (px) in response to fish kairomone exposure across four population types (A_F, A_NF, NA_F, NA_NF).(A) Reaction norm plot of estimated marginal means under no-fish and fish conditions. Error bars represent 95% confidence intervals. (B) Fish kairomone effect sizes from post-hoc pairwise comparisons (Table S12). Significance codes: **p<0.01.*

***Table** 5: Results of ANOVA type III performed on the model fitted on the distance travelled*

Fixed effect	X^2	Df	p
Condition	0.82	1	0.365
Population type	2.79	3	0.436
Condition x population type	8.72	3	**0.033***

When looking at **nearest neighbour distance** (NND) it is expected that under fish kairomone exposure the distance should increase (Langer et al., 2019). Looking at the reaction norms (Fig. 11A) both fish absent population groups showed a negative slope, which means the distance between them becomes smaller, opposite to expected. In populations with fish presence, A_F and NA_F, a positive slope is seen, thus an increase in NND. However, after post-hoc pairwise comparison, fish effect was non-significant in all population types. Between population types Bonferroni post-hoc comparison showed no significant difference between groups (Table S15).

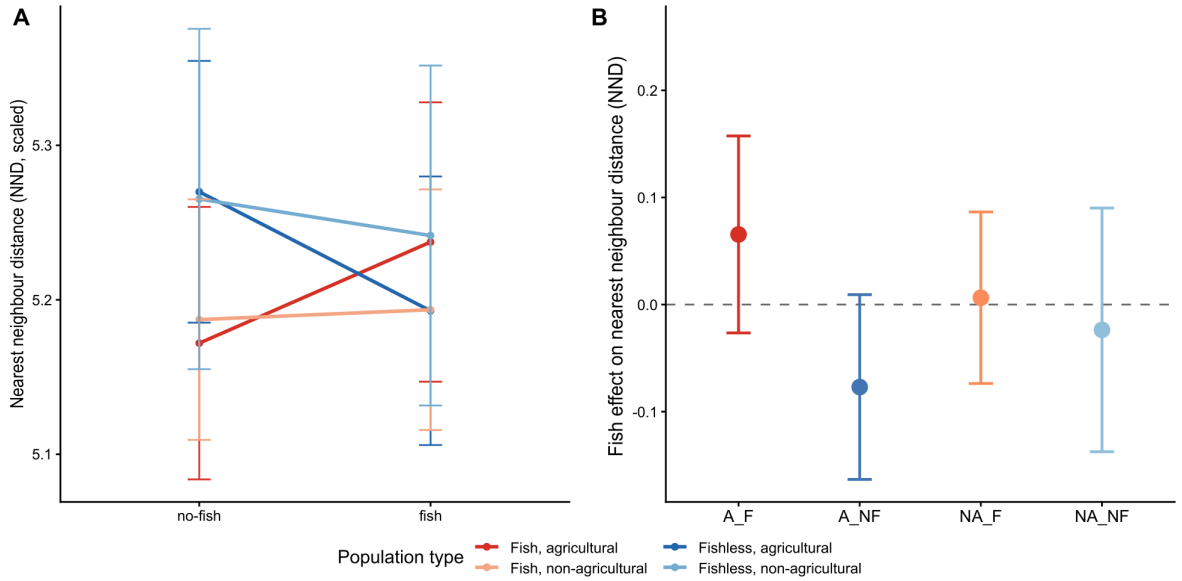


Figure 11: Nearest neighbour distance (scaled) in response to fish kairomone exposure across four population types (A_F, A_NF, NA_F, NA_NF). (A) Reaction norm plot of estimated scaled marginal means under no-fish and fish conditions. Error bars represent 95% confidence intervals. (B) Fish kairomone effect sizes from post-hoc pairwise comparisons (Table S14).

***Table** 6: Results of ANOVA type III performed on the model fitted on the nearest neighbour distance*

Fixed effect	X^2	Df	p
Condition	1.99	1	0.159
Population type	3.98	3	0.264
Condition x population type	5.19	3	0.158

3. GWAS

Genotyping and sample quality

Prior to GWAS, principal component analysis (PCA) was performed on 98 *D. magna* genotypes (excluded three pilot clones, based on PCA outlier status; see methods) using 1,467,196 SNPs. The first two principal components explained 3.74793% and 2.83836 % of genetic variance, respectively, with subsequent components explaining progressively less (PC3: 2.5597 %, PC4: 2.2646%). The PCA revealed broad population structure consistent with pond of origin, with no single separation between fish exposed and fish free populations, suggesting that geographic separation is the most likely explanation for genetic differences between ponds. These first four PCs were retained as covariates in the linear mixed model to account for residual population stratification.

Association analysis was performed using GEMMA v0.98.3, implementing a linear mixed model with a centred kinship matrix and four genomic PCs as fixed-effect covariates, across 1,067,310 SNPs and 98 individuals. The overall genomic inflation factor was λ **= 1.124**. The QQ plot shows that most points follow the null-model and that only few detach from the line in the upper tail (Fig. 12), consistent with genuine association signal rather than widespread stratification-driven inflation. The QQ plot below is for the GWAS on vertical position in the control condition, additional QQ plots are provided in supplementary material.

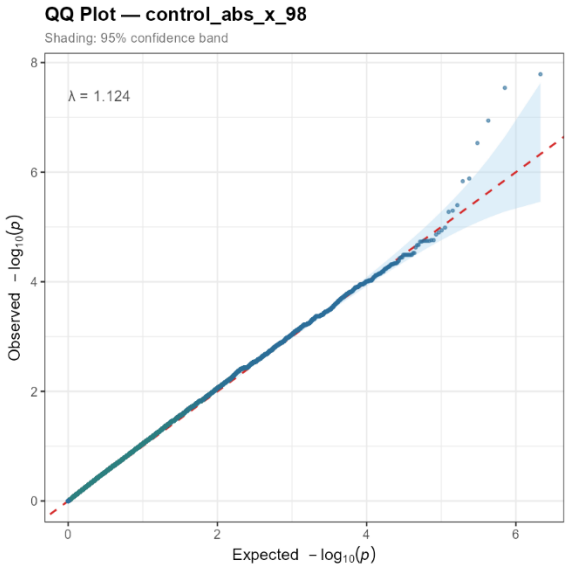


Figure 12: QQ plot based on the vertical position of the control group as phenotype, based on GEMMA results of 98 genotypes.

Suggestive and significant SNPS

GWAS was performed on all metrics previously reported, however, only those yielding significant results are shown while the rest can be found in supplementary materials (Figs. S10-26). If the GWAS returned significant SNPs (p<Bonferroni-value; **~4.68*10^{-8}**) which fell within an annotated gene, the protein sequence of that gene is considered in further analyses (InterPro and BLAST, to infer biological function). If it fell outside an annotated gene, but within ± 5kb of neighbouring genes, their gene function was identified and discussed. Many alterations of the same phenotype were considered, yielding a lot of suggestive SNPs (p<1 x 10^{-5}), to minimize these and as a conservative measure, we considered only those that had overlap with other suggestive SNPs from the other phenotype representations.

Phenotype: vertical position control (no-fish exposure)

Across the four vertical position phenotype representations, GWAS identified a consistent set of significantly associated loci on chromosome 9 (Table 7). In the primary analysis of absolute depth in 98 individuals, two SNPs reached genome-wide significance (p<4.68 x 10^{-8}): **Scaffold_9:7079725** (hereafter referred to as **locus VPC1**), (p=1.64x10^{-8}), β = 238.25 ± 40.06) located within gene OUZ56_029317 and **Scaffold_9:7135106** (hereafter referred to as **locus VPC2**) (p = 2.90×10^{-8}, β = 346.04 ± 59.62), located within 5kb of the gene OUZ56_029343 (Fig. 13B). Genotype-phenotype analysis at locus VPC1 (ref-alt: C T) revealed a significant additive effect on vertical position: T/T homozygotes were positioned significantly deeper than both C/C homozygotes (p<0.001) and C/T heterozygotes (p<0.01), while the difference between C/C and C/T individuals was non-significant (Fig. 13C). Seven additional SNPs in close proximity reached the suggestive threshold (p<1 x 10^{-5}).

Replication of the analysis on the full 101-clone dataset (λ **= 1.10**) recovered the same major effect SNP on locus VPC1 (Scaffold_9:7079725, p = 2.50×10^{-9}, β = 246.57 ± 39.93), further supporting the result of the primary analysis. A second significant hit on chromosome 3 (Scaffold_3:4215049, p = 1.17×10^{-8}, β = −289.84 ± 49.09) was identified. While possibly interesting, I did not investigate further into this SNP, because it was deemed a likely artefact due to lack of support from neighbouring variants (Fig. S10).

Allele frequency at locus VPC1 varied considerably across ponds (Fig. 13D). The T/T genotype was unevenly distributed across the 20 ponds. When ranking boxplots based on mean vertical position, no clear relationship emerged between the proportion of T/T carriers and the observed mean position, suggesting that pond-level variation in vertical position is not solely explained by this locus. The three pilot clones are also included in Fig. 13D: C1242 carried the C/T genotype, P_{132},85 the T/T homozygote and P_{132},96 the C/C genotype. Notably, this contrasts with the genotype-phenotype pattern in Fig. 13C, where T/T homozygotes showed the deepest positioning. While P_{132},96 (C/C) showed the lowest vertical position among pilot clones. This mismatch suggests that additional loci contribute to vertical positioning in *Daphnia*.

The proportion of phenotypic variance explained was estimated for each major effect locus SNP from GEMMA-derived effect sizes and allele frequencies (see M&M). Locus VPC1 explained **5.85%** of phenotypic variance in vertical position (R^2=0.059), and locus VPC2 explained **5.47%** (R^2=0.055). The z-score normalised (μ=0, SD=1) did not find significant peaks, but found 11 suggestive SNPs. The categorical run identified a significant SNP, Scaffold_9:7135106 (p = 9.55×10^{-9}), overlapping with the 98-individual result of locus VPC2. Across all four phenotype representations, one suggestive SNP was consistent: Scaffold_9:7134580, which maps to a region within 5kb from OUZ56_029343 (Table 8).

Table 7: Significant SNPs for different vertical position phenotypes (fell outside of gene, most proximate gene; **likely artefact, so no gene noteworthy)*

phenotype	CHR	BP	P	beta	se	af	logl_h1	gene
abs_98	9	7079725	1.64E-08	238.2533	40.05729	0.26	-679.494	OUZ56_029317
abs_98	9	7135106	2.90E-08	346.0438	59.6158	0.097	-680.049	OUZ56_029343*
abs_101	9	7079725	2.50E-09	246.5694	39.93456	0.27	-701.363	OUZ56_029317
abs_101	3	4215049	1.17E-08	-289.843	49.08778	0.277	-702.862	NA**
categorical	9	7135106	9.55E-09	-2.54508	0.421624	0.097	-199.378	OUZ56_029343*

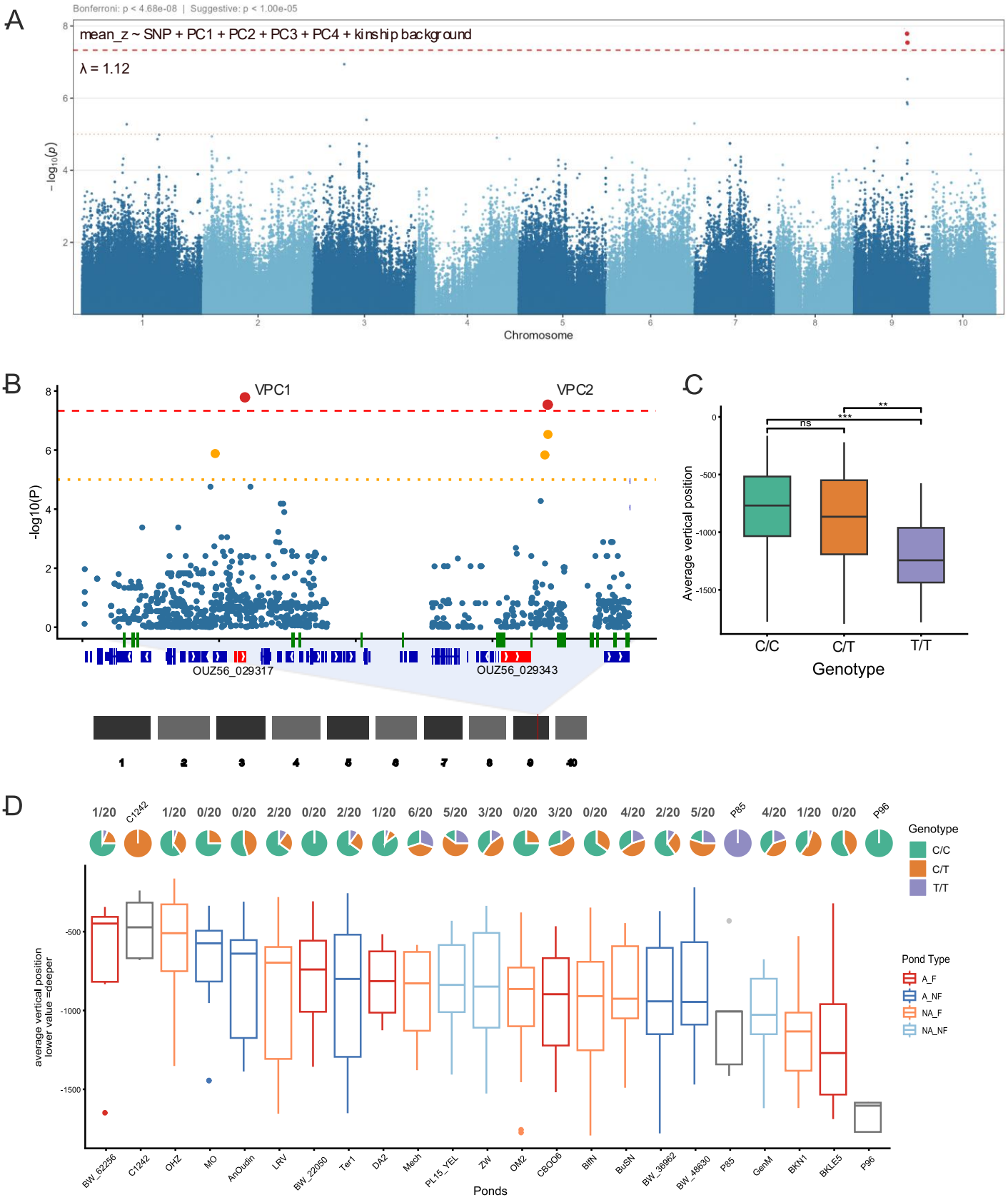


*Figure 13: GWAS results for vertical position (A) Manhattan plot across all scaffolds with the model fitted by GEMMA, and the genomic inflation factor in the top right corner. Red dashed and orange dotted lines indicate Bonferroni and suggestive thresholds respectively. The SNPs crossing each threshold are coloured accordingly. (B) Zoomed regional plot (scaffold_9:7,050,000-7,150,000). The top SNP (Locus VPC1, red) exceeds the Bonferroni threshold and falls within the gene highlighted in red (OUZ56_029317). Green bars in A and B show the chromatin accessible regions. (C) Average vertical position by genotype at the lead SNP (C/C: reference homozygote, C/T: heterozygote, T/T: alternative homozygote). Significance brackets: **p<0.01, ***p<0.001. (D) Average vertical position per pond (box plots, coloured by pond type), with pie charts showing the proportion of T/T carriers among all sequenced clones per pond.*

Phenotype: vertical position fish kairomone exposed

In contrast, no genome-wide significant associations were identified for vertical position under fish kairomone exposure across any of the three phenotype representations (Figs. S13-15). The number of suggestive hits ($p<10x10^{-8}$) was a lot higher than in the control condition, with 50, 12, and 25 suggestive SNPs identified in the absolute depth (n=101), z-score normalised (n=100), and categorical (n=100) analyses respectively. This could potentially reflect an increased phenotypic variance under kairomone exposure. Across the three representations, three SNPs were consistent (Table 8): two located on chromosome 6, and one on chromosome 9, locus VPC1, the same locus that reached genome-wide significance in the control condition. The presence of locus VPC1 further strengthens the assumption that this SNP may influence baseline behaviour, but also plays a part in vertical positioning in FK-exposed condition.

Plasticity of the response

To identify loci underlying phenotypic plasticity of vertical positioning, five representations of the plasticity phenotype were tested in GWAS (see Methods). None returned genome-wide significant associations (Figs. S16-20). The mean slope and z-score normalised mean slope phenotypes (both n = 101) identified 19 and 20 suggestive SNPs, respectively, of which 13 were shared between the two representations (Table 8). The more extreme plasticity phenotypes, based on most extreme genotype values, its absolute value, and a subset restricted to the top and bottom 30% of the plastic response (n = 63), returned 8, 4, and 30 suggestive SNPs respectively. No consensus overlap was observed across phenotype representations, even within a ±5 kb window. This indicates the suggestive SNPs identified are highly dependent on how the phenotype is encoded. The mean slope showed the lowest genomic inflation (λ = 1.038) and is taken as the primary representation of plasticity suggestive SNPs. The overlapping suggestive SNPs of the mean slope phenotype and the scaled mean slope phenotype was taken into consideration as representative (Table 8).

Table 8: Suggestive SNPs of the three vertical positional phenotypes: control, kairomone exposed and plasticity (overlap mean slope and mean slope scaled). SNPs shown below are based on overlap between suggestive SNPs of the different representations of the same phenotype. Per SNP the location is given (Scaffold and base pair), whether it fell within an exon or intron region or not, and the accompanying gene name, its protein ID. If it did not fall within an annotated gene, the closest gene was considered.

phenotype	scaffold	bp	exon/intron	gene name	protein ID	closest gene
control position	9	7135139	/			OUZ56_029343
control position	3	7192883	exon	OUZ56_009051	KAK4023650.1	
control position	9	7134580	/			OUZ56_029343
control position	9	7074289	intron	OUZ56_029315	KAK4037279.1	
fish position	6	3360442	/			OUZ56_019126
fish position	9	7079725	exon	OUZ56_029317	KAK4037281.1	
fish position	6	3360622	/			OUZ56_019126
plasticity	1	4920046	/			OUZ56_001141
plasticity	2	1388450	/			OUZ56_004077
plasticity	3	478378	/			OUZ56_007467
plasticity	4	10400888	exon	OUZ56_013436	KAK4008293.1	
plasticity	4	10400934	exon	OUZ56_013436	KAK4008293.1	
plasticity	4	10401681	exon	OUZ56_013436	KAK4008293.1	
plasticity	4	10384885	exon	OUZ56_013429	KAK4008284.1	
plasticity	4	10388903	intron	OUZ56_013433	KAK4008289.1	
plasticity	4	10396361	intron	OUZ56_013436	KAK4008293.1	
plasticity	4	10400614	exon	OUZ56_013436	KAK4008293.1	
plasticity	6	4837497	exon	OUZ56_019589	KAK4010446.1	
plasticity	6	4960084	intron	OUZ56_019640	KAK4010497.1	
plasticity	10	6657819	/			OUZ56_031840

GWAS swimming speed

For swimming speed, no genome-wide significant associations were identified for absolute speed under control or kairomone conditions, nor for the signed speed delta between conditions (λ = 0.998).

A categorical representation of control swimming speed did return significant SNPs (λ = 1.210), however these values were excluded from further consideration because all significant hits shared identical p-values, effect sizes, and allele frequencies, which indicate full LD rather than independent association. As this pattern provides no evidence for multiple independent associations and occurred only in the categorical phenotype representation, the signal was considered insufficiently robust for biological representation.

GWAS on the absolute value of speed change between conditions (speed absolute delta, λ = 1,074; Fig. 24 & S26) identified three genome-wide significant SNPs across two chromosomes. Two SNPs on chromosome 1 (Scaffold_1:4,979,537 and Scaffold_1:4,995,205; $p = 2.44\times10^{-8}$ and 9.97×10^{-10} respectively) likely coincide on the same locus, with neighbouring genes (within 5kb). The SNP Scaffold_1:4,995,205 fell within a 5kb range of both OUZ56_001158 and OUZ56_001160, and SNP Scaffold_1:4,979,537 fell within a 5kb range of OUZ56_001155. An independent hit on chromosome 3 (Scaffold_3:6,740,262; $p = 2.38\times10^{-9}$) falls within an intron of OUZ56_008941. Significant SNP coordinates, effect sizes, and nearest annotated genes are reported in Table 9.

*Table 9:significant SNPs for the absolute paired difference of control and fish kairomone condition. *closest gene within 5kb*

CHR	BP	P	beta	se	af	logl_h1	Gene
1	4995205	9.97E-10	0.275211	0.042652	0.036	84.47382	OUZ56_001158*
1	4979537	2.44E-08	0.333804	0.057608	0.02	81.36397	OUZ56_001155*
3	6740262	2.38E-09	0.358401	0.057112	0.02	83.62387	OUZ56_008941 (intron)

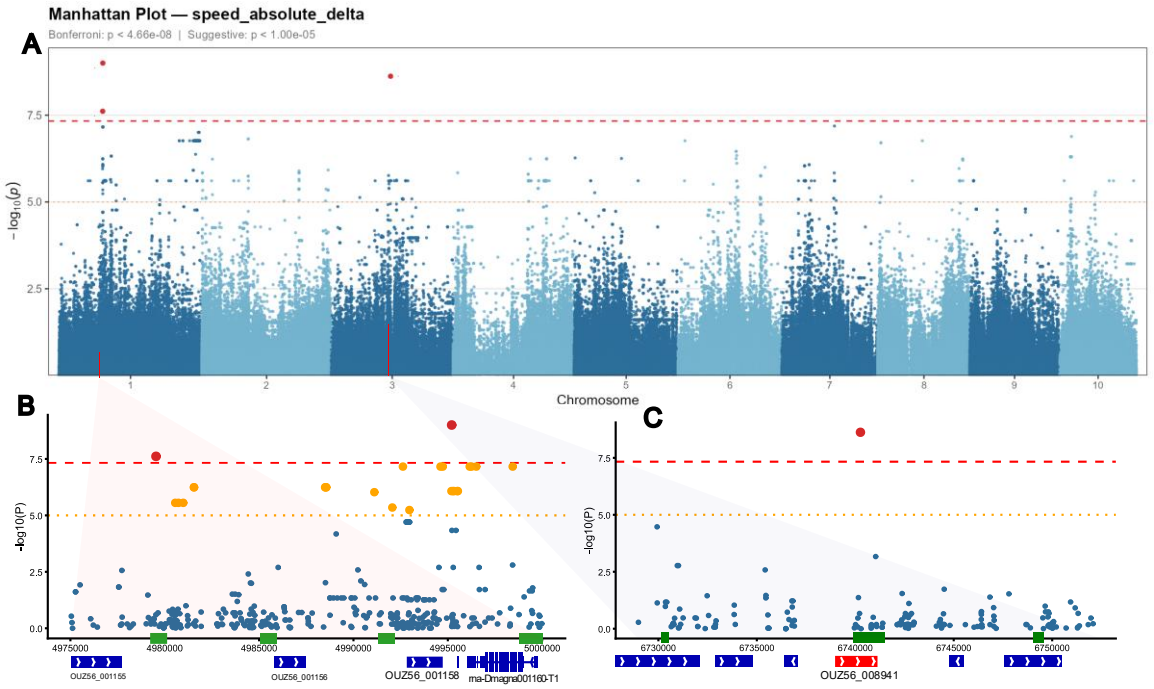


Figure 14: Manhattan plot of GWAS results for the absolute difference in swimming speed between control and kairomone-exposed conditions. (A) Full Manhattan plot with suggestive ($p<1x10^{-5}$) and Bonferroni ($p<4.66x10^{-8}$) significance thresholds indicated by orange dotted and red dashed line, respectively. SNPs exceeding each threshold are coloured accordingly. (B) Inset of scaffold_1:4,975,000-5,000,000 with gene models shown in blue and consensus ATAC-seq accessible regions in green. (C) Inset of scaffold_3:6,727,762-6,752,762, with gene annotation in blue. OUZ56_008941, the gene in which the significant SNP is present is highlighted in red. Consensus accessible regions are shown in green.

Overlap with ATAC-seq peaks

Integration with consensus ATAC-seq peaks was used to determine GWAS-identified SNPs corresponded to consensus regions of open chromatin. For the vertical position phenotype, all significant and suggestive peaks fell outside of consensus accessible regions. For the speed phenotype, two of the three significant SNPs overlapped with accessible chromatin regions: scaffold_1:4979537 and scaffold_3:6740262 (Figs. 14B & C).

BLAST and missense mutations

Protein sequences of significant and suggestive GWAS candidate genes were aligned to RefSeq database (Arthropoda taxid:6656) using BLAST to identify putative homologues and assign gene function based on sequence similarity to annotated arthropod proteins.

Significant loci vertical position

For the significant vertical position locus VPC1, within gene OUZ56_029317 carried InterPro annotations IPR000276, IPR000856, and IPR017452, and aligned with 99.74% identity to Compound eye opsin BCRH2 in *D. magna* (query cover 100%; Table S18). Locus VPC2, near gene OUZ56_029343, carried Zinc-finger Sec23/Sec24-type domain annotations (InterPro), with BLAST top hits to protein transport protein Sec24C-like sequences across *Daphnia* species (percent identity >87%. Table S18), with the highest identity to *D. magna*.

Suggestive loci plasticity vertical position

For the suggestive plasticity loci on chromosome 4, five SNPs mapped to OUZ56_013436, which carried a Zinc finger NF-X1-type domain annotation, with BLAST top hits to NFX1-type zinc finger-containing protein 1 isoform (Table S18). OUZ56_019640 aligned to Zwei IG domain protein zig-8 in *D. magna* (Table S18). OUZ56_004077 aligned to domesticated amidase effector 2-like protein in *Daphnia carinata*, and additionally to NPC intracellular cholesterol transporter 2 homolog in *D. magna*. OUZ56_019589, OUZ56_013429 and OUZ56_001141 matched uncharacterized proteins and OUZ56_007467 and OUZ56_031840 were of insufficient length for reliable alignment.

Significant loci speed absolute delta

Regarding the significant SNPs for the absolute paired difference in speed there was one which fell within an intron of OUZ56_008941. The protein sequence of this gene mapped best to a zinc finger protein rotund like isoform protein sequence of *Daphnia pulex* (Table S18), with the same protein from *D. magna* as the third hit. The other hits fell outside of genes, but within a 5kb region of other genes, however, the protein sequence of OUZ56_001158 was of insufficient length for alignment. The OUZ56_001155 protein sequence aligned best with the Ubiquitin carboxyl-terminal hydrolase 36 isoform of *D. magna* (Table S18).

Missense mutations

When checking the missense mutations, I only considered the GWAS SNP hits in exons of genes. The mutation on locus VPC1 was a synonymous mutation, it was in the third base of the codon on exon 6. The reference codon is GTC and the mutation is GTT, both coding for Valine. Locus VPC2 fell outside a gene region, and the peaks of speed absolute delta fell outside genes and within an intron region.

RNA-seq

Differentially expressed genes under fish kairomone exposure

RNA-seq of clone P_{132},85 under fish kairomone versus control conditions identified 701 differentially expressed genes (DEGs; FDR<0.05), of which 286 were upregulated and 415 downregulated (Fig. 15). The most statistically significant DEG was OUZ56_033583 (adj = 2.52×10^{-22}, Log2FC = −0.38), encoding a serine type endopeptidase inhibitor and showing modest downregulation under fish kairomone exposure. Both most extremely up and down regulated genes lacked the GO terms within the GO databases consulted for these analyses. None of the 17 GWAS hits were among the differentially expressed genes.

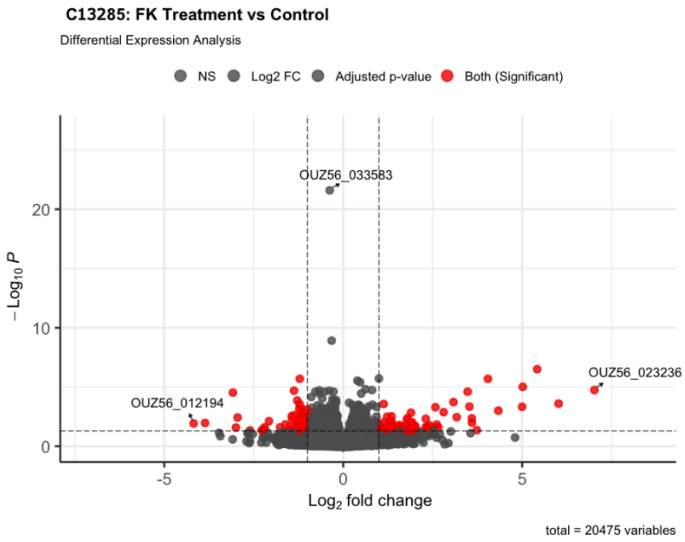


Figure 15: Volcano plot of control vs fish kairomone exposed condition of clone P_{132},85. Red highlighted are the DEG (|LFC|>1) and FDR<0.05. Labelled are the most significantly differentially expressed gene (OUZ56_033583), the most upregulated (OUZ56_023236) and most downregulated (OUZ56_012194).

GO overrepresentation analysis

GO overrepresentation analysis (ORA) against the EggNOG full proteome annotation background identified significant enrichment in mitochondrial energy metabolism, including ATP metabolic process, aerobic respiration, and tricarboxylic acid cycle, forming a densely interconnected cluster of functionally related terms (Fig. 16). The enrichment map can be roughly grouped into four functional groups: (i) mitochondrial respiration and ATP production, (ii) nucleotide and nucleoside triphosphate metabolism, (iii) organic acid and central carbon metabolism, and (iv) chromatin organization and histone modification. This suggests that modulation of the energy metabolism is very important for the response.

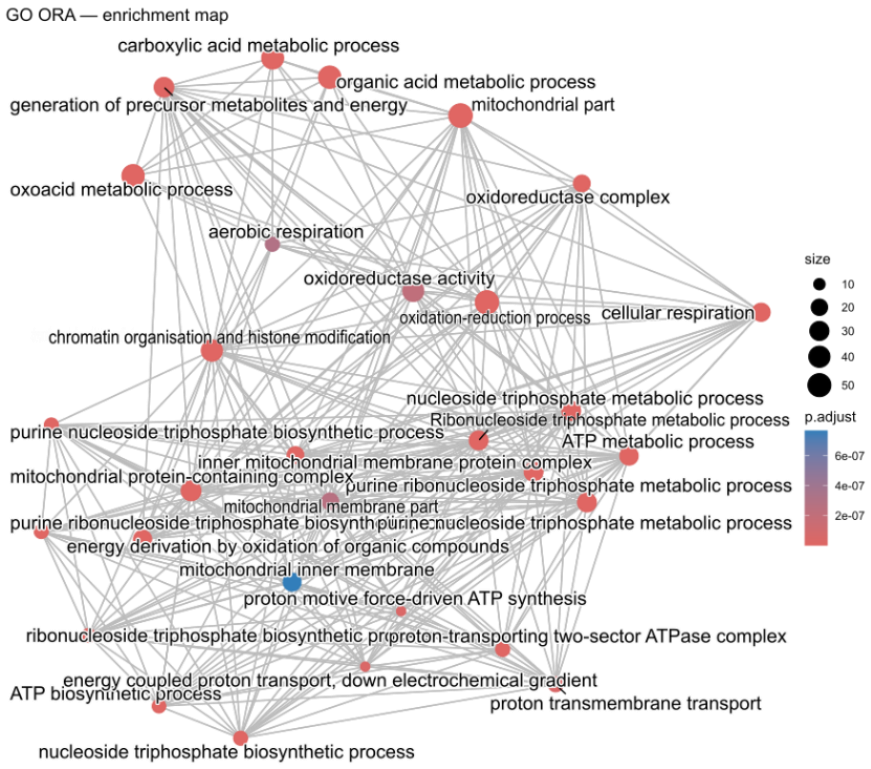


Figure 16:Enrichment plot map, a network like representation of enriched GO term, clustering GO terms which are alike into the same cluster. The hubs are coloured according to their p-value. The size is dependent on how many connections is has with other clusters.

GO gene set enrichment analysis

GO gene set enrichment analysis (GSEA) revealed more directionality in these signals across the full ranked gene list (Fig. 17) among upregulated gene sets, acetylgalactosaminyl-transferase activity, (positive) regulation of Notch signalling pathway and structural constituent of chitin-based larval cuticle were upregulated under fish kairomone exposure. Suggesting increased investment in cuticle biosynthesis and developmental signalling under kairomone exposure. While three metabolic processes showed negative enrichment scores suggesting a downregulation of these genes. (Fig. 17). Additionally, chromatin organization and histone modification were in the downregulated set, which might suggest chromatin accessibility change upon kairomone exposure.

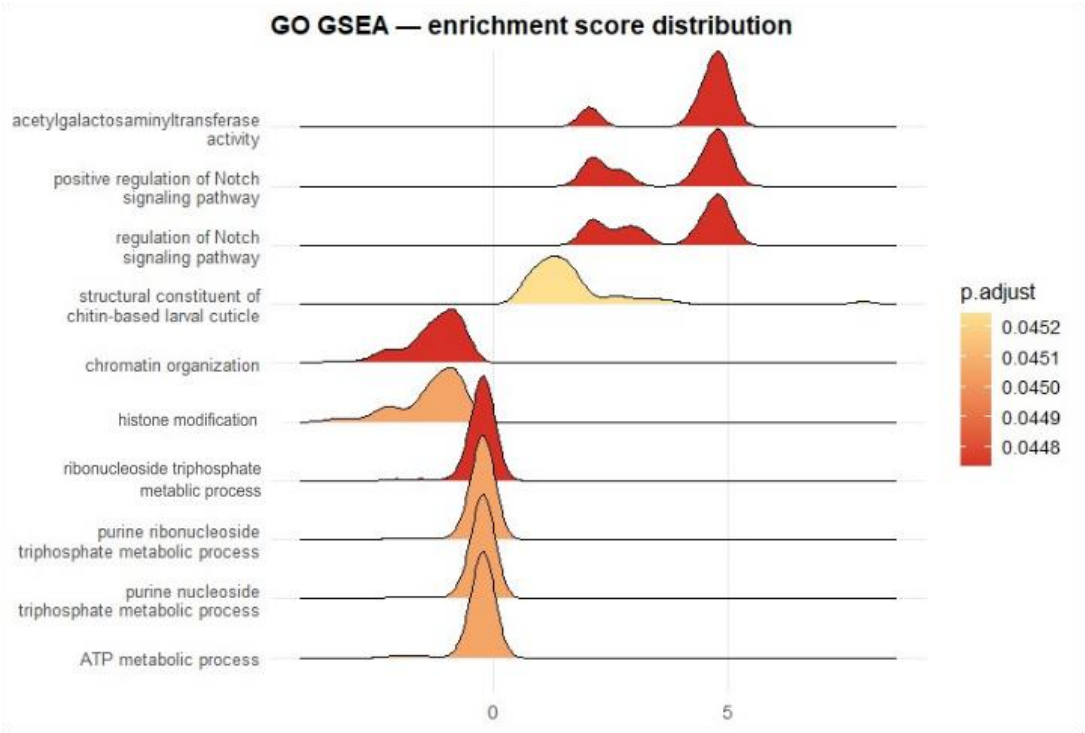


Figure 17: Gene Set Enrichment Analysis (GSEA) enrichment scores distributions for the top 10 significantly enriched Gene Ontology (GO) terms identified in the fish kairomone-exposed versus control comparison in D. magna. Each ridge represents the distribution of enrichment scores for a given GO term. Positive enrichment scores indicate enrichment among the upregulated genes under fish-kairomone exposure. Fill colour is based on their adjusted p-value.

KEGG gene set enrichment analysis

KEGG GSEA revealed uniform suppression, with all enriched gene sets showing negative normalised enrichment scores (NES) between -2.0 and -2.5 (Fig.18). The most significantly suppressed terms included myosin V, ankyrin repeat domain-containing proteins, and apoptosis-stimulating of p53 protein. The KEGG gene-concept network (Fig. 19) identified kallikrein 8, alpha-amylase, and acyl-CoA dehydrogenase as pathway hubs, with connected genes predominantly downregulated. A noticeable exception was OUZ56_019390, strongly upregulated (Log2FC ~4-5) within the kallikrein 8 network, suggesting a potentially counter regulatory response in a suppressed proteolytic pathway (Fig. 19).

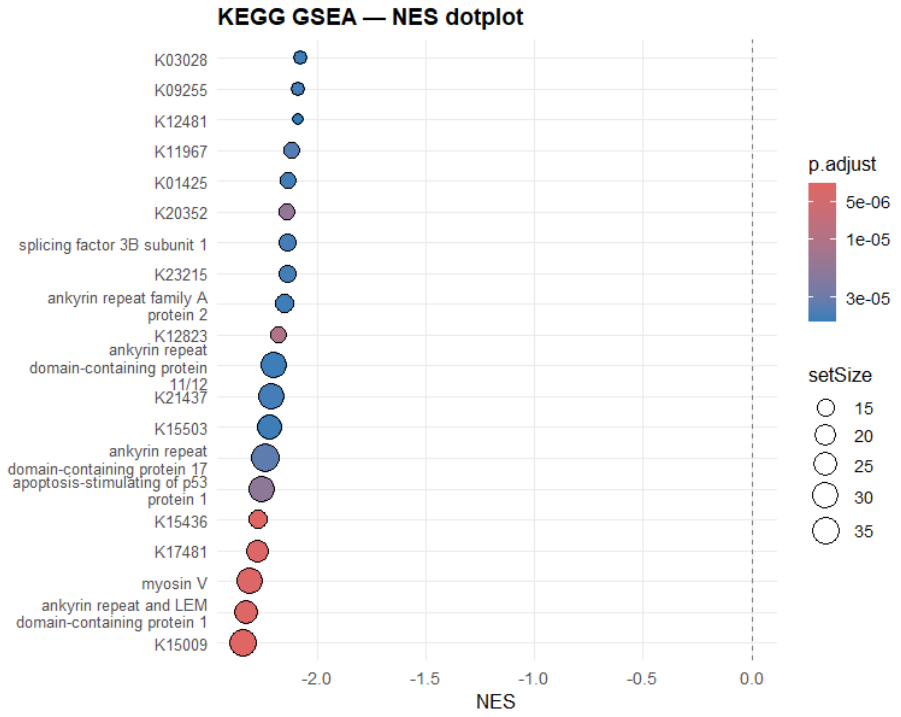


Figure 18: Normalised enrichment scores (NES) for significantly enriched KEGG pathways identified by gene set enrichment analysis (GSEA). Each dot represents one KEGG pathway. Dot size corresponds to the number of genes contributing to this pathway, and dot colour is based on adjusted p-values. Negative NES values show that these pathways are downregulated.

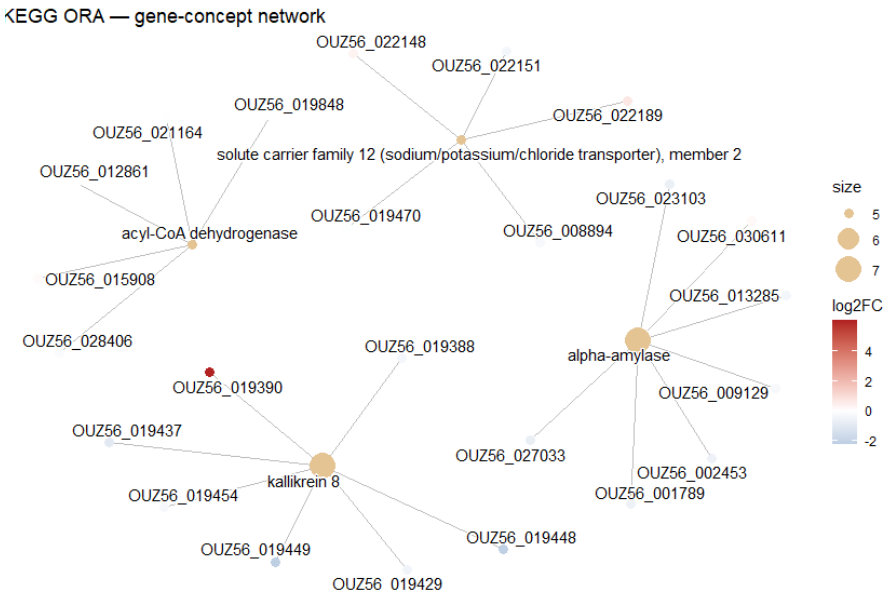


Figure 19: KEGG ORA gene-concept network (cnetplot) of over-represented pathways in fish kairomone-exposed D. magna. Nodes are either KEGG pathways (large, centred circles, size based on the number of interacting gens) or individual genes (smaller circles). Edges connect genes to their corresponding pathway. Node colour is based on the Log2FC representing up- (red) or downregulation (blue).

GO terms overlap literature

A predetermined GO-term dataset was made based on previous studies regarding sensory and neuronal signalling (Bedrossiantz et al., 2021; Weiss et al., 2012) and light dependence of DVM (S. I. Dodson et al., 1997; Weiss, 2019). DEGs identified under fish kairomone exposure showed overlap with several GO categories associated with neuronal signalling and sensory perception (Table S16). The strongest overlap was with GO terms related to synaptic and receptor-mediated signalling, including ionotropic glutamate receptor activity (GO:0004970; 9 overlapping DEGs), followed by locomotory behaviour (GO:0007626; 5 overlapping DEGs) and G protein-coupled receptor activity (GO:0004930; 5 overlapping DEGs). Additionally, DEGs overlapped with GO categories involved in photoreception and light detection, including phototransduction (GO:0007602), G protein-coupled opsin signalling pathway (GO:0016056), and detection of light stimulus (GO:0050953), each showing two overlapping genes. No overlaps were detected for GO terms related to cholinergic, GABAergic, glutaminergic or dopaminergic signalling specifically.

Together, these results may point toward transcriptional changes in genes broadly associated with synaptic communication, GPCR-mediated signalling, and sensory perception, including phototransduction pathways. However, none of these GO terms were statistically significant in the over-representation analysis. Regardless, even this statistically underpowered result could be biologically meaningful, given the limitation of annotation depth in *D. magna* (Chaturvedi et al., 2023).

Suggestive GRN

The suggestive GRN was reconstructed by integrating chromatin accessibility data from ATAC-seq with gene expression profiles from RNA-seq. TF binding sites (TFBS) were mapped within open chromatin regions across three distinct regulatory regions: promoter, proximal and distal. Candidate TFs were identified by BLASTp alignment of DEG protein sequences against a curated TF database, enabling assignment of TF domain homology to differentially expressed genes.

The full, unfiltered GRN contains 674 nodes (Fig. S27). Within this network, two hub TFs show exceptionally high connectivity: FOXL1/FOXI1/FOXS1 (Hub 1) with 917 edges, and ftz/HOXC13 (Hub 2) with 253 edges. Both hubs are themselves differentially expressed under fish kairomone exposure, making them biologically relevant entry points into the broader regulatory landscape.

To focus on the most interpretable regulatory interactions, the network was filtered to retain only these hub genes that were themselves differentially expressed. Target genes were subsequently filtered to include only those containing TF-binding motifs in their promoter regions and showing differential expression under fish kairomone exposure. The resulting putative GRN consists of 17 nodes and 22 edges, representing a hierarchical view of transcription factors controlling the DVM response (Fig. 20). GO term annotations for each node are provided in Table S17.

The target genes of Hub 2 completely overlap with a subset of those regulated by Hub 1. Under fish-exposed condition, Hub 1 is downregulated, while Hub 2 is upregulated, creating opposing regulatory inputs onto shared targets. For example, *SP5* is repressed by Hub 1 and activated by Hub 2, because downregulation of the repression and upregulation of activational TF, it results in the upregulation of *SP5.* Alternatively, a reverse pattern can be seen for *Dorsal/NF-kB*.

Although the 15 target genes are differentially expressed and carry TF domain homology, no further downstream genes were identified within the filtered network. Relaxing the false discovery rate (FDR) in the raw data revealed eight possible downstream targets of SP5, none of which were differentially expressed.

One GWAS hit (OUZ56_001155) identified in the delta speed phenotype, shared overlapping TFBS motifs with the curated TF database, matching the Q9W268_DROME protein, also known as defective proboscis extension (dve) in *Drosophila melanogaster.* This gene showed no structural or regulatory interactions with any of node in either the filtered or raw GRN, and is therefore represented as an isolated independent node in Fig. 20 (orange diamond).

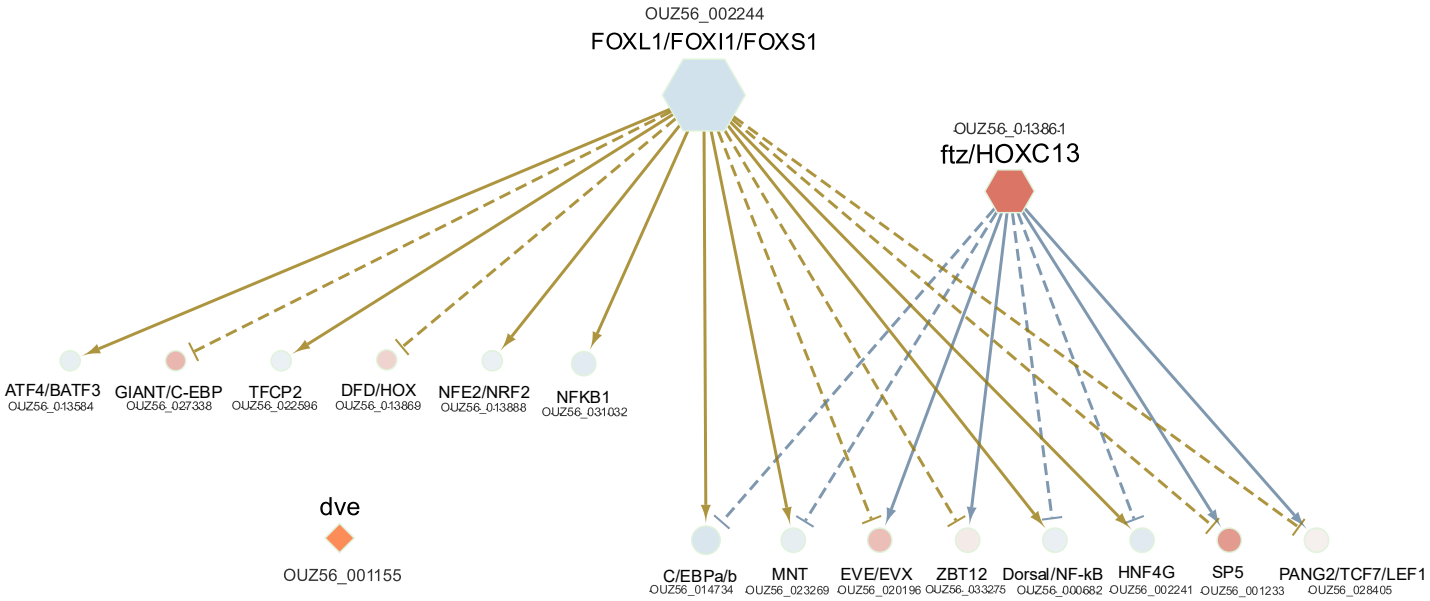


Figure 20: Graphical representation of a putative GRN where two hub genes (hexagons) and their downstream targets (circles). The GWAS hit which also had TF motifs is displayed as a diamond. The interactions between the genes are shown by full lines with arrowhead for activation and dashed line with T end for repression. The nodes are coloured based on their differential expression levels, blue – red gradient based on their logfc. Interactions out of the hubs is shown in different colour to distinguish them easier from each other. Names of the hubs are based on homology of TFs, their corresponding gene names are also shown beneath.

Discussion:

1. Change in phototactic behaviour (objectives 1 and 2)

1.1 Validation of the experimental setup

To see whether the experimental setup produced reliable phototactic data, three clones with well documented phototactic responses upon fish kairomone exposure were included as a proof of concept: C1242 (constitutive positive phototaxis), P_{132},85 (phenotypically plastic), and P_{132},96 (constitutive negative phototaxis). All three responded consistently with previously described behaviour (Pauwels et al., 2005). C1242 maintained a higher vertical position (closer to the surface) under both conditions, P_{132},96 remained near the bottom regardless of the fish kairomone exposure, and P_{132},85 showed a significant downward shift in vertical position and phototactic index upon fish kairomone exposure (Figs. 6 and 7). The use of phototactic index as a metric for phototaxis provided a more resilient metric for phototactic behaviour. Not all daphnids showed a similar behavioural response upon exposure to fish kairomones, despite sharing a common genotype. This individuality in behaviour can be attributed to ontogenetic development and individual consistency (Heuschele et al., 2017). To control for the maternal effects as best as possible, only the second brood was considered for the phenotype experiment. This controls as much as possible for the differences in ontogenetic development.

1.2 Phototactic responses across population types

The phototactic responses observed across GWAS population types were contrary to expected classical predator-avoidance behaviour. Populations with a history of fish predation (A_F, NA_F) were expected to respond to fish kairomones by altering their position towards deeper parts of the arena, a well-documented inducible defence mediated by negative phototaxis (Cousyn et al., 2001; De Meester, 1993). Instead the fish-exposed population types showed no significant shift in mean vertical position or phototactic index upon fish kairomone exposure. The fishless populations (A_NF and NA_NF) responded differently by becoming more phototactic upon fish kairomone exposure, with the NA_NF population type significantly altering its mean vertical position and phototactic index. This is the exact opposite of the expected response. Possible explanations for these observed unexpected patterns are explored below.

1.3 The absence of response in fish-exposed populations

The most plausible explanation is the experimental setup, which was used for the first time in this study. It is similar to others, using a top light structure, however, earlier setups like Cousyn et al. (2001) and De Meester (1993) used halogen light source whereas we used LED lights. With this, Bedrossiantz et al. (2021) showed that a light intensity too high produced less contrasting phototactic responses between fish-kairomone exposed conditions, suggesting that possibly the light source used here was too bright to produce sufficient contrasting phenotypes between conditions.

A second explanation concerns defence trade-offs. A lack of behavioural change upon fish kairomone exposure may reflect investment in alternative defence strategies, such as morphological or life history traits, rather than behavioural plasticity (Boersma et al., 1998). Behavioural changes in response to fish kairomones are known to occur in about 13 hours time, however morphological changes are expected to take longer exposure time and may only be induced during specific juvenile stages (De Meester & Cousyn, 1997). As the *D. magna* in this study were first exposed after five days of development, prior fish-exposed populations may have relied more strongly on constitutive morphological or life history defences. However because this study did not account for life history traits, this cannot be stated with certainty. It provides useful insight and a possible consideration for future studies.

The absence of a consistent response in the population types with prior fish-exposure might be due to the diversity of the plasticity between the clones (Figs. S3-7). Clones from different ponds were grouped together, while possibly experiencing different levels of predation pressure in their pond of origin. Selection on phototactic behaviour was likely not uniform across the different ponds, causing the standing genetic variation as well as variation in the response to fish to result in an inconsistent pattern in response to fish kairomones.

Phototactic behaviour is shown to shift rapidly under changing predation pressure while retaining considerable genetic variation (Cousyn et al., 2001; Landy et al., 2020). This pattern is also reflected in the distribution of the causal SNP in locus VPC1 across ponds (Fig. 13D).

A last contributing factor may be the effect of pesticide runoff on the chemosensory system of *Daphnia* from agriculturally exposed ponds (A_F and A_NF). Chemical detection of fish kairomones depends on the chemosensory system and is essential for triggering an appropriate phototactic response (Weiss, 2019). Agricultural runoff is shown to affect the chemically-mediated avoidance behaviour in *Daphnia* (López-Valcárcel et al., 2025) suggesting that the chemosensory system is likely to be involved. However it is unclear whether this extends to biotic chemical cues such as fish kairomones. This is a more speculative but plausible contributing factor to the absence of response in the agriculturally exposed populations.

1.4 Paradoxical upward shift in fish-naïve populations

The upward shift in phototactic index observed in fishless populations (A_NF and NA_NF) under fish kairomone exposure is one of the more surprising patterns seen in our data. Since it is the exact opposite of the classical predator avoidance prediction. However, this surprising result has previously been found by a study investigating the multiple predator defence strategies in *Daphnia pulex* (Boeing et al., 2006). The study found that clonal lines originating from habitats lacking fish frequently displayed unexpected upward migration when exposed to fish kairomones, whereas clones from habitats where fish naturally co-occur migrated downward (Boeing et al., 2006). This may suggest that *Daphnia* populations without prior exposure to fish predation do not exhibit an adaptive antipredator response to unfamiliar predator cues. When animals first come into contact with a new environment, the plastic response observed are often non-adaptive or even maladaptive because selection has not had the chance to work on it (Ghalambor et al., 2007). Landy et al. (2020) further demonstrated that ancestral *Daphnia* populations have extensive standing genetic variation in plasticity, including maladaptive plastic responses that move phenotypes away from the predator-adapted optimum (Lalejini et al., 2021). Which might explain the fact that fish-naïve *Daphnia* do not react according to expectations, because for them the presence of FK is a new environment, which they are not yet adapted to. An additional explanation is that surface waters typically offer warmer temperatures and greater food availability. The upward movement may therefore reflect a foraging response that increases energy intake and reproduction in the absence of an established antipredator response.

DVM is generally considered a costly strategy. Spending time in deeper, darker waters during the day reduces metabolic activity and reproductive output (Loose & Dawidowicz, 1994), while also limiting foraging time. Furthermore, energy obtained from feeding is increasingly allocated to swimming rather than reproduction. Together, these costs can reduce overall fitness (De Meester et al., 1999; S. Dodson, 1990; Loose & Dawidowicz, 1994). In environments without fish predation expressing DVM is non-beneficial and does not contribute to fitness, making it maladaptive. It is therefore likely that the upward phototactic shift observed reflects a non-adaptive plastic response. Fish kairomones represent a novel cue for these populations, and without historical fish-mediated selection, the behavioural machinery required for displaying a fish mediated DVM response has not been shaped by selection in their pond of origin.

2. Change in swimming kinematics (objectives 1 and 2)

2.1 Swimming speed and distance travelled

A significant reduction in swimming speed was observed in fish-naïve clones (Fig. 8). Such shift may reflect a general increase in caution in response to an unfamiliar stressor. A decrease in swimming speed is more metabolically efficient (Hinch & Rand, 2011), which might help with the reallocation of this energy to alternative defence traits (Jeschke et al., 2008). In contrast the non-significant change in *Daphnia* with prior fish exposure could be linked to its escape behaviour. Brewer et al. (1999) showed that the average swimming speed is not significantly altered when exposed to fish kairomone, because this would increase their metabolic rate. Whereas their alertness and escape speed was increased when exposed to fish kairomones, which could explain the lack of significance in these populations.

The absolute swimming speed recorded here (5.5-6.5mm/s) were substantially lower that the approximately 15 mm/s reported by Langer et al. (2019) for *D. magna.* This difference likely reflects differences in experimental setup rather than a biological inconsistency. Langer et al. used a three-dimensional tracking arena (20 x 20 x 85 cm) that captured movement in all directions, whereas this thesis used a narrow arena (3.1 x 13.8 x 25 cm) in which movement was quantified in two dimensions. The limited width of the arena constrained movement along the third axis, meaning most tracked locomotion occurred in the vertical and horizontal plane. This likely contributes to the lower swimming speeds observed in this thesis.

Distance travelled showed a similar pattern to swimming speed (Fig. 10). NA_NF clones travelled significantly shorter distances under FK exposure ($p < 0.01$), whereas no significant changes were observed in the other population types. Fish-exposed populations again showed a slight increase in movement. The consistency between swimming speed and distance travelled strengthens the conclusion that the reduction in locomotory activity observed in NA_NF clones represents a genuine behavioural response to fish kairomones rather than a measurement artefact, as two complementary metrics show at same pattern.

2.2 Nearest neighbour distance

Nearest neighbour distance (NND) showed no statistically significant response to FK exposure in any population type. Directional trends, however, were consistent with previous findings in speed and distance travelled. Fish-exposed types (A_F, NA_F) showed a slight increase in NND, while fish-naïve types (A_NF, NA_NF) showed a slight decrease (Fig. 11). The expected response from literature is an increase in NND under FK exposure (Langer et al., 2019), which was only directionally supported in fish-exposed groups. The decrease in NND in fish-naïve groups is more likely to be a consequence of reduced locomotor activity than an active aggregation response. Animals moving less in a confined area will naturally remain closer to their initial position and to one another.

2.3 Overall behavioural change and interclonal variation

Across all behavioural metrics examined (phototactic index, mean vertical position, swimming speed, distance travelled, and nearest neighbour distance) the most consistent and statistically significant FK-induced responses were observed in fish-naïve conditions, particularly NA_NF. Fish-exposed populations (A_F, NA_F) showed practically no plastic responses upon FK exposure, which is contrary to expectation. It was expected that these clones would show a lower baseline vertical position and a more pronounced plastic response (Cousyn et al., 2001). The findings that fish-naïve population types respond in shifting upwards is in line with findings by Boeing et al. (2006). Which might suggest that the absence of fish predation has an effect on the preferred behaviour expressed in these populations.

A key factor underlying the inconsistency of responses across population types is the high degree of inter-clonal variation within ponds, visible in the allele frequency distribution across ponds (Fig. 13D) and in the variation of mean vertical position under control conditions between ponds of the same type. A study investigating the responses to invertebrate kairomones (*Chaoborus*) suggested that the observed inconsistency might be because of genetic diversity in induced behaviour within the population (Oram & Spitze, 2013). This study considers 98 clones from 20 ponds, which is a substantially larger scale than conventional studies, using only a handful of clones. While it provides a more representative picture of phenotypic diversity in *Daphnia* responses to fish kairomones, it also increases complexity of population level interpretation. The four population type groupings capture ecologically meaningful variation in fish and agricultural exposure, but cannot fully account for the clonal diversity within each group. Which is likely to contribute to the absence of consistent response in fish-exposed population types. As for intra-clonal, the experiments were limited to 3 replicates per clone per condition, which allowed us to work with 98 clones in total, but at the same time made it difficult for statistical reproducibility especially in behaviour, which inherently is a very variable and dependent trait to observe.

3. GWAS (objective 3)

3.1 Sample size and statistical power

A sample size of 101 clones (98 C1-clones and 3 pilot-clones) allowed for genomic investigation of the observed phenotypes through a GWAS on vertical position and swimming speed. However, this sample size is on the lower end of for GWAS, which typically require hundreds to thousands of individuals. Such large sample sizes are more common in human studies, where funding for whole genome sequencing is considerably greater than in non-model organisms. Although 400 whole genome sequences are available for *D. magna*, time constraints and practical feasibility led us to aim for 100 clones with 3 replicates per condition, to ensure a reliable phenotype estimate for each genotype. This resulted in 630 samples (including pilot clones), each consisting of 6-7 tracked *Daphnia*, meaning the phenotype per genotype represents the mean of 18-21 individuals sharing the same genotype. In total 4346 *Daphnia* were tracked, representing 101 genomes.

3.2 Population stratification and genomic inflation

Since the sampled *Daphnia* originate from 20 different ponds, population stratification was accounted for using a kinship matrix and principal component analysis (PCA). Despite this, the first 4 PC axes together explained only 11.41% of the genetic variance associated with pond of origin. *Daphnia* from the same pond are expected to be more genetically similar to one another than to individuals from a different pond, and given that *Daphnia* reproduce primarily clonally, genetic similarity within populations is expected to be high. These factors likely both contribute to the elevated genomic inflation factor observed in the GWAS of vertical position ($\lambda = 1.124$). Ideally λ approaches 1, indicating full control for population stratification. The residual inflation seen here likely reflects two interacting sources. First, the use of 4 PC axes may provide incomplete correction for underlying population structure, as residual stratification is commonly observed even after PC-based correction, particularly when fine-scale or recent population history is not fully captured by the PCs (A. L. Price et al., 2010; Zaidi & Mathieson, 2020). Second, the relatively small sample size reduces statistical power and increases the uncertainty in effect size estimates, making it harder to detect polygenic signals (Yang et al., 2011). Methods to test for these factors have been developed, but they require substantially larger sample sizes. Minor allele frequency is also an important consideration, although not explicitly filtered for, GEMMA excludes alleles with frequencies below 0.01 by default.

3.3 Vertical position in the control condition

The GWAS of vertical position in the control condition revealed a significant peak on Scaffold 9 (Fig. 13A). The associated SNP had an allele frequency of 0.26, which supports it as a true finding, and not an artefact driven by a rare, population-specific variant. Since GWAS peaks do not pinpoint single causal SNPs, but rather implicates a genomic region associated with the trait (Korte & Farlow, 2013). BLAST analysis of the protein sequences of the significant and suggestive SNPs allowed us to infer biological function based on sequence conservation.

The top hit, locus VPC1, falls within an exon of gene OUZ56_029317, whose best BLAST match is the BCRH2 opsin-like protein in *D. magna*. Opsins are key components of the visual phototransduction pathway and have been implicated in regulation of light-dependent behaviours (Randel & Jékely, 2016). In Antarctic krill (*Euphausia superba*), a pelagic crustacean that performs diel vertical migration behaviour (Cresswell et al., 2009), homologous Rh1-like opsins show strong diurnal expression patterns and have been proposed to contribute to the perception of environmental light cues that synchronize daily behavioural rhythms (De Pittà et al., 2013). Given that DVM is driven primarily by light intensity changes (Ringelberg, 1999), an opsin-like gene is a biologically plausible candidate for baseline vertical positioning.

The BCRH2 opsin was first characterized in the crab *Hemigrapsus sanguineus* with a spectral sensitivity peak of approximately 480nm (Sakamoto et al., 1996). This wavelength falls within the blue-green range that penetrates deepest in freshwater environments, suggesting that a BCRH2-like opsin may be suited for detecting subtle light gradients that trigger vertical migration. Variation in this locus may therefore reflect differences in light sensitivity among clones, which might contribute to the observed clonal variation in vertical positioning.

D. magna has around 32 opsins, this great variety of different opsins is hypothesized to capture the large variation of light intensity experienced by *Daphnia* (Brandon et al., 2017). The VPC1 SNP itself was found to be a synonymous mutation. However, there were additional SNPs present in the neighbouring regions of locus VPC1, which could influence the structure of the protein (Fig. 13B). Despite this, VPC1 alone explains only 5.85% of variance in the mean vertical position, suggesting that other genes contribute to the trait. While it was found that if clones had the homozygote mutation, their mean vertical position was significantly lower than those with homozygote reference or heterozygote (Fig. 13C). No clear pattern emerged when the ponds were ranked based on their mean vertical position with the accompanying allele distribution. These observations suggest that while VPC1 is a meaningful contributor, vertical position is likely to be influenced by other genes as well.

The second significant SNP on locus VPC2, located within 5kb of Sec23/Sec24 vesicle transport locus, likely represents a passenger signal driven by linkage disequilibrium (LD) rather than an independent functional association. Physically proximal loci tend to be co-inherited (McManus et al., 2023), this most likely tags along the VPC1 locus. However, it remains possible that this intergenic SNP has a cis-regulatory function. Non-coding variants situated within flanking regions can act as distal enhancers or insulators (Maurano et al., 2012), meaning this locus could actively modulate the transcriptional efficiency or chromatin accessibility of the adjacent opsin gene rather than functioning as a purely neutral marker.

3.4 Vertical position under fish kairomone exposure

The drop from genome-wide significance to suggestive level of the opsin-like locus in the FK-exposed condition may reflect a gene-by-environment (GxE) interaction (Chari & Dworkin, 2013), where the genetic effect of this locus on vertical positioning is partially modified in the presence of predator cues. Rather than stating that the effect of this locus is not present in kairomone exposed conditions, its effect is likely dependent on environment and other interacting loci (Saltz et al., 2018).

The absence of additional significant hits in the FK-exposed condition may additionally reflect insufficient statistical power to detect polygenic effects on a behaviourally complex response. Especially considering the modest sample size of 101 genotypes. Increasing sample size and further refinement of the experimental setup would improve power to identify the genetic basis of predator-induced behavioural plasticity. By increasing a sample size in GWAS, it is possible to elevate SNPs identified in the suggestive level significance to genome-wide significance level (Hammond et al., 2021).

3.5 Plasticity of vertical position

For the GWAS performed on the plasticity phenotype of vertical position, no significant peaks were identified. Strikingly however, five suggestive hits fell within the same gene, OUZ56_013436, either within exon or intron regions. BLAST analysis identified this gene as a NFX1 zinc-finger containing protein 1 isoform X2 in *D. magna* (Table S18). NFX1 is primarily known as an antiviral defence protein involved in immune homeostasis, which makes it an odd candidate for regulation of plasticity. However, NFX1-type proteins do retain DNA-binding capacity through their zinc finger domain. Zinc-finger proteins more broadly are known to interact with RNA and DNA modifying the gene expression (Klug, 1999). Variation in this locus could influence the magnitude of the transcriptional response to fish kairomones, contributing to the variation seen DVM plasticity. Given that these hits remain at the suggestive threshold, a causal role for this locus cannot be established with confidence. Increasing sample size would improve statistical power and may resolve whether this association is a true underlying signal.

3.6 Swimming speed plasticity

GWAS on the plasticity in speed identified three significant SNPS of which only one fell within a gene (OUZ56_008941). This gene encodes a conserved C2H2 zinc-finger TF homologous to Rotund (RN). Rotund-family proteins function as developmental transcriptional regulators controlling downstream gene expression programs (Seetharam et al., 2010), and Rotund has specifically been shown to be important for the development of the olfactory system and antenna patterning of *Drosophila* (Q. Li et al., 2015). The chemosensory system of *Daphnia* is located within the antennules, identified as the primary site of fish kairomone detection (Graeve et al., 2026). Variation in OUZ56_008941 may therefore influence behavioural plasticity indirectly, through transcriptional control of sensory development or function in the antennules.

3.7 Overall evaluation and future directions

Overall, the GWAS on vertical position in the control condition yielded a compelling result, with a significant peak within an opsin-like gene that provides a biologically defendable candidate for the genetic basis of light-dependent vertical positioning in *D. magna*. This finding demonstrates that even with a modest sample size of 101 genotypes, GWAS can identify meaningful associations for well-expressed behavioural traits with a reliable consistency in phenotype. However, the lack of pronounced phenotypic responses found in the phenotypic experiments limited the power to detect genetic associations underlying plasticity between conditions. Plasticity phenotypes, derived as differences between conditions, might be less reliable than a single measurement in the conditions, which makes it harder to find the genetic basis of the trait (Craddock et al., 2009). Although the suggestive hits identified for plasticity phenotypes, particularly the clustering of five SNPs within a single NFX1-type protein, are encouraging for future study. This suggests that larger sample size and a more consistent predator-induced response may reveal the genetic basis of plasticity. Expanding the sample size to include the full 400 genomes logical next step for future research.

4. Differential gene expression and GRN (objective 4 & 5)

The RNA-seq analysis of clone P_{132},85 identified 701 differentially expressed genes, with more down (415) than upregulated (286) genes. GO overrepresentation analysis revealed significant enrichment in mitochondrial energy metabolism, including the TCA-cycle and ATP metabolic processes, indicating a broad suppression of energy production. This is consistent with the reduction in swimming speed observed under fish kairomone exposure (Langer et al., 2019), as reduced mitochondrial function would limit energy availability for sustained locomotion. This metabolic suppression may reflect the energetic demands of the acute predator response, including the activation of signalling cascades and early transcriptional reprogramming that precede the morphological and life history adjustments observed over longer exposure windows in *Daphnia* (Boersma et al., 1998; Graeve et al., 2026).

KEGG GSEA provided further support for this pattern (Fig. 18), with all gene sets showing negative normalised enrichment scores, suggesting uniform suppression. Alpha-amylase was one of the most connected hubs, with seven associated genes, suggesting suppression of digestive carbohydrate metabolism as a part of the broader metabolic downregulation (Janeček et al., 2013). Another significantly suppressed pathway is myosin V, an organelle and vesicle transporter (Donovan & Bretscher, 2012).

A notable limitation of KEGG pathway annotation via EggNOG orthology is that the biological functions are inferred from sequence similarity to characterized genes in model organisms rather than experimentally validated in *Daphnia*. For instance, the kallikrein 8 network is specific to mammals (Hecker et al., 2017), however the broader serine peptidase it represents may be functionally conserved, as serine protease expression has been shown to increase to meet higher metabolic demands *D. pulex* (Dölling et al., 2016). Notably, the kallikrein 8 cluster (Fig. 19) was almost entirely downregulated, except for one gene, suggesting a counter regulatory response in an otherwise suppressed pathway. Indicating that the function of serine protease activity might still be important under fish kairomone exposure.

4.1 Overlap with kairomone-relevant signalling pathways

Comparison of DEGs against a set of GO terms associated with signalling pathways previously implicated in kairomone-induced responses in *Daphnia* (Table S16; (Miyakawa et al., 2015; Weiss et al., 2012) revealed overlap with neurological processes linked to synaptic signalling, locomotory behaviour, GPCR activity, and ligand-gated ion channel activity. In addition, DEGs overlapped with GO terms involved in light perception and processing, including phototransduction, GPCR-coupled opsin signalling and detection of light signal.

Despite not being enriched, overlap with these GO terms suggests that these pathways are likely involved in the fish kairomone response. Synaptic signalling is crucial for the neurological differences expected upon kairomone exposure (Weiss, 2019; Weiss et al., 2012). Additionally, ligand gated ionotropic channels have been shown to be important for the perception of fish kairomones, becoming differentially expressed under exposure (Graeve et al., 2026), which was also found in our analysis. The differential expression of genes involved in locomotory behaviour was consistent with previous findings that *D. magna* becomes significantly slower when exposed to fish kairomones (Langer et al., 2019). The differential expression within genes coupled with phototransduction, integration of light signal, and GPCR-coupled opsin signalling further suggest that light is an important factor and that opsin-like proteins are responsible for the response to light (Ringelberg, 1999; Weiss, 2019). This interpretation is further supported by the GWAS results for baseline vertical position, where the VPC1 locus showed homology to the crustacean opsin BCRH2. Suggesting a possible role for light perception in determining vertical positioning behaviour.

Despite previous studies linking fish kairomone exposure and GABAergic, cholinergic and dopaminergic signalling (Miyakawa et al., 2015; Weiss et al., 2012), no overlap was found with these specific GO terms. This may reflect an annotation gap, because the assigned GO terms were more general, including neurological signalling, synaptic signalling, etc. This limitation is mainly due to the fact that chemoreceptor identification in *Daphnia* largely relied on sequence homology with other arthropods, with few direct validation studies (Weiss, 2019). Nevertheless, the overlap with phototransduction terms is interesting, as light is the primary environmental variable driving fish-induced DVM in *Daphnia* (Ringelberg, 1999; Weiss, 2019). Transcriptional changes within these opsin-related genes may reflect modulation of the light-sensitivity component of the DVM response. A finding in line with the VPC1 GWAS signal discussed above.

4.2 ATAC-seq chromatin accessibility

The chromatin accessibility primarily provided a way identify the edges of the GRN to see which regions containing a TF binding site were accessible. Since ATAC-seq is relatively novel in *D. magna*, this study used consensus peaks instead of clear separated view of chromatin accessibility in control and fish kairomone-exposed conditions. A consensus approach pools signal across conditions to maximise peak detection sensitivity, but at the cost of condition specific accessibility. In future studies this condition specific view of chromatin accessibility might provide interesting insights into the changes upon fish kairomone exposure.

4.3 Putative GRN

The putative GRN was constructed from differentially expressed genes, and consists of two hubs with 15 downstream nodes, all of which are DEGs. All nodes additionally showed TF homology, indicating that they are likely TFs themselves.

The primary hub show homology with FOXL1, FOXI1, and FOXS1, all members of the Forkhead (FOX) family of TFs, which regulate genes involved in cell growth, differentiation, and longevity in arthropods. In *D. melanogaster*, FOXL1 is expressed in the musculature and plays an important role in organ placement during development. Of this family, only FOXL1 has been characterized in *D. magna* (Schomburg et al., 2022), and the function of FOX genes in *Daphnia* and other crustaceans more broadly remains largely understudied. The second hub shows homology with FTZ and HOXC: FTZ is important for the neurogenesis in *Drosophila* (Doe et al., 1988), while HOXC genes are regulate anterior-posterior axis development in vertebrates (Min et al., 2013).

The functional homologies of both hubs suggest that musculature and neurological signalling are relevant to the *Daphnia* response to fish kairomones (D. H. Kim et al., 2018; Nicolini et al., 2023). The downregulation of the primary FOX hub is consistent with a reallocation of energy away from muscular maintenance, which aligns with the broader metabolic suppression observed in the RNA-seq data and the hypothesis that energy is redirected towards other inducible traits, like morphological changes (Boersma et al., 1998). The upregulation of the secondary FTZ/HOXC hub, implicated in neurogenesis in *Drosophila,* is consistent with the hypothesis that neurological changes play a role in the behavioural response to fish kairomones, consistent with previous findings in *Daphnia* (Weiss et al., 2012). It should be noted, however, that these functional inferences are based on homology with *Drosophila*, and direct experimental validation in *Daphnia* is lacking (D. H. Kim et al., 2018; Nicolini et al., 2023).

The downstream genes from both hubs were themselves TFs, though no further differentially expressed genes were identified beyond this level. When including non-differentially expressed genes, eight downstream genes were found beneath node SP5. SP5 is a homolog of *btd* in *Drosophila*, where it is important for patterning and formation of the anterior region, with expression in the central and peripheral nervous system during later embryogenesis (Schaeper et al., 2010), suggesting a possible role in neuronal development in *Daphnia*. The GWAS hit associated with absolute speed difference also showed TF homology, with *dve* (defective proventriculus) protein. However, BLAST alignment identified this sequence as a ubiquitin carboxyl-terminal hydrolase 36 isoform X4, which has no known TF function. The remaining BLAST hits returned uncharacterised proteins in *D. magna*, leaving open the possibility that this locus encodes a TF not yet described in *Daphnia* (Table S18).

A key limitation of this analysis concerns the completeness of TF assignment. Candidate TFs were identified by BLASTp alignment of DEG protein sequences against a curated TF binding motif database spanning human, C. elegans, plant, fungal and *Drosophila* references. While this broad taxonomic coverage maximizes motif detections, the match rate is incomplete. *Daphnia* TFs are poorly annotated, and their binding motifs are largely absent from existing databases, meaning that functionally relevant TFs may go undetected. Functional inference is further complicated by the phylogenetic distance between *Daphnia* and the model organisms mostly present in reference database. This limits the assignment of highly specific GO terms derived from *Drosophila* or vertebrates to *Daphnia* genes. Despite these constraints, the TFs identified here through both GWAS and GRN analyses represent putative regulators with homology to genes implicated in neurological signalling and behavioural responses to kairomone exposure. As such these findings are meaningful candidates for further functional investigation.

Taken together, the results from differential gene expression, pathway analysis, and GRN inference all point to a metabolic suppression under fish kairomone exposure, accompanied by transcriptional changes in potentially neurologically relevant genes. Homology-based inference contributes little to specific interpretations in *D. magna*, particularly for distantly related vertebrate systems such as HOX genes. Yet broad orthology relationships can still reveal general functional associations. The neurological implications of several GRN nodes in *Drosophila* are more informative given their closer phylogenetic relationship. The overlap of DEGs with phototransduction-related and ionotropic GO terms and the involvement of neurologically implicated TF together supports the hypothesis that neurological signalling plays a central role in integrating the DVM response in the presence of fish kairomones, consistent with previous research (Weiss et al., 2012).

In conclusion, my analyses identified several putative candidates involved in the response to fish kairomones. A natural next step would be functional validation of these candidates through RNAi-mediated knockdown, an approach shown to work in *Daphnia* through feeding (Schumpert et al., 2015) or microinjection (Toyota et al., 2016). Measuring the effects of such knockdowns on phototactic behaviour and vertical positioning would allow direct testing of whether the identified loci and TF nodes are involved in the fish kairomone response. Along with this, qPCR quantification of opsin gene expression across light-dark cycle could reveal whether the cyclical diurnal expression patterns observed in opsins of *Euphausia superba* (De Pittà et al., 2013) are conserved in *Daphnia*. If opsin expression in *D. magna* follows a similar rhythmic pattern, this would strengthen the case for light-perception mechanism underlying DVM. Gene editing experiments targeting the VPC1 opsin gene could further test whether and which mutations can shift vertical positioning behaviour, providing a functional link between GWAS signal and observed phenotype.

Conclusion and future perspective

In this thesis, behavioural assays were performed on 98 *D. magna* clones originating from 20 Flemish ponds, and three well-documented pilot clones, to characterize variation in phototactic behaviour and responses to fish kairomone exposure. At the metapopulation level, fish kairomones did not induce a significant overall shift in phototactic behaviour or locomotory traits. However, when considering evolutionary history, clones with no prior fish predation exposure (NA_NF) responded significantly to fish kairomones by becoming more phototactic and reducing swimming speed. Which suggests that the absence of fish predation causes an opposite response to fish kairomones than expected.

These behavioural phenotypes were used as the basis for a genome-wide association study across 101 *D. magna* clones, investigating both the genomic associations of baseline behaviour and the genotype-by-environment (GxE) interaction underlying plasticity. A genome-wide significant locus, VPC1, was identified for vertical positioning in the control condition. This showed homology to a BCRH2 opsin-like protein, implicating light perception in the regulation of vertical positioning. GWAS on plasticity of vertical positioning did not identify significant loci, though five suggestive SNPs were identified within a ZNFX1-type zinc-finger gene. The plasticity of speed did find a significant associated SNP, a C2H2 zinc-finger TF homologous to Rotund protein.

Differential gene expression of publicly available RNA-dataset identified 701 differentially expressed genes in response to fish kairomone exposure. GO overrepresentation and KEGG pathway analyses showed broad suppression of mitochondrial energy metabolism and associated energy consuming processes. Integration of RNA-seq with ATAC-seq data enabled reconstruction of a putative GRN, identifying two TF hubs with homology to FOX family genes and FTZ/HOXC genes respectively, linking musculature-related and neurogenic regulatory programs to the kairomone response.

Further expansion of the sample size to the full set of 400 clones would be an interesting move to further investigate whether the suggestive hits reach significant levels. Functional genomics of VPC1 locus through RNAi would allow direct testing whether the gene contributes to the vertical positioning. Repeating ATAC-seq to investigate the condition dependent chromatin accessibility would show how it changes upon fish kairomone exposure, providing additional insight. Finally, the qPCR quantification of opsin expression across light-dark cycle could test whether the diurnal expression of other crustacean opsins is conserved in *D. magna* and overexpression experiments could directly show if expression levels are linked to observed phototactic behaviour.

Use of generative AI

Generative artificial intelligence (AI) tools (Claude, ChatGPT) have been used in this thesis to improve text flow, clarity, and overall reading fluency. It was also used to help improve R and Python code. These tools were not used to generate scientific content, conduct analyses, interpret results, or formulate conclusions.

Bibliography

aaronkiggen/daphnia-ATAC-pipeline. (n.d.). Retrieved June 3, 2026, from https://github.com/aaronkiggen/daphnia-ATAC-pipeline

Balloux, F., Lehmann, L., & De Meeûs, T. (2003). The population genetics of clonal and partially clonal diploids. *Genetics*, *164*(4), 1635–1644. https://doi.org/10.1093/GENETICS/164.4.1635

Barabási, A. L., & Oltvai, Z. N. (2004). Network biology: understanding the cell's functional organization. *Nature Reviews Genetics 2004 5:2*, *5*(2), 101–113. https://doi.org/10.1038/nrg1272

Barbasch, T. A., Abuwa, V. I., Carswell, B., & Bell, A. M. (2024). Managing the tradeoff between reproduction and survival requires flexibility in behaviour and gene regulation in three-spined stickleback. *Proceedings of the Royal Society B: Biological Sciences*, *291*(2036). https://doi.org/10.1098/rspb.2024.2296

Baudach, A., & Vilcinskas, A. (2021). The European Map Butterfly Araschnia levana as a Model to Study the Molecular Basis and Evolutionary Ecology of Seasonal Polyphenism. *Insects*, *12*(4). https://doi.org/10.3390/INSECTS12040325

Bedrossiantz, J., Fuertes, I., Raldua, D., & Barata, C. (2021). Pharmacological modulation of fish-induced depth selection in D. magna: the role of cholinergic and GABAergic signalling. *Scientific Reports 2021 11:1*, *11*(1), 19407-. https://doi.org/10.1038/s41598-021-98886-w

Beldade, P., Mateus, A. R. A., & Keller, R. A. (2011). Evolution and molecular mechanisms of adaptive developmental plasticity. *Molecular Ecology*, *20*(7), 1347–1363. https://doi.org/10.1111/J.1365-294X.2011.05016.X

Bellot, M., Gómez-Canela, C., & Barata, C. (2022). Phototactic behaviour and neurotransmitter profiles in two Daphnia magna clones: Vertical and horizontal responses to fish kairomones and psychotropic drugs. *Science of The Total Environment*, *830*, 154684. https://doi.org/10.1016/J.SCITOTENV.2022.154684

Bendesky, A., & Bargmann, C. I. (2011). Genetic contributions to behavioural diversity at the gene-environment interface. *Nature Reviews. Genetics*, *12*(12), 809–820. https://doi.org/10.1038/NRG3065

Boeing, W. J., Ramcharan, C. W., & Riessen, H. P. (2006). Multiple predator defence strategies in Daphnia pulex and their relation to native habitat. *Journal of Plankton Research*, *28*(6), 571–584. https://doi.org/10.1093/PLANKT/FBI142

Boersma, M., Spaak, P., & De Meester, L. (1998). Predator-mediated plasticity in morphology, life history, and behavior of Daphnia: the uncoupling of responses. *The American Naturalist*, *152*(2), 237–248. https://doi.org/10.1086/286164

Brandon, C. S., Greenwold, M. J., & Dudycha, J. L. (2017). Ancient and Recent Duplications Support Functional Diversity of Daphnia Opsins. *Journal of Molecular Evolution*, *84*(1), 12–28. https://doi.org/10.1007/S00239-016-9777-1/TABLES/2

Bravo González-Blas, C., De Winter, S., Hulselmans, G., Hecker, N., Matetovici, I., Christiaens, V., Poovathingal, S., Wouters, J., Aibar, S., & Aerts, S. (2023). SCENIC+: single-cell multiomic inference of enhancers and gene regulatory networks. *Nature Methods*, *20*(9), 1355–1367. https://doi.org/10.1038/s41592-023-01938-4

Brewer, M. C., Dawidowicz, P., & Dodson, S. I. (n.d.). *Interactive effects of fish kairomone and light on Daphnia escape behavior*.

Buenrostro, J. D., Giresi, P. G., Zaba, L. C., Chang, H. Y., & Greenleaf, W. J. (2013). Transposition of native chromatin for fast and sensitive epigenomic profiling of open chromatin, DNA-binding proteins and nucleosome position. *Nature Methods 2013 10:12*, *10*(12), 1213–1218. https://doi.org/10.1038/nmeth.2688

Buenrostro, J. D., Wu, B., Chang, H. Y., & Greenleaf, W. J. (2015). ATAC-seq: A Method for Assaying Chromatin Accessibility Genome-Wide. *Current Protocols in Molecular Biology*, *109*, 21.29.1-21.29.9. https://doi.org/10.1002/0471142727.MB2129S109

Carrillo, M. P., Piña, B., Vila-Costa, M., & Barata, C. (2025). Molecular mechanisms that regulate scopolamine effects on inducible fish antipredation responses in Daphnia magna. *Comparative Biochemistry and Physiology Part C: Toxicology & Pharmacology*, *289*, 110116. https://doi.org/10.1016/J.CBPC.2024.110116

Chang, J., Xu, Y., Fu, Y., Liu, J., Jiang, D., Pan, J., Ouyang, H., Liu, W., Xu, J., Tian, Y., Huang, Y., Ruan, J., & Shen, X. (2024). The dynamic landscape of chromatin accessibility and active regulatory elements in the mediobasal hypothalamus influences the seasonal activation of the reproductive axis in the male quail under long light exposure. *BMC Genomics*, *25*(1), 197. https://doi.org/10.1186/S12864-024-10097-5

Chari, S., & Dworkin, I. (2013). The Conditional Nature of Genetic Interactions: The Consequences of Wild-Type Backgrounds on Mutational Interactions in a Genome-Wide Modifier Screen. *PLOS Genetics*, *9*(8), e1003661. https://doi.org/10.1371/JOURNAL.PGEN.1003661

Chaturvedi, A., Li, X., Dhandapani, V., Marshall, H., Kissane, S., Cuenca-Cambronero, M., Asole, G., Calvet, F., Ruiz-Romero, M., Marangio, P., Guigó, R., Rago, D., Mirbahai, L., Eastwood, N., Colbourne, J. K., Zhou, J., Mallon, E., & Orsini, L. (2023). The hologenome of Daphnia magna reveals possible DNA methylation and microbiome-mediated evolution of the host genome. *Nucleic Acids Research*, *51*(18), 9785–9803. https://doi.org/10.1093/NAR/GKAD685

Chen, Z. L., Meng, J. M., Cao, Y., Yin, J. L., Fang, R. Q., Fan, S. B., Liu, C., Zeng, W. F., Ding, Y. H., Tan, D., Wu, L., Zhou, W. J., Chi, H., Sun, R. X., Dong, M. Q., & He, S. M. (2019). A high-speed search engine pLink 2 with systematic evaluation for proteome-scale identification of cross-linked peptides. *Nature Communications 2019 10:1*, *10*(1), 3404-. https://doi.org/10.1038/s41467-019-11337-z

Chevin, L. M., Leung, C., Le Rouzic, A., & Uller, T. (2022). Using phenotypic plasticity to understand the structure and evolution of the genotype–phenotype map. *Genetica*, *150*(3–4), 209–221. https://doi.org/10.1007/s10709-021-00135-5

Choi, T. J., Han, S. M., Malik, A., & Kim, C. B. (2023). Comparative transcriptome analysis of two Daphnia galeata genotypes displaying contrasting phenotypic variation induced by fish kairomones in the same environment of the Han River, Korea. *BMC Genomics*, *24*(1). https://doi.org/10.1186/S12864-023-09701-X

Colbourne, J. K., Pfrender, M. E., Gilbert, D., Thomas, W. K., Tucker, A., Oakley, T. H., Tokishita, S., Aerts, A., Arnold, G. J., Basu, M. K., Bauer, D. J., Cáceres, C. E., Carmel, L., Casola, C., Choi, J. H., Detter, J. C., Dong, Q., Dusheyko, S., Eads, B. D., … Boore, J. L. (2011). The Ecoresponsive Genome of Daphnia pulex. *Science (New York, N.Y.)*, *331*(6017), 555. https://doi.org/10.1126/SCIENCE.1197761

Corces, M. R., Trevino, A. E., Hamilton, E. G., Greenside, P. G., Sinnott-Armstrong, N. A., Vesuna, S., Satpathy, A. T., Rubin, A. J., Montine, K. S., Wu, B., Kathiria, A., Cho, S. W., Mumbach, M. R., Carter, A. C., Kasowski, M., Orloff, L. A., Risca, V. I., Kundaje, A., Khavari, P. A., … Chang, H. Y. (2017). An improved ATAC-seq protocol reduces background and enables interrogation of frozen tissues. *Nature Methods*, *14*(10), 959–962. https://doi.org/10.1038/NMETH.4396

Cousyn, C., De Meester, L., Colbourne, J. K., Brendonck, L., Verschuren, D., & Volckaert, F. (2001). Rapid, local adaptation of zooplankton behavior to changes in predation pressure in the absence of neutral genetic changes. *Proceedings of the National Academy of Sciences*, *98*(11), 6256–6260. https://doi.org/10.1073/pnas.111606798

Craddock, N., Kendler, K., Neale, M., Nurnberger, J., Purcell, S., Rietschel, M., Perlis, R., Santangelo, S. L., Schulze, T., Smoller, J. W., & Thapar, A. (2009). Dissecting the phenotype in genome-wide association studies of psychiatric illness. *The British Journal of Psychiatry : The Journal of Mental Science*, *195*(2), 97. https://doi.org/10.1192/BJP.BP.108.063156

Cresswell, K. A., Tarling, G. A., Thorpe, S. E., Burrows, M. T., Wiedenmann, J., & Mangel, M. (2009). Diel vertical migration of Antarctic krill (Euphausia superba) is flexible during advection across the Scotia Sea. *Journal of Plankton Research*, *31*(10), 1265–1281. https://doi.org/10.1093/PLANKT/FBP062

Crispo, E. (2007). The Baldwin effect and genetic assimilation: Revisiting two mechanisms of evolutionary change mediated by phenotypic plasticity. In *Evolution* (Vol. 61, Number 11, pp. 2469–2479). https://doi.org/10.1111/j.1558-5646.2007.00203.x

De Meester, L. (1993). Genotype, fish-mediated chemicals, and phototactic behavior in Daphnia magna. *Ecology*, *74*(5), 1467. https://kuleuven.e-bronnen.be/login?url=https://www.proquest.com/scholarly-journals/genotype-fish-mediated-chemicals-phototactic/docview/219002166/se-2?accountid=17215

De Meester, L. (1996). EVOLUTIONARY POTENTIAL AND LOCAL GENETIC DIFFERENTIATION IN A PHENOTYPICALLY PLASTIC TRAIT OF A CYCLICAL PARTHENOGEN, DAPHNIA MAGNA. *Evolution*, *50*(3), 1293–1298. https://doi.org/10.1111/j.1558-5646.1996.tb02369.x

De Meester, L., & Cousyn, C. (1997). The change in phototactic behaviour of a Daphnia magna clone in the presence of fish kairomones: The effect of exposure time. *Hydrobiologia*, *360*(1), 169–175. https://doi.org/10.1023/A:1003119827390/METRICS

De Meester, L., Dawidowicz, P., & Gool, E. (1999). Ecology and evolution of predator-induced behavior of zooplankton: Depth selection behavior and diel vertical migration. *The Ecology and Evolution of Inducible Defences*, 160–176.

De Pittà, C., Biscontin, A., Albiero, A., Sales, G., Millino, C., Mazzotta, G. M., Bertolucci, C., & Costa, R. (2013). The Antarctic Krill Euphausia superba Shows Diurnal Cycles of Transcription under Natural Conditions. *PLOS ONE*, *8*(7), e68652. https://doi.org/10.1371/JOURNAL.PONE.0068652

Decaestecker, E., Gaba, S., Raeymaekers, J. A. M., Stoks, R., Van Kerckhoven, L., Ebert, D., & De Meester, L. (2007). Host-parasite "Red Queen" dynamics archived in pond sediment. *Nature*, *450*(7171), 870–873. https://doi.org/10.1038/NATURE06291

Des Marais, D. L., Hernandez, K. M., & Juenger, T. E. (2013). Genotype-by-environment interaction and plasticity: Exploring genomic responses of plants to the abiotic environment. In *Annual Review of Ecology, Evolution, and Systematics* (Vol. 44, pp. 5–29). Annual Reviews Inc. https://doi.org/10.1146/annurev-ecolsys-110512-135806

Dingemanse, N. J., Kazem, A. J. N., Réale, D., & Wright, J. (2010). Behavioural reaction norms: animal personality meets individual plasticity. *Trends in Ecology & Evolution*, *25*(2), 81–89. https://doi.org/10.1016/J.TREE.2009.07.013

Dodson, S. (1990). Predicting diel vertical migration of zooplankton. *Limnology and Oceanography*, *35*(5), 1195–1200. https://doi.org/10.4319/LO.1990.35.5.1195

Dodson, S. I., Ryan, S., Tollrian, R., & Lampert, W. (1997). Individual swimming behavior of Daphnia: Effects of food, light and container size in four clones. *Journal of Plankton Research*, *19*(10), 1537–1552. https://doi.org/10.1093/PLANKT/19.10.1537

Doe, C. Q., Hiromi, Y., Gehring, W. J., & Goodman, C. S. (1988). Expression and function of the segmentation gene fushi tarazu during Drosophila neurogenesis. *Science (New York, N.Y.)*, *239*(4836), 170–175. https://doi.org/10.1126/SCIENCE.2892267

Dölling, R., Becker, D., Hawat, S., Koch, M., Schwarzenberger, A., & Zeis, B. (2016). Adjustments of serine proteases of Daphnia pulex in response to temperature changes. *Comparative Biochemistry and Physiology Part B: Biochemistry and Molecular Biology*, *194–195*, 1–10. https://doi.org/10.1016/J.CBPB.2016.01.001

Donovan, K. W., & Bretscher, A. (2012). Myosin-V is activated by binding secretory cargo and released in coordination with Rab/exocyst function. *Developmental Cell*, *23*(4), 769. https://doi.org/10.1016/J.DEVCEL.2012.09.001

Ebert, D. (2022). Daphnia as a versatile model system in ecology and evolution. *EvoDevo 2022 13:1*, *13*(1), 16-. https://doi.org/10.1186/S13227-022-00199-0

Falconer, D. S. . (1996). *Introduction to quantitative genetics*. Prentice Hall.

Ferreira, M. S., Alves, P. C., Callahan, C. M., Giska, I., Farelo, L., Jenny, H., Mills, L. S., Hackländer, K., Good, J. M., & Melo-Ferreira, J. (2020). Transcriptomic regulation of seasonal coat color change in hares. *Ecology and Evolution*, *10*(3), 1180. https://doi.org/10.1002/ECE3.5956

Ghalambor, C. K., McKay, J. K., Carroll, S. P., & Reznick, D. N. (2007). Adaptive versus non-adaptive phenotypic plasticity and the potential for contemporary adaptation in new environments. *Functional Ecology*, *21*(3), 394–407. https://doi.org/10.1111/J.1365-2435.2007.01283.X

Graeve, A., Huster, J., Mayweg, J., Fiedler, R., Plaßmann, J., Görl, D., Keilmann, A., Alev, S., Wahle, P., & Weiss, L. C. (2026). Predator cue detection in Daphnia involves ionotropic receptors IR25a and IR93a. *Proceedings of the Royal Society B: Biological Sciences*, *293*(2070). https://doi.org/10.1098/RSPB.2025.3283

Graeve, A., Ioannidou, I., Reinhard, J., Görl, D. M., Faissner, A., & Weiss, L. (2021). Brain volume increase and neuronal plasticity underly predator-induced morphological defense expression in Daphnia longicephala. *Scientific Reports 2021 11:1*, *11*(1), 12612-. https://doi.org/10.1038/s41598-021-92052-y

Gross, K., Pasinelli, G., & Kunc, H. P. (2010). Behavioral Plasticity Allows Short-Term Adjustment to a Novel Environment. *Https://Doi.Org/10.1086/655428*, *176*(4), 456–464. https://doi.org/10.1086/655428

Grunau, C., Augusto, R. de C., Rey, O., Cosseau, C., Chaparro, C., Vidal-Dupiol, J., Allienne, J. F., Duval, D., Pinaud, S., Tönges, S., Andriantsoa, R., Luquet, E., Aubret, F., Dia Sow, M., David, P., Thomson, V., Joly, D., Gomes Lima, M., Federico, D., … Minoda, A. (2021). A simple ATAC-seq protocol for population epigenetics. *Wellcome Open Research*, *5*, 121. https://doi.org/10.12688/WELLCOMEOPENRES.15552.2

Gusev, A., Mancuso, N., Won, H., Kousi, M., Finucane, H. K., Reshef, Y., Song, L., Safi, A., McCarroll, S., Neale, B. M., Ophoff, R. A., O'Donovan, M. C., Crawford, G. E., Geschwind, D. H., Katsanis, N., Sullivan, P. F., Pasaniuc, B., & Price, A. L. (2018). Transcriptome-wide association study of schizophrenia and chromatin activity yields mechanistic disease insights. *Nature Genetics*, *50*(4), 538–548. https://doi.org/10.1038/S41588-018-0092-1

Hahn, M., & von Elert, E. (2022). One Kairomone and Multiple Effects in Daphnia Species—5α-Cyprinol Sulfate Induces Morphological Defenses in the Invasive Species Daphnia lumholtzi. *Frontiers in Ecology and Evolution*, *10*, 804521. https://doi.org/10.3389/FEVO.2022.804521/TEXT

Hammond, R. K., Pahl, M. C., Su, C., Cousminer, D. L., Leonard, M. E., Lu, S., Doege, C. A., Wagley, Y., Hodge, K. M., Lasconi, C., Johnson, M. E., Pippin, J. A., Hankenson, K. D., Leibel, R. L., Chesi, A., Wells, A. D., & Grant, S. F. A. (2021). Biological constraints on GWAS SNPs at suggestive significance thresholds reveal additional BMI loci. *ELife*, *10*, 1–19. https://doi.org/10.7554/ELIFE.62206

Hecker, N., Sharma, V., & Hiller, M. (2017). Transition to an Aquatic Habitat Permitted the Repeated Loss of the Pleiotropic KLK8 Gene in Mammals. *Genome Biology and Evolution*, *9*(11), 3179. https://doi.org/10.1093/GBE/EVX239

Heinz, S., Benner, C., Spann, N., Bertolino, E., Lin, Y. C., Laslo, P., Cheng, J. X., Murre, C., Singh, H., & Glass, C. K. (2010). Simple combinations of lineage-determining transcription factors prime cis-regulatory elements required for macrophage and B cell identities. *Molecular Cell*, *38*(4), 576–589. https://doi.org/10.1016/J.MOLCEL.2010.05.004

Herman, J. J., & Sultan, S. E. (2011). Adaptive transgenerational plasticity in plants: case studies, mechanisms, and implications for natural populations. *Frontiers in Plant Science*, *2*(DEC). https://doi.org/10.3389/FPLS.2011.00102

Hernández-Plaza, A., Deng, Z., Robledo-Yagüe, F., Szklarczyk, D., von Mering, C., Bork, P., & Huerta-Cepas, J. (2026). eggNOG v7: phylogeny-based orthology predictions and functional

annotations. *Nucleic Acids Research*, *54*(D1), D402–D408. https://doi.org/10.1093/NAR/GKAF1249

Herrel, A., Joly, D., & Danchin, E. (2020). Epigenetics in ecology and evolution. *Functional Ecology*, *34*(2), 381–384. https://doi.org/10.1111/1365-2435.13494

Heuschele, J., Ekvall, M. T., Bianco, G., Hylander, S., & Hansson, L. A. (2017). Context-dependent individual behavioral consistency in Daphnia. *Ecosphere*, *8*(2), e01679. https://doi.org/10.1002/ECS2.1679

Hinch, S. G., & Rand, P. S. (2011). Optimal swimming speeds and forward-assisted propulsion: energy-conserving behaviours of upriver-migrating adult salmon. *Https://Doi.Org/10.1139/F00-238*, *57*(12), 2470–2478. https://doi.org/10.1139/F00-238

Hitzemann, R., Bottomly, D., Darakjian, P., Walter, N., Iancu, O., Searles, R., Wilmot, B., & Mcweeney, S. (2013). Genes, behavior and next-generation RNA sequencing. *Genes, Brain and Behavior*, *12*(1), 1–12. https://doi.org/10.1111/gbb.12007

Huang, S. (2009). Reprogramming cell fates: Reconciling rarity with robustness. *BioEssays*, *31*(5), 546–560. https://doi.org/10.1002/bies.200800189

Hutchings, J. A. (2011). Old wine in new bottles: reaction norms in salmonid fishes. *Heredity 2011 106:3*, *106*(3), 421–437. https://doi.org/10.1038/hdy.2010.166

Irschick, D. J., Albertson, R. C., Brennan, P., Podos, J., Johnson, N. A., Patek, S., & Dumont, E. (2013). Evo-devo beyond morphology: From genes to resource use. *Trends in Ecology and Evolution*, *28*(5), 267–273. https://doi.org/10.1016/j.tree.2012.12.004

Janeček, Š., Svensson, B., & MacGregor, E. A. (2013). α-Amylase: an enzyme specificity found in various families of glycoside hydrolases. *Cellular and Molecular Life Sciences: CMLS*, *71*(7), 1149. https://doi.org/10.1007/S00018-013-1388-Z

Jeschke, J. M., Laforsch, C., & Tollrian, R. (2008). Animal Prey Defenses. *Encyclopedia of Ecology, Five-Volume Set*, *1–5*, 189–194. https://doi.org/10.1016/B978-008045405-4.00858-2

Jones, B. M., Rao, V. D., Gernat, T., Jagla, T., Cash-Ahmed, A. C., Rubin, B. E. R., Comi, T. J., Bhogale, S., Husain, S. S., Blatti, C., Middendorf, M., Sinha, S., Chandrasekaran, S., & Robinson, G. E. (2020). Individual differences in honey bee behavior enabled by plasticity in brain gene regulatory networks. *ELife*, *9*, 1–28. https://doi.org/10.7554/ELIFE.62850

Kim, D. H., Lee, B. Y., Kim, H. S., Jeong, C. B., Hwang, D. S., Kim, I. C., & Lee, J. S. (2018). Identification and characterization of homeobox (Hox) genes and conservation of the single Hox cluster (324.6 kb) in the water flea Daphnia magna. *Journal of Experimental Zoology Part B: Molecular and Developmental Evolution*, *330*(2), 76–82. https://doi.org/10.1002/JEZ.B.22793

Kim, D., Paggi, J. M., Park, C., Bennett, C., & Salzberg, S. L. (2019). Graph-based genome alignment and genotyping with HISAT2 and HISAT-genotype. *Nature Biotechnology*, *37*(8), 907–915. https://doi.org/10.1038/S41587-019-0201-4

Klug, A. (1999). Zinc finger peptides for the regulation of gene expression. *Journal of Molecular Biology*, *293*(2), 215–218. https://doi.org/10.1006/JMBI.1999.3007

Korte, A., & Farlow, A. (2013). The advantages and limitations of trait analysis with GWAS: A review. In *Plant Methods* (Vol. 9, Number 1). https://doi.org/10.1186/1746-4811-9-29

Lafuente, E., Duneau, D., & Beldade, P. (2018). Genetic basis of thermal plasticity variation in Drosophila melanogaster body size. *PLOS Genetics*, *14*(9), e1007686. https://doi.org/10.1371/JOURNAL.PGEN.1007686

Lalejini, A., Ferguson, A. J., Grant, N. A., & Ofria, C. (2021). Adaptive Phenotypic Plasticity Stabilizes Evolution in Fluctuating Environments. *Frontiers in Ecology and Evolution | Www.Frontiersin.Org*, *1*, 715381. https://doi.org/https://doi.org/10.3389/fevo.2021.715381

Landry, L., & Bernatchez, L. (2010). Role of epibenthic resource opportunities in the parallel evolution of lake whitefish species pairs (*Coregonus* sp.). *Journal of Evolutionary Biology*, *23*(12), 2602–2613. https://doi.org/10.1111/j.1420-9101.2010.02121.x

Landy, J. A., Oschmann, A., Munch, S. B., & Walsh, M. R. (2020). Ancestral genetic variation in phenotypic plasticity underlies rapid evolutionary changes in resurrected populations of waterfleas. *Proceedings of the National Academy of Sciences of the United States of America*, *117*(51), 32535–32544. https://doi.org/10.1073/PNAS.2006581117/-/DCSUPPLEMENTAL

Langer, S. M., Weiss, L. C., Ekvall, M. T., Bianco, G., Hansson, L., & Tollrian, R. (2019). A three-dimensional perspective of *Daphnia* 's swimming behavior with and without predator cues. *Limnology and Oceanography*, *64*(4), 1515–1525. https://doi.org/10.1002/lno.11132

Lee, B. Y., Choi, B. S., Kim, M. S., Park, J. C., Jeong, C. B., Han, J., & Lee, J. S. (2019). The genome of the freshwater water flea Daphnia magna: A potential use for freshwater molecular ecotoxicology. *Aquatic Toxicology*, *210*, 69–84. https://doi.org/10.1016/J.AQUATOX.2019.02.009

Li, H., & Barrett, J. (2011). A statistical framework for SNP calling, mutation discovery, association mapping and population genetical parameter estimation from sequencing data. *Bioinformatics*, *27*(21), 2987–2993. https://doi.org/10.1093/BIOINFORMATICS/BTR509

Li, H., Handsaker, B., Wysoker, A., Fennell, T., Ruan, J., Homer, N., Marth, G., Abecasis, G., & Durbin, R. (2009). The Sequence Alignment/Map format and SAMtools. *Bioinformatics*, *25*(16), 2078–2079. https://doi.org/10.1093/BIOINFORMATICS/BTP352

Li, Q., Barish, S., Okuwa, S., & Volkan, P. C. (2015). Examination of Endogenous Rotund Expression and Function in Developing Drosophila Olfactory System Using CRISPR-Cas9–Mediated Protein Tagging. *G3 Genes|Genomes|Genetics*, *5*(12), 2809–2816. https://doi.org/10.1534/G3.115.021857

Liao, Y., Smyth, G. K., & Shi, W. (2014). featureCounts: an efficient general purpose program for assigning sequence reads to genomic features. *Bioinformatics*, *30*(7), 923–930. https://doi.org/10.1093/BIOINFORMATICS/BTT656

Loose, C. J., & Dawidowicz, P. (1994). Trade-Offs in Diel Vertical Migration by Zooplankton: The Costs of Predator Avoidance. *Ecology*, *75*(8), 2255–2263. https://doi.org/10.2307/1940881

López-Valcárcel, M. E., del Arco, A., Araújo, C. V. M., & Parra, G. (2025). Reduced avoidance behaviour in Daphnia magna due to agrochemical-induced vulnerability. *Ecotoxicology and Environmental Safety*, *291*, 117673. https://doi.org/10.1016/J.ECOENV.2025.117673

Love, M. I., Huber, W., & Anders, S. (2014). Moderated estimation of fold change and dispersion for RNA-seq data with DESeq2. *Genome Biology*, *15*(12), 550-. https://doi.org/10.1186/S13059-014-0550-8/FIGURES/9

Lynch, M., Ye, Z., Urban, L., Maruki, T., & Wei, W. (2022). The Linkage-Disequilibrium and Recombinational Landscape in Daphnia pulex. *Genome Biology and Evolution*, *14*(11). https://doi.org/10.1093/gbe/evac145

Maurano, M. T., Humbert, R., Rynes, E., Thurman, R. E., Haugen, E., Wang, H., Reynolds, A. P., Sandstrom, R., Qu, H., Brody, J., Shafer, A., Neri, F., Lee, K., Kutyavin, T., Stehling-Sun, S., Johnson, A. K., Canfield, T. K., Giste, E., Diegel, M., … Stamatoyannopoulos, J. A. (2012). Systematic localization of common disease-associated variation in regulatory DNA. *Science (New York, N.Y.)*, *337*(6099), 1190–1195. https://doi.org/10.1126/SCIENCE.1222794

McManus, J. N. J., Lovelett, R. J., Lowengrub, D., & Christensen, S. (2023). A unifying statistical framework to discover disease genes from GWASs. *Cell Genomics*, *3*(3), 100264. https://doi.org/10.1016/J.XGEN.2023.100264

Min, H., Lee, J. Y., & Kim, M. H. (2013). Hoxc Gene Collinear Expression and Epigenetic Modifications Established during Embryogenesis Are Maintained until after Birth. *International Journal of Biological Sciences*, *9*(9), 960. https://doi.org/10.7150/IJBS.6739

Miyakawa, H., Sato, M., Colbourne, J. K., & Iguchi, T. (2015). Ionotropic Glutamate Receptors Mediate Inducible Defense in the Water Flea Daphnia pulex. *PLOS ONE*, *10*(3), e0121324. https://doi.org/10.1371/JOURNAL.PONE.0121324

Muñoz, J., Chaturvedi, A., De Meester, L., & Weider, L. J. (2016). Characterization of genome-wide SNPs for the water flea Daphnia pulicaria generated by genotyping-by-sequencing (GBS). *Scientific Reports*, *6*(1), 28569. https://doi.org/10.1038/srep28569

Nicolini, F., Martelossi, J., Forni, G., Savojardo, C., Mantovani, B., & Luchetti, A. (2023). Comparative genomics of Hox and ParaHox genes among major lineages of Branchiopoda with emphasis on tadpole shrimps. *Frontiers in Ecology and Evolution*, *11*. https://doi.org/10.3389/fevo.2023.1046960

Nussey, D. H., Wilson, A. J., & Brommer, J. E. (2007). The evolutionary ecology of individual phenotypic plasticity in wild populations. *Journal of Evolutionary Biology*, *20*(3), 831–844. https://doi.org/10.1111/J.1420-9101.2007.01300.X

Oram, E., & Spitze, K. (2013). Depth selection by Daphnia pulex in response to Chaoborus kairomone. *Freshwater Biology*, *58*(2), 409–415. https://doi.org/10.1111/FWB.12069

Orsini, L., Gilbert, D., Podicheti, R., Jansen, M., Brown, J. B., Solari, O. S., Spanier, K. I., Colbourne, J. K., Rush, D., Decaestecker, E., Asselman, J., De Schamphelaere, K. A. C., Ebert, D., Haag, C. R., Kvist, J., Laforsch, C., Petrusek, A., Beckerman, A. P., Little, T. J., … Frilander, M. J. (2016). Daphnia magna transcriptome by RNA-Seq across 12 environmental stressors. *Scientific Data 2016 3:1*, *3*(1), 160030-. https://doi.org/10.1038/sdata.2016.30

Panhwar, W. A., & Mustafa, S. B. (2022). Phenotypic plasticity in grasshoppers and locusts: a review. *Asian Journal of Science, Engineering and Technology (AJSET)*, *1*(1), 38–51. https://doi.org/10.47264/idea.ajset/1.1.4

Pauwels, K., Stoks, R., & De Meester, L. (2005). Coping with predator stress: Interclonal differences in induction of heat-shock proteins in the water flea Daphnia magna. *Journal of Evolutionary Biology*, *18*(4), 867–872. https://doi.org/10.1111/j.1420-9101.2005.00890.x

Pigliucci, M. (2005). Evolution of phenotypic plasticity: where are we going now? *Trends in Ecology & Evolution*, *20*(9), 481–486. https://doi.org/10.1016/j.tree.2005.06.001

Pigliucci, M., & Murren, C. J. (2003). EVOLUTION I N T E R N A T I O N A L J O U R N A L O F O R G A N I C E V O L U T I O N PUBLISHED BY THE SOCIETY FOR THE STUDY OF EVOLUTION PERSPECTIVE: GENETIC ASSIMILATION AND A POSSIBLE EVOLUTIONARY PARADOX: CAN MACROEVOLUTION SOMETIMES BE SO FAST AS TO PASS US BY? In *Evolution* (Vol. 57, Number 7). https://academic.oup.com/evolut/article/57/7/1455/6756153

Pijanowska, J., & Kowalczewski, A. (1997). Predators can induce swarming behaviour and locomotory responses in Daphnia. *Freshwater Biology*, *37*(3), 649–656. https://doi.org/10.1046/j.1365-2427.1997.00192.x

Price, A. L., Zaitlen, N. A., Reich, D., & Patterson, N. (2010). New approaches to population stratification in genome-wide association studies. *Nature Reviews. Genetics*, *11*(7), 459. https://doi.org/10.1038/NRG2813

Price, T. D., Qvarnström, A., & Irwin, D. E. (2003). The role of phenotypic plasticity in driving genetic evolution. In *Proceedings of the Royal Society B: Biological Sciences* (Vol. 270, Number 1523, pp. 1433–1440). Royal Society. https://doi.org/10.1098/rspb.2003.2372

R Core Team (2025). _R: A Language and Environment for Statistical Computing_. R Foundation for Statistica Computing, Vienna, Austria. https://www.R-project.org/

Randel, N., & Jékely, G. (2016). Phototaxis and the origin of visual eyes. *Philosophical Transactions of the Royal Society B: Biological Sciences*, *371*(1685), 20150042. https://doi.org/10.1098/RSTB.2015.0042

Ringelberg, J. (1999). The photobehaviour of Daphnia spp. as a model to explain diel vertical migration in zooplankton. *Biological Reviews*, *74*(4), 397–423. https://doi.org/10.1111/J.1469-185X.1999.TB00036.X

Robinson, G. E., Grozinger, C. M., & Whitfield, C. W. (2005). Sociogenomics: social life in molecular terms. *Nature Reviews. Genetics*, *6*(4), 257–270. https://doi.org/10.1038/NRG1575

Posit team (2025). RStudio: Integrated Development Environment for R. Posit Software, PBC, Boston, MA. URL http://www.posit.co/.

Sakamoto, K., Hisatomi, O., Tokunaga, F., & Eguchi, E. (1996). Two Opsins From the Compound Eye of the Crab Hemigrapsus Sanguineus. *Journal of Experimental Biology*, *199*(2), 441–450. https://doi.org/10.1242/JEB.199.2.441

Saltz, J. B., Bell, A. M., Flint, J., Gomulkiewicz, R., Hughes, K. A., & Keagy, J. (2018). Why does the magnitude of genotype-by-environment interaction vary? *Ecology and Evolution*, *8*(12), 6342–6353. https://doi.org/10.1002/ECE3.4128

Schaeper, N. D., Prpic, N.-M., & Wimmer, E. A. (2010). *A clustered set of three Sp-family genes is ancestral in the Metazoa: evidence from sequence analysis, protein domain structure, developmental expression patterns and chromosomal location*. https://doi.org/10.1186/1471-2148-10-88

Schlichting, C. D., & Pigliucci, M. (1998). *Phenotypic evolution : a reaction norm perspective*. Sinauer Associates.

Schneider, H. M. (2022). Characterization, costs, cues and future perspectives of phenotypic plasticity. *Annals of Botany*, *130*(2), 131. https://doi.org/10.1093/AOB/MCAC087

Schomburg, C., Janssen, R., & Prpic, N. M. (2022). Phylogenetic analysis of forkhead transcription factors in the Panarthropoda. *Development Genes and Evolution*, *232*(1), 39–48. https://doi.org/10.1007/S00427-022-00686-3/FIGURES/3

Schumpert, C. A., Dudycha, J. L., & Patel, R. C. (2015). Development of an efficient RNA interference method by feeding for the microcrustacean Daphnia. *BMC Biotechnology*, *15*(1). https://doi.org/10.1186/S12896-015-0209-X

Seetharam, A., Bai, Y., & Stuart, G. W. (2010). A survey of well conserved families of C2H2 zinc-finger genes in Daphnia. *BMC Genomics*, *11*(1), 276. https://doi.org/10.1186/1471-2164-11-276

Shackelford, T. K., & Weekes-Shackelford, V. A. (2021). Encyclopedia of Evolutionary Psychological Science. In *Encyclopedia of Evolutionary Psychological Science*. Springer Science+Business Media. https://doi.org/10.1007/978-3-319-19650-3

Shannon, P., Markiel, A., Ozier, O., Baliga, N. S., Wang, J. T., Ramage, D., Amin, N., Schwikowski, B., & Ideker, T. (2003). Cytoscape: a software environment for integrated models of biomolecular interaction networks. *Genome Research*, *13*(11), 2498–2504. https://doi.org/10.1101/GR.1239303

Sih, A., Bell, A., & Johnson, J. C. (2004). Behavioral syndromes: an ecological and evolutionary overview. *Trends in Ecology & Evolution*, *19*(7), 372–378. https://doi.org/10.1016/J.TREE.2004.04.009

Sih, A., Ferrari, M. C. O., & Harris, D. J. (2011). Evolution and behavioural responses to human-induced rapid environmental change. *Evolutionary Applications*, *4*(2), 367–387. https://doi.org/10.1111/J.1752-4571.2010.00166.X

Sinha, S., Jones, B. M., Traniello, I. M., Bukhari, S. A., Halfon, M. S., Hofmann, H. A., Huang, S., Katz, P. S., Keagy, J., Lynch, V. J., Sokolowski, M. B., Stubbs, L. J., Tabe-Bordbar, S., Wolfner, M. F., & Robinson, G. E. (2020). Behavior-related gene regulatory networks: A new level of organization in the brain. *Proceedings of the National Academy of Sciences of the United States of America*, *117*(38), 23270–23279. https://doi.org/10.1073/PNAS.1921625117/ASSET/7C854164-3081-48B9-9E79-E40BDF1C14C6/ASSETS/IMAGES/LARGE/PNAS.1921625117FIG02.JPG

Slatkin, M. (2008). Linkage disequilibrium - Understanding the evolutionary past and mapping the medical future. In *Nature Reviews Genetics* (Vol. 9, Number 6, pp. 477–485). https://doi.org/10.1038/nrg2361

Snell-Rood, E. C. (2013). An overview of the evolutionary causes and consequences of behavioural plasticity. *Animal Behaviour*, *85*(5), 1004–1011. https://doi.org/10.1016/J.ANBEHAV.2012.12.031

Stoks, R., Govaert, L., Pauwels, K., Jansen, B., & De Meester, L. (2016). Resurrecting complexity: The interplay of plasticity and rapid evolution in the multiple trait response to strong changes in predation pressure in the water flea Daphnia magna. *Ecology Letters*, *19*(2), 180–190. https://doi.org/10.1111/ele.12551

Swaegers, J., & Koch, E. L. (2022). Gene expression studies of plastic and evolutionary responses to global warming. In *Current Opinion in Insect Science* (Vol. 51). Elsevier Inc. https://doi.org/10.1016/j.cois.2022.100918

The MathWorks Inc. (2023). Optimization Toolbox version: 9.14 (R2023a), Natick, Massachusetts: The MathWorks Inc. https://www.mathworks.com

Tollrian, R., & Harvell, C. D. (Eds.). (1999). *The Ecology and Evolution of Inducible Defenses*. Princeton University Press. https://doi.org/10.2307/j.ctv1ddd1cn

Toyota, K., Miyagawa, S., Ogino, Y., & Iguchi, T. (2016). Microinjection-Based RNA Interference Method in the Water Flea, Daphnia pulex and Daphnia magna. *RNA Interference*. https://doi.org/10.5772/61485

Traniello, I. M., Bukhari, S. A., Dibaeinia, P., Serrano, G., Avalos, A., Ahmed, A. C., Sankey, A. L., Hernaez, M., Sinha, S., Zhao, S. D., Catchen, J., & Robinson, G. E. (2023). Single-cell dissection of aggression in honeybee colonies. *Nature Ecology and Evolution*, *7*(8), 1232–1244. https://doi.org/10.1038/s41559-023-02090-0

Tuomainen, U., & Candolin, U. (2011). Behavioural responses to human-induced environmental change. *Biological Reviews*, *86*(3), 640–657. https://doi.org/10.1111/j.1469-185X.2010.00164.x

Van Kleunen, M., & Fischer, M. (2005). Constraints on the evolution of adaptive phenotypic plasticity in plants. *New Phytologist*, *166*(1), 49–60. https://doi.org/10.1111/J.1469-8137.2004.01296.X

Van Tienderen, P. H., & Koelewijn, H. P. (1994). Selection on reaction norms, genetic correlations and constraints. *Genetics Research*, *64*(2), 115–125. https://doi.org/10.1017/S0016672300032729

Velotta, J. P., & Cheviron, Z. A. (2018). Remodeling Ancestral Phenotypic Plasticity in Local Adaptation: A New Framework to Explore the Role of Genetic Compensation in the Evolution of Homeostasis. *Integrative and Comparative Biology*, *58*(6), 1098–1110. https://doi.org/10.1093/ICB/ICY117

Waddington, C. H. (1942). CANALIZATION OF DEVELOPMENT AND THE INHERITANCE OF ACQUIRED CHARACTERS. *Nature 1942 150:3811*, *150*(3811), 563–565. https://doi.org/10.1038/150563a0

Waddington, C. H. (1952). Selection of the Genetic Basis for an Acquired Character. *Nature 1952 169:4302*, *169*(4302), 625–626. https://doi.org/10.1038/169625b0

Wang, Z., Gerstein, M., & Snyder, M. (2009). RNA-Seq: a revolutionary tool for transcriptomics. *Nature Reviews Genetics 2008 10:1*, *10*(1), 57–63. https://doi.org/10.1038/nrg2484

Weiss, L. C. (2019). Sensory ecology of predator-induced phenotypic plasticity. *Frontiers in Behavioral Neuroscience*, *12*, 427852. https://doi.org/10.3389/FNBEH.2018.00330/XML

Weiss, L. C., Kruppert, S., Laforsch, C., & Tollrian, R. (2012). Chaoborus and Gasterosteus Anti-Predator Responses in Daphnia pulex Are Mediated by Independent Cholinergic and Gabaergic Neuronal Signals. *PLOS ONE*, *7*(5), e36879. https://doi.org/10.1371/JOURNAL.PONE.0036879

West-Eberhard, M. J. (1989). Phenotypic Plasticity and the Origins of Diversity. *Annual Review of Ecology and Systematics*, *20*, 249–278. http://www.jstor.org/stable/2097092

Wund, M. A., Baker, J. A., Clancy, B., Golub, J. L., & Foster, S. A. (2008). A test of the “flexible stem” model of evolution: Ancestral plasticity, genetic accommodation, and morphological divergence

in the threespine stickleback radiation. *American Naturalist*, *172*(4), 449–462. https://doi.org/10.1086/590966

Yang, J., Weedon, M. N., Purcell, S., Lettre, G., Estrada, K., Willer, C. J., Smith, A. V., Ingelsson, E., O'Connell, J. R., Mangino, M., Mägi, R., Madden, P. A., Heath, A. C., Nyholt, D. R., Martin, N. G., Montgomery, G. W., Frayling, T. M., Hirschhorn, J. N., McCarthy, M. I., … Visscher, P. M. (2011). Genomic inflation factors under polygenic inheritance. *European Journal of Human Genetics 2011 19:7*, *19*(7), 807–812. https://doi.org/10.1038/ejhg.2011.39

Yu, G., Wang, L. G., Han, Y., & He, Q. Y. (2012). clusterProfiler: an R Package for Comparing Biological Themes Among Gene Clusters. *OMICS : A Journal of Integrative Biology*, *16*(5), 284. https://doi.org/10.1089/OMI.2011.0118

Yuan, W., Zhou, Y., Chen, Y., Liu, X., & Wang, J. (2020). Toxicological effects of microplastics and heavy metals on the Daphnia magna. *Science of The Total Environment*, *746*, 141254. https://doi.org/10.1016/J.SCITOTENV.2020.141254

Zaidi, A. A., & Mathieson, I. (2020). Demographic history mediates the effect of stratification on polygenic scores. *ELife*, *9*, 1–30. https://doi.org/10.7554/ELIFE.61548

Zhou, X., & Stephens, M. (2012). Genome-wide efficient mixed-model analysis for association studies. *Nature Genetics*, *44*(7), 821–824. https://doi.org/10.1038/NG.2310

Addendum

Tables

Table S1: Tukey Post-hoc pairwise comparison test for differences in vertical position (scaled) within population types between control (no-fish) and kairomone exposed (fish)

contrast	type	estimate	SE	df	z.ratio	p.value
fish - (no-fish)	A_F	0.052794	0.121265	Inf	0.435364	0.663298
fish - (no-fish)	A_NF	0.210596	0.115373	Inf	1.825343	0.067949
fish - (no-fish)	NA_F	-0.08349	0.103454	Inf	-0.807	0.419665
fish - (no-fish)	NA_NF	0.507859	0.150511	Inf	3.374241	**0.00074**
fish - (no-fish)	C1242	-0.5305	0.48395	Inf	-1.09618	0.272998
fish - (no-fish)	P_{132},85	-1.1221	0.465725	Inf	-2.40936	**0.015981**
fish - (no-fish)	P_{132},96	0.171932	0.550008	Inf	0.312599	0.754585

Table S2:Bonferroni Post-hoc comparison test for differences in vertical position between population types in the control (no-fish) and kairomone exposed (fish) conditions

contrast	condition	estimate	SE	df	z.ratio	p.value
A_F - A_NF	no-fish	0.116943	0.20169	Inf	0.579814	0.786857
A_F - C1242	no-fish	1.123275	0.714565	Inf	1.57197	0.256913
A_F - P_{132},85	no-fish	-0.33674	0.707141	Inf	-0.4762	0.800059
A_F - P_{132},96	no-fish	-2.23239	0.740618	Inf	-3.01423	**0.013831**
A_F - NA_F	no-fish	-0.0152	0.19285	Inf	-0.07883	0.937165
A_F - NA_NF	no-fish	-0.07236	0.23398	Inf	-0.30927	0.836812
A_NF - C1242	no-fish	1.006332	0.713893	Inf	1.40964	0.30287
A_NF - P_{132},85	no-fish	-0.45368	0.706482	Inf	-0.64217	0.781143
A_NF - P_{132},96	no-fish	-2.34933	0.740007	Inf	-3.17474	**0.013831**
A_NF - NA_F	no-fish	-0.13215	0.18879	Inf	-0.69996	0.781143
A_NF - NA_NF	no-fish	-0.18931	0.231279	Inf	-0.81852	0.722858
C1242 - P_{132},85	no-fish	-1.46001	0.944975	Inf	-1.54503	0.256913
C1242 - P_{132},96	no-fish	-3.35566	0.975238	Inf	-3.44087	**0.012177**
C1242 - NA_F	no-fish	-1.13848	0.711	Inf	-1.60123	0.256913
C1242 - NA_NF	no-fish	-1.19564	0.723074	Inf	-1.65355	0.256913
P_{132},85 - P_{132},96	no-fish	-1.89565	0.94594	Inf	-2.00399	0.15775
P_{132},85 - NA_F	no-fish	0.321536	0.703571	Inf	0.457006	0.800059
P_{132},85 - NA_NF	no-fish	0.264376	0.715717	Inf	0.369386	0.83048
P_{132},96 - NA_F	no-fish	2.217187	0.737229	Inf	3.007459	**0.013831**
P_{132},96 - NA_NF	no-fish	2.160027	0.748765	Inf	2.884785	**0.016451**
NA_F - NA_NF	no-fish	-0.05716	0.222442	Inf	-0.25697	0.837065
A_F - A_NF	fish	0.274744	0.20618	Inf	1.332543	0.274023
A_F - C1242	fish	0.539981	0.703342	Inf	0.767737	0.546795
A_F - P_{132},85	fish	-1.51163	0.725016	Inf	-2.08496	0.070775
A_F - P_{132},96	fish	-2.11325	0.732026	Inf	-2.88686	**0.027238**
A_F - NA_F	fish	-0.15149	0.193898	Inf	-0.78126	0.546795

A_F - NA_NF	fish	0.382702	0.237367	Inf	1.612279	0.172687
A_NF - C1242	fish	0.265237	0.702608	Inf	0.377504	0.741089
A_NF - P_{132},85	fish	-1.78638	0.724375	Inf	-2.46609	**0.040979**
A_NF - P_{132},96	fish	-2.388	0.731432	Inf	-3.26482	**0.011501**
A_NF - NA_F	fish	-0.42623	0.19098	Inf	-2.2318	0.059799
A_NF - NA_NF	fish	0.107958	0.234794	Inf	0.459798	0.713626
C1242 - P_{132},85	fish	-2.05161	0.952077	Inf	-2.15488	0.065459
C1242 - P_{132},96	fish	-2.65323	0.964773	Inf	-2.75011	**0.029574**
C1242 - NA_F	fish	-0.69147	0.699058	Inf	-0.98914	0.451632
C1242 - NA_NF	fish	-0.15728	0.7119	Inf	-0.22093	0.825147
P_{132},85 - P_{132},96	fish	-0.60162	0.95703	Inf	-0.62863	0.617855
P_{132},85 - NA_F	fish	1.360147	0.720883	Inf	1.886779	0.103583
P_{132},85 - NA_NF	fish	1.894334	0.733436	Inf	2.582822	**0.034299**
P_{132},96 - NA_F	fish	1.961767	0.72796	Inf	2.694882	**0.029574**
P_{132},96 - NA_NF	fish	2.495954	0.740436	Inf	3.370925	**0.011501**
NA_F - NA_NF	fish	0.534187	0.223861	Inf	2.386239	**0.044682**

Table S3: Tukey Post-hoc pairwise comparison test for differences in vertical position (scaled) within populations (ponds) between control (no-fish) and kairomone exposed (fish)

contrast	pond.code	estimate	SE	df	z.ratio	p.value
(no-fish) - fish	A1_AnOudin	0.151924	0.265428	Inf	0.572372	0.56707
(no-fish) - fish	A2_BuSN	0.385203	0.278963	Inf	1.38084	0.167328
(no-fish) - fish	A3_Mech	-0.68345	0.263764	Inf	-2.59114	**0.009566**
(no-fish) - fish	A4_PL15_YEL	0.2524	0.256002	Inf	0.985931	0.324167
(no-fish) - fish	A5_GenM	0.845752	0.251409	Inf	3.36404	**0.000768**
(no-fish) - fish	B1_BKN1	0.437302	0.30642	Inf	1.427136	0.153541
(no-fish) - fish	B2_OM2	0.006129	0.230427	Inf	0.026597	0.978781
(no-fish) - fish	B3_ZW	0.416245	0.257565	Inf	1.616074	0.106078
(no-fish) - fish	B4_OHZ	-0.54333	0.274892	Inf	-1.97654	**0.048094**
(no-fish) - fish	B5_DA2	-0.12885	0.261803	Inf	-0.49216	0.622608
(no-fish) - fish	C1_BlfN	-0.02571	0.284476	Inf	-0.09037	0.927993
(no-fish) - fish	C2_MO	0.416939	0.257722	Inf	1.617783	0.105709
(no-fish) - fish	C3_Ter1	0.394931	0.265304	Inf	1.488599	0.136593
(no-fish) - fish	C4_BW_48630	0.027402	0.229151	Inf	0.11958	0.904816
(no-fish) - fish	C5_BW_36962	0.137953	0.25329	Inf	0.544645	0.585998
(no-fish) - fish	D1_CBOO6	-0.04849	0.256958	Inf	-0.18871	0.850316
(no-fish) - fish	D2_LRV	-0.01228	0.263587	Inf	-0.04658	0.962849
(no-fish) - fish	D3_BKLE5	0.322432	0.246345	Inf	1.308861	0.190582
(no-fish) - fish	D4_BW_62256	-0.10306	0.289695	Inf	-0.35577	0.722015
(no-fish) - fish	D5_BW_22050	0.164038	0.287855	Inf	0.569862	0.568771

Table S4: Tukey Post-hoc pairwise comparison test for differences in vertical position (scaled) within population types between control (no-fish) and kairomone exposed (fish)

contrast	type	estimate	SE	df	z.ratio	p.value
(no-fish) - fish	A_F	-0.09708	0.124558	Inf	-0.77941	0.435738
(no-fish) - fish	A_NF	-0.2149	0.117258	Inf	-1.83273	0.066842
(no-fish) - fish	NA_F	0.123064	0.107692	Inf	1.142742	0.253146
(no-fish) - fish	NA_NF	-0.4771	0.154521	Inf	-3.08761	**0.002018**
(no-fish) - fish	C1242	0.522246	0.489858	Inf	1.066118	0.28637
(no-fish) - fish	P_{132},85	1.075458	0.507407	Inf	2.119516	**0.034047**
(no-fish) - fish	P_{132},96	-0.40635	0.661016	Inf	-0.61474	0.538726

Table S5: Tukey Post-hoc pairwise comparison test for difference in vertical position (scaled) within clones between control (no-fish) and kairomone exposed (fish)

contrast	clone	estimate	SE	df	z.ratio	p.value
(no-fish) - fish	1	-0.31845	0.627478	Inf	-0.50751	0.611796
(no-fish) - fish	2	-0.13488	0.554946	Inf	-0.24305	0.807969
(no-fish) - fish	3	-0.43171	0.592783	Inf	-0.72827	0.466449
(no-fish) - fish	4	0.653678	0.489113	Inf	1.336457	0.1814
(no-fish) - fish	5	0.474808	0.414408	Inf	1.145752	0.251898
(no-fish) - fish	6	0.074926	0.582635	Inf	0.128598	0.897676
(no-fish) - fish	7	0.698994	0.536004	Inf	1.304083	0.192205
(no-fish) - fish	8	0.511635	0.69251	Inf	0.738812	0.460021
(no-fish) - fish	9	0.372945	0.489596	Inf	0.761741	0.446214
(no-fish) - fish	10	0.233085	0.514017	Inf	0.453457	0.650219
(no-fish) - fish	11	-0.02203	0.468789	Inf	-0.04699	0.962518
(no-fish) - fish	12	-0.43435	0.476865	Inf	-0.91084	0.362381
(no-fish) - fish	13	-2.5925	0.684234	Inf	-3.78891	**0.000151**
(no-fish) - fish	14	-0.54817	0.48381	Inf	-1.13304	0.2572
(no-fish) - fish	15	-0.46974	0.483099	Inf	-0.97236	0.330874
(no-fish) - fish	16	-0.44254	0.486641	Inf	-0.90938	0.36315
(no-fish) - fish	17	-0.02603	0.505592	Inf	-0.05149	0.958934
(no-fish) - fish	18	0.740524	0.502838	Inf	1.472689	0.140835
(no-fish) - fish	19	0.413467	0.498559	Inf	0.829325	0.40692
(no-fish) - fish	20	0.576199	0.475424	Inf	1.211969	0.225524
(no-fish) - fish	21	1.035264	0.513842	Inf	2.014753	0.043931
(no-fish) - fish	22	1.320288	0.509224	Inf	2.592742	**0.009521**
(no-fish) - fish	23	0.668975	0.511432	Inf	1.308044	0.190858
(no-fish) - fish	24	0.569787	0.485869	Inf	1.172717	0.240909
(no-fish) - fish	25	0.661476	0.431118	Inf	1.534328	0.124949
(no-fish) - fish	26	0.909842	0.496664	Inf	1.831906	0.066965
(no-fish) - fish	27	0.169012	0.474225	Inf	0.356396	0.721544
(no-fish) - fish	28	1.077497	0.608122	Inf	1.771843	0.076421
(no-fish) - fish	30	-0.4376	0.589915	Inf	-0.7418	0.458208
(no-fish) - fish	31	-0.80094	0.490027	Inf	-1.63447	0.102159
(no-fish) - fish	32	0.541325	0.337068	Inf	1.605979	0.108279
(no-fish) - fish	33	0.568558	0.486143	Inf	1.169529	0.242191

(no-fish) - fish	34	-0.06266	0.538862	Inf	-0.11629	0.907425
(no-fish) - fish	35	-0.53325	0.463381	Inf	-1.15078	0.249822
(no-fish) - fish	36	0.430102	0.504989	Inf	0.851705	0.394378
(no-fish) - fish	37	-0.67988	0.487545	Inf	-1.3945	0.163166
(no-fish) - fish	38	0.246843	0.557504	Inf	0.442764	0.657936
(no-fish) - fish	39	1.15485	0.499584	Inf	2.311624	**0.020798**
(no-fish) - fish	40	0.915534	0.486132	Inf	1.883303	0.059659
(no-fish) - fish	41	-0.60103	0.661101	Inf	-0.90914	0.363276
(no-fish) - fish	42	-0.97145	0.518932	Inf	-1.87201	0.061205
(no-fish) - fish	43	-0.24676	0.544582	Inf	-0.45312	0.650461
(no-fish) - fish	44	-1.0628	0.511402	Inf	-2.07822	**0.037689**
(no-fish) - fish	45	0.441632	0.676931	Inf	0.652403	0.514141
(no-fish) - fish	46	0.648065	0.441326	Inf	1.468449	0.141982
(no-fish) - fish	47	-1.10251	0.489109	Inf	-2.25412	**0.024189**
(no-fish) - fish	48	0.841096	0.840892	Inf	1.000243	0.317193
(no-fish) - fish	49	0.109618	0.477798	Inf	0.229423	0.81854
(no-fish) - fish	50	-0.46213	0.489427	Inf	-0.94422	0.345056
(no-fish) - fish	52	-0.2016	0.478373	Inf	-0.42143	0.673441
(no-fish) - fish	53	0.421391	0.587282	Inf	0.717529	0.473048
(no-fish) - fish	54	-0.11649	0.527987	Inf	-0.22064	0.825376
(no-fish) - fish	55	-0.30733	0.490395	Inf	-0.62669	0.530861
(no-fish) - fish	56	0.112334	0.449554	Inf	0.24988	0.80268
(no-fish) - fish	57	1.258954	0.465302	Inf	2.705671	**0.006817**
(no-fish) - fish	58	0.326529	0.54761	Inf	0.59628	0.550988
(no-fish) - fish	59	-0.3444	0.528897	Inf	-0.65117	0.51494
(no-fish) - fish	60	0.481287	0.572309	Inf	0.840957	0.400372
(no-fish) - fish	61	-1.07683	0.631157	Inf	-1.70612	0.087986
(no-fish) - fish	62	0.033493	0.461587	Inf	0.07256	0.942157
(no-fish) - fish	63	2.334982	0.608917	Inf	3.834647	**0.000126**
(no-fish) - fish	64	0.176029	0.530502	Inf	0.331816	0.740028
(no-fish) - fish	65	0.326885	0.557694	Inf	0.586137	0.557783
(no-fish) - fish	66	-0.30347	0.535566	Inf	-0.56663	0.570964
(no-fish) - fish	67	0.556467	0.335296	Inf	1.65963	0.096989
(no-fish) - fish	68	0.026909	0.476015	Inf	0.05653	0.95492
(no-fish) - fish	69	0.016826	0.529919	Inf	0.031751	0.97467
(no-fish) - fish	70	-0.84247	0.498875	Inf	-1.68873	0.091271
(no-fish) - fish	71	0.549245	0.548244	Inf	1.001826	0.316428
(no-fish) - fish	72	1.010511	0.59092	Inf	1.710064	0.087254
(no-fish) - fish	73	0.12759	0.557895	Inf	0.228698	0.819103
(no-fish) - fish	74	-0.33843	0.416563	Inf	-0.81243	0.416543
(no-fish) - fish	75	-0.12202	0.547036	Inf	-0.22305	0.823499
(no-fish) - fish	76	-0.25913	0.512127	Inf	-0.50599	0.612861
(no-fish) - fish	77	0.942734	0.488447	Inf	1.930062	0.053599
(no-fish) - fish	78	-0.51078	0.489859	Inf	-1.0427	0.297085
(no-fish) - fish	79	-0.06781	0.445132	Inf	-0.15233	0.87893
(no-fish) - fish	80	-0.09838	0.551899	Inf	-0.17826	0.858523

(no-fish) - fish		81	-0.06519	0.427137	Inf	-0.15261	0.878703
(no-fish) - fish		82	-0.06528	0.542851	Inf	-0.12025	0.904285
(no-fish) - fish		83	-0.40699	0.489548	Inf	-0.83137	0.405766
(no-fish) - fish		84	-0.18645	0.795989	Inf	-0.23424	0.814799
(no-fish) - fish		85	0.419355	0.537726	Inf	0.779867	0.435469
(no-fish) - fish		86	-0.49966	0.515644	Inf	-0.969	0.332543
(no-fish) - fish		87	0.588341	0.551322	Inf	1.067146	0.285906
(no-fish) - fish		88	0.946342	0.390014	Inf	2.426432	**0.015248**
(no-fish) - fish		89	0.068168	0.623218	Inf	0.10938	0.912901
(no-fish) - fish		90	-0.02117	0.518344	Inf	-0.04085	0.967418
(no-fish) - fish		91	-0.25395	0.672324	Inf	-0.37772	0.70564
(no-fish) - fish		92	-0.82749	0.671352	Inf	-1.23257	0.217735
(no-fish) - fish		93	0.605538	0.486221	Inf	1.245397	0.212986
(no-fish) - fish		94	-1.30138	0.859776	Inf	-1.51362	0.130121
(no-fish) - fish		95	-0.05746	0.421976	Inf	-0.13617	0.891685
(no-fish) - fish		96	0.856283	0.463378	Inf	1.847916	0.064614
(no-fish) - fish		97	-0.60443	0.960383	Inf	-0.62936	0.529111
(no-fish) - fish		98	-0.2865	0.517052	Inf	-0.5541	0.579513
(no-fish) - fish		99	1.38672	0.812043	Inf	1.707693	0.087693
(no-fish) - fish		100	-0.63489	0.484241	Inf	-1.3111	0.189823
(no-fish) - fish	C1242		-0.55744	0.415774	Inf	-1.34074	0.180005
(no-fish) - fish	P_{132},85		-1.16822	0.397982	Inf	-2.93537	**0.003332**
(no-fish) - fish	P_{132},96		0.189226	0.497857	Inf	0.38008	0.703886

Table S6: Bonferroni Post-hoc comparison test for differences in Phototactic Index (PI) between population types in the control (no-fish) and kairomone exposed (fish) conditions

contrast	condition	estimate	SE	df	z.ratio	p.value
A_F - A_NF	no-fish	-0.10439	0.218637	Inf	-0.47744	0.891471
A_F - C1242	no-fish	-0.99595	0.757036	Inf	-1.31559	0.445519
A_F - P_{132},85	no-fish	0.262967	0.772099	Inf	0.340587	0.891471
A_F - P_{132},96	no-fish	2.601424	0.823587	Inf	3.158649	**0.008321**
A_F - NA_F	no-fish	-0.01122	0.209126	Inf	-0.05365	0.957215
A_F - NA_NF	no-fish	0.047831	0.253575	Inf	0.188628	0.892904
A_NF - C1242	no-fish	-0.89156	0.756268	Inf	-1.1789	0.455202
A_NF - P_{132},85	no-fish	0.367354	0.771328	Inf	0.476261	0.891471
A_NF - P_{132},96	no-fish	2.705811	0.822914	Inf	3.288085	**0.008321**
A_NF - NA_F	no-fish	0.093168	0.204718	Inf	0.455105	0.891471
A_NF - NA_NF	no-fish	0.152219	0.250682	Inf	0.607218	0.891471
C1242 - P_{132},85	no-fish	1.258916	1.01814	Inf	1.236486	0.454184
C1242 - P_{132},96	no-fish	3.597373	1.063389	Inf	3.382933	**0.008321**
C1242 - NA_F	no-fish	0.98473	0.752959	Inf	1.307813	0.445519
C1242 - NA_NF	no-fish	1.04378	0.766445	Inf	1.361847	0.445519
P_{132},85 - P_{132},96	no-fish	2.338457	1.051716	Inf	2.223468	0.091645
P_{132},85 - NA_F	no-fish	-0.27419	0.768013	Inf	-0.35701	0.891471
P_{132},85 - NA_NF	no-fish	-0.21514	0.781272	Inf	-0.27537	0.891471

P_{132},96 - NA_F	no-fish	-2.61264	0.819843	Inf	-3.18676	**0.008321**
P_{132},96 - NA_NF	no-fish	-2.55359	0.832181	Inf	-3.06855	**0.009034**
NA_F - NA_NF	no-fish	0.059051	0.241165	Inf	0.244855	0.891471
A_F - A_NF	fish	-0.22221	0.22284	Inf	-0.99717	0.447101
A_F - C1242	fish	-0.37662	0.747686	Inf	-0.50372	0.716872
A_F - P_{132},85	fish	1.435506	0.771229	Inf	1.861324	0.131667
A_F - P_{132},96	fish	2.292153	0.804946	Inf	2.847585	**0.030837**
A_F - NA_F	fish	0.208927	0.209813	Inf	0.995779	0.447101
A_F - NA_NF	fish	-0.33219	0.256793	Inf	-1.2936	0.3163
A_NF - C1242	fish	-0.15441	0.746743	Inf	-0.20678	0.87799
A_NF - P_{132},85	fish	1.657715	0.770323	Inf	2.151973	0.082424
A_NF - P_{132},96	fish	2.514361	0.804404	Inf	3.125744	**0.018622**
A_NF - NA_F	fish	0.431135	0.206614	Inf	2.086675	0.086141
A_NF - NA_NF	fish	-0.10998	0.254067	Inf	-0.43287	0.735121
C1242 - P_{132},85	fish	1.812127	1.012364	Inf	1.789996	0.140232
C1242 - P_{132},96	fish	2.668774	1.053158	Inf	2.534068	**0.047354**
C1242 - NA_F	fish	0.585548	0.742832	Inf	0.788263	0.531847
C1242 - NA_NF	fish	0.044434	0.757024	Inf	0.058696	0.953194
P_{132},85 - P_{132},96	fish	0.856647	1.052925	Inf	0.813587	0.531847
P_{132},85 - NA_F	fish	-1.22658	0.766385	Inf	-1.60047	0.191614
P_{132},85 - NA_NF	fish	-1.76769	0.780255	Inf	-2.26553	0.076957
P_{132},96 - NA_F	fish	-2.08323	0.800729	Inf	-2.60166	**0.047354**
P_{132},96 - NA_NF	fish	-2.62434	0.814052	Inf	-3.2238	**0.018622**
NA_F - NA_NF	fish	-0.54111	0.242496	Inf	-2.23143	0.076957

Table S7: Tukey Post-hoc comparison test for differences in phototactic index within populations (ponds) between control (no-fish) and kairomone exposed (fish)

contrast	pond.code	estimate	SE	df	z.ratio	p.value
(no-fish) - fish	A1_AnOudin	-0.29285	0.235886	Inf	-1.24148	0.21443
(no-fish) - fish	A2_BuSN	-0.37829	0.294807	Inf	-1.28316	0.199436
(no-fish) - fish	A3_Mech	0.753358	0.287302	Inf	2.622178	**0.008737**
(no-fish) - fish	A4_PL15_YEL	-0.16678	0.274082	Inf	-0.60852	0.542845
(no-fish) - fish	A5_GenM	-0.76501	0.227966	Inf	-3.35582	**0.000791**
(no-fish) - fish	B1_BKN1	-0.39157	0.331268	Inf	-1.18202	0.237198
(no-fish) - fish	B2_OM2	-0.18242	0.16848	Inf	-1.08275	0.278918
(no-fish) - fish	B3_ZW	-0.38597	0.276956	Inf	-1.39361	0.163434
(no-fish) - fish	B4_OHZ	0.660446	0.28355	Inf	2.329209	**0.019848**
(no-fish) - fish	B5_DA2	0.00214	0.249145	Inf	0.008588	0.993148
(no-fish) - fish	C1_BlfN	0.203826	0.279715	Inf	0.728691	0.466191
(no-fish) - fish	C2_MO	-0.30305	0.223459	Inf	-1.35619	0.175039
(no-fish) - fish	C3_Ter1	-0.16017	0.272169	Inf	-0.58848	0.556209
(no-fish) - fish	C4_BW_48630	-0.06407	0.216073	Inf	-0.29653	0.766827
(no-fish) - fish	C5_BW_36962	-0.51081	0.227914	Inf	-2.24122	**0.025012**
(no-fish) - fish	D1_CBOO6	-0.02864	0.237014	Inf	-0.12083	0.903824
(no-fish) - fish	D2_LRV	-0.06876	0.257225	Inf	-0.2673	0.78924

(no-fish) - fish	D3_BKLE5	-0.37255	0.197056	Inf	-1.89057	0.058682
(no-fish) - fish	D4_BW_62256	0.156946	0.247167	Inf	0.634979	0.525442
(no-fish) - fish	D5_BW_22050	-0.48065	0.268342	Inf	-1.79117	0.073266

Table S8: Tukey Post-hoc comparison test for differences in swimming speed within population types between control (no-fish) and kairomone exposed (fish)

contrast	type	estimate	SE	df	t.ratio	p.value
(no-fish) - fish	A_F	-0.27919	0.155183	490.7443	-1.79909	0.072619
(no-fish) - fish	A_NF	0.095377	0.145454	481.6959	0.655716	0.51232
(no-fish) - fish	NA_F	-0.03684	0.134844	487.0635	-0.27321	0.784805
(no-fish) - fish	NA_NF	0.475725	0.192327	477.8172	2.473523	**0.013725**

Table S9: Bonferroni Post-hoc comparison test for differences in swimming speed between population types in the control (no-fish) and kairomone exposed (fish) conditions

contrast	condition	estimate	SE	df	t.ratio	p.value
A_F - A_NF	no-fish	-0.51395	0.29028	19.74413	-1.77054	0.276233
A_F - NA_F	no-fish	-0.55358	0.276176	21.78203	-2.00443	0.276233
A_F - NA_NF	no-fish	-0.30315	0.337149	20.22458	-0.89916	0.642384
A_NF - NA_F	no-fish	-0.03963	0.271786	20.54168	-0.1458	0.885502
A_NF - NA_NF	no-fish	0.210798	0.334045	19.54335	0.631049	0.642384
NA_F - NA_NF	no-fish	0.250424	0.320709	20.68713	0.780847	0.642384
A_F - A_NF	fish	-0.13938	0.294097	20.76216	-0.47394	0.640489
A_F - NA_F	fish	-0.31123	0.277387	22.16586	-1.122	0.410805
A_F - NA_NF	fish	0.451763	0.337727	20.36446	1.337658	0.391512
A_NF - NA_F	fish	-0.17184	0.273544	21.01686	-0.62821	0.640489
A_NF - NA_NF	fish	0.591147	0.334591	19.65499	1.766778	0.278375
NA_F - NA_NF	fish	0.762991	0.319873	20.45514	2.385292	0.161017

Table S10: Tukey Post-hoc comparison test for differences in swimming speed within groups based on prior exposure between control (no-fish) and kairomone exposed (fish)

contrast	fish	estimate	SE	df	t.ratio	p.value
(no-fish) - fish	N	0.413694	0.16172	479.4521	2.558091	**0.010831**
(no-fish) - fish	Y	-0.09221	0.086996	491.2117	-1.05998	0.289676

Table S11: Bonferroni Post-hoc comparison test for differences in swimming speed between groups based on prior exposure to fish in the control (no-fish) and kairomone exposed (fish) conditions

contrast	condition	estimate	SE	df	t.ratio	p.value
N - Y	no-fish	-0.10802	0.259936	22.09654	-0.41558	0.681729
N - Y	fish	-0.61393	0.259308	21.87559	-2.36758	**0.027173**

Table S12: Tukey Post-hoc comparison test for differences in distance travelled within population types between control (no-fish) and kairomone exposed (fish)

contrast	type	estimate	SE	df	t.ratio	p.value
(no-fish) - fish	A_F	-43.0733	47.6129	494.2829	-0.90466	0.366089
(no-fish) - fish	A_NF	23.51858	44.67028	484.9257	0.526493	0.598787

(no-fish) - fish	NA_F	-27.5958	41.39425	490.7642	-0.66666	0.505304
(no-fish) - fish	NA_NF	161.0872	59.08805	481.1254	2.726223	**0.00664**

Table S13: Bonferroni Post-hoc comparison test for differences in distance travelled between population types in the control (no-fish) and kairomone exposed (fish) conditions

contrast	condition	estimate	SE	df	t.ratio	p.value
A_F - A_NF	no-fish	-93.7487	80.51826	21.0626	-1.16432	0.531633
A_F - NA_F	no-fish	-121.155	76.78968	23.41702	-1.57774	0.531633
A_F - NA_NF	no-fish	-106.846	93.53304	21.60913	-1.14233	0.531633
A_NF - NA_F	no-fish	-27.4058	75.46762	21.97635	-0.36315	0.888852
A_NF - NA_NF	no-fish	-13.097	92.57137	20.79617	-0.14148	0.888852
NA_F - NA_NF	no-fish	14.30884	89.01568	22.14104	0.160745	0.888852
A_F - A_NF	fish	-27.1568	81.7595	22.32968	-0.33216	0.74287
A_F - NA_F	fish	-105.677	77.21999	23.94982	-1.36852	0.374886
A_F - NA_NF	fish	97.31481	93.75055	21.80508	1.038019	0.374886
A_NF - NA_F	fish	-78.5202	75.98463	22.51296	-1.03337	0.374886
A_NF - NA_NF	fish	124.4716	92.73104	20.91532	1.342287	0.374886
NA_F - NA_NF	fish	202.9919	88.71009	21.81765	2.288261	0.193092

Table S14: Tukey Post-hoc comparison test for differences in nearest neighbour distance (NND) within population types between control (no-fish) and kairomone exposed (fish)

contrast	type	estimate	SE	df	z.ratio	p.value
(no-fish) - fish	A_F	-0.06586	0.046701	Inf	-1.41024	0.158469
(no-fish) - fish	A_NF	0.077447	0.043787	Inf	1.768716	0.076941
(no-fish) - fish	NA_F	-0.00669	0.04067	Inf	-0.1646	0.869257
(no-fish) - fish	NA_NF	0.023588	0.057744	Inf	0.408489	0.682915

Table S15: Bonferroni Post-hoc comparison test for difference in nearest neighbour distance between population types in the control (no-fish) and kairomone exposed (fish) condition

contrast	condition	estimate	SE	df	z.ratio	p.value
A_F - A_NF	no-fish	-0.09881	0.061524	Inf	-1.606	0.374017
A_F - NA_F	no-fish	-0.01514	0.059309	Inf	-0.25529	0.944282
A_F - NA_NF	no-fish	-0.09386	0.0719	Inf	-1.30546	0.374017
A_NF - NA_F	no-fish	0.083666	0.057719	Inf	1.449527	0.374017
A_NF - NA_NF	no-fish	0.004944	0.070742	Inf	0.069888	0.944282
NA_F - NA_NF	no-fish	-0.07872	0.068338	Inf	-1.15194	0.374017
A_F - A_NF	fish	0.044501	0.063324	Inf	0.702748	0.739255
A_F - NA_F	fish	0.044025	0.060007	Inf	0.733666	0.739255
A_F - NA_NF	fish	-0.00441	0.072449	Inf	-0.06094	0.993529
A_NF - NA_F	fish	-0.00048	0.058676	Inf	-0.00811	0.993529
A_NF - NA_NF	fish	-0.04892	0.071326	Inf	-0.6858	0.739255
NA_F - NA_NF	fish	-0.04844	0.068385	Inf	-0.70833	0.739255

Table S16: Table of GO terms with linked function to the fish kairomones induced changes. Genes which overlapped are seen in the second column

GO term	genes	description
GO:0007602	OUZ56_003987 OUZ56_009856	phototransduction
GO:0016056	OUZ56_003987 OUZ56_009856	G protein-coupled opsin signalling pathway
GO:0050953	/	sensory perception of light stimulus
GO:0009583	OUZ56_003987 OUZ56_009856	detection of light stimulus
GO:0099536	OUZ56_001370 OUZ56_004510 OUZ56_008471 OUZ56_011008 OUZ56_019698 OUZ56_019861 OUZ56_025184 OUZ56_025188 OUZ56_027743	synaptic signalling
GO:0004970	/	ionotropic glutamate receptor activity
GO:0015276	OUZ56_001370 OUZ56_015553 OUZ56_015660 OUZ56_025225	ligand-gated ion channel activity
GO:0016917	/	GABA receptor activity
GO:0030594	/	neurotransmitter receptor activity
GO:0007626	OUZ56_006604 OUZ56_006846 OUZ56_008886 OUZ56_009240 OUZ56_022400	locomotory behaviour
GO:0004930	OUZ56_004876 OUZ56_016031 OUZ56_022400 OUZ56_031120 OUZ56_031365	G protein-coupled receptor activity
GO:0007210	/	serotonin receptor signalling pathway
GO:0007212	/	dopamine receptor signalling pathway
GO:0007213	/	G protein-coupled acetylcholine receptor
GO:0007207	/	phospholipase C-activating G protein-coupled acetylcholine receptor signalling pathway
GO:0004965	/	G protein-coupled GABA receptor activity
GO:0051932	/	Synaptic transmission, GABAergic
GO:0008066	/	Glutamate receptor activity
GO:0007215	/	Glutamate signalling and binding pathway
GO:0004952	/	dopamine receptor activity
GO:0060158	/	phospholipase C-activating dopamine receptor signalling pathway

*Table S17: GO annotation of the nodes of the suggestive GRN (**Fig.** 20) with hub genes in bold.*

gene	GO terms	description
OUZ56_023269	GO:0000978; GO:0000981, GO:0006357, GO:0046983, GO:0000978, GO:0000981, GO:0003677, GO:0003700, GO:0005634, GO:0005654, GO:0006355, GO:0009952, GO:0045944	RNA polymerase II cis-regulatory region sequence-specific DNA binding / DNA-binding transcription factor activity, RNA polymerase II-specific / regulation of transcription by RNA polymerase II / protein dimerization activity / RNA polymerase II cis-regulatory region sequence-specific DNA binding / DNA-binding transcription factor activity, RNA polymerase II-specific/ DNA binding / DNA-binding transcription factor activity / nucleus / nucleoplasm / regulation of DNA-templated transcription / anterior/posterior pattern specification / positive regulation of transcription by RNA polymerase II
OUZ56_013869	GO:0000978, GO:0000981, GO:0003677, GO:0003700, GO:0005515, GO:0005737, GO:0006355	RNA polymerase II cis-regulatory region sequence-specific DNA binding / DNA-binding transcription factor activity, RNA polymerase II-specific / DNA binding / DNA-binding transcription factor activity / protein binding / cytoplasm / regulation of DNA-templated transcription
OUZ56_031032	GO:0000977, GO:0001228, GO:0003700, GO:0005634, GO:0006355, GO:0006357	RNA polymerase II transcription regulatory region sequence-specific DNA binding / DNA-binding transcription activator activity, RNA polymerase II-specific / DNA-binding transcription factor activity / nucleus / regulation of DNA-templated transcription / regulation of transcription by RNA polymerase II
OUZ56_013584	GO:0000978, GO:0000981, GO:0003700, GO:0006351, GO:0006355, GO:0006357	RNA polymerase II cis-regulatory region sequence-specific DNA binding / DNA-binding transcription factor activity, RNA polymerase II-specific / DNA-binding transcription factor activity/ DNA-templated transcription / regulation of DNA-templated transcription / regulation of transcription by RNA polymerase II
OUZ56_014734	GO:0000122, GO:0000978, GO:0000981, GO:0003677, GO:0005634, GO:0006355, GO:0006357, GO:0009952	negative regulation of transcription by RNA polymerase II / RNA polymerase II cis-regulatory region sequence-specific DNA binding / DNA-binding transcription factor activity, RNA polymerase II-specific / DNA binding / nucleus /regulation of DNA-templated transcription / regulation of transcription by RNA polymerase II / anterior/posterior pattern specification
OUZ56_013861 (hub)	GO:0000978, GO:0003677, GO:0003700, GO:0003707, GO:0005634, GO:0006355, GO:0008270, GO:0043565	RNA polymerase II cis-regulatory region sequence-specific DNA binding / DNA binding / DNA-binding transcription factor activity / nuclear steroid receptor activity / nucleus / regulation of DNA-templated transcription / zinc ion binding / sequence-specific DNA binding
OUZ56_002241	GO:0000978, GO:0003677, GO:0003700, GO:0003707, GO:0005634, GO:0006355, GO:0008270, GO:0043565	RNA polymerase II cis-regulatory region sequence-specific DNA binding / DNA binding / DNA-binding transcription factor activity / nuclear steroid receptor activity / nucleus / regulation of DNA-templated transcription / zinc ion binding / sequence-specific DNA binding
OUZ56_001155 (GWAS hit)	GO:0002376, GO:0006325, GO:0006351, GO:0006355, GO:0022414, GO:0030154, GO:0036211, GO:0048856, GO:0048870, GO:0098542	Immune system process / chromatin organization / DNA-templated transcription / regulation of DNA-templated transcription / reproductive process / cell differentiation / protein modification process / anatomical structure development / cell motility / defence response to other organism

OUZ56_027338	GO:0000978, GO:0000981, GO:0003700, GO:0005634, GO:0006355, GO:0006357	RNA polymerase II cis-regulatory region sequence-specific DNA binding DNA-binding transcription factor activity, RNA polymerase II-specific DNA-binding transcription factor activity nucleus regulation of DNA-templated transcription regulation of transcription by RNA polymerase II
OUZ56_013888	GO:0000978, GO:0000981, GO:0003677, GO:0003700, GO:0005634, GO:0006355, GO:0006357	RNA polymerase II cis-regulatory region sequence-specific DNA binding / DNA-binding transcription factor activity, RNA polymerase II-specific / DNA binding / DNA-binding transcription factor activity / nucleus / regulation of DNA-templated transcription / regulation of transcription by RNA polymerase II
OUZ56_000682	GO:0000978, GO:0000981, GO:0003677, GO:0003700, GO:0005634, GO:0005737, GO:0006355, GO:0006954, GO:0007249, GO:0033554, GO:0034097, GO:0038061, GO:0045087, GO:0045944	RNA polymerase II cis-regulatory region sequence-specific DNA binding / DNA-binding transcription factor activity, RNA polymerase II-specific / DNA binding / DNA-binding transcription factor activity / nucleus / cytoplasm / regulation of DNA-templated transcription / inflammatory response / canonical NF-kappaB signal transduction / cellular response to stress / response to cytokine / non-canonical NF-kappaB signal transduction / innate immune response / positive regulation of transcription by RNA polymerase II
OUZ56_001233	GO:0000978, GO:0000981, GO:0006357	RNA polymerase II cis-regulatory region sequence-specific DNA binding / DNA-binding transcription factor activity, RNA polymerase II-specific / regulation of transcription by RNA polymerase II
OUZ56_004422 (hub)	GO:0000978, GO:0000981, GO:0003700, GO:0006355, GO:0006357, GO:0009653, GO:0030154, GO:0043565	RNA polymerase II cis-regulatory region sequence-specific DNA binding / DNA-binding transcription factor activity, RNA polymerase II-specific / DNA-binding transcription factor activity / regulation of DNA-templated transcription /regulation of transcription by RNA polymerase II / anatomical structure morphogenesis / cell differentiation / sequence-specific DNA binding
OUZ56_033275	GO:0000981, GO:0005515, GO:0005634, GO:0006357	DNA-binding transcription factor activity, RNA polymerase II-specific / protein binding / nucleus / regulation of transcription by RNA polymerase II
OUZ56_022596	GO:0000978, GO:0001228, GO:0003700, GO:0005634, GO:0006357	RNA polymerase II cis-regulatory region sequence-specific DNA binding / DNA-binding transcription activator activity, RNA polymerase II-specific / DNA-binding transcription factor activity / nucleus / regulation of transcription by RNA polymerase II
OUZ56_020196	GO:0000978, GO:0000981, GO:0003677, GO:0005634, GO:0006355, GO:0006357	RNA polymerase II cis-regulatory region sequence-specific DNA binding / DNA-binding transcription factor activity, RNA polymerase II-specific / DNA binding / nucleus /regulation of DNA-templated transcription / regulation of transcription by RNA polymerase II
OUZ56_028405	GO:0000785, GO:0000978, GO:0000981, GO:0006357, GO:0016055, GO:0060070, GO:1990907	chromatin / RNA polymerase II cis-regulatory region sequence-specific DNA binding / DNA-binding transcription factor activity, RNA polymerase II-specific / regulation of transcription by RNA polymerase II / Wnt signalling pathway / canonical Wnt signalling pathway /beta-catenin-TCF complex

Table S18: BLAST results of GWAS significant and suggestive SNPs in genes

gene	description	max score	total score	query cover	E-value	per. Ident	acc. length	accession
OUZ56_001141	uncharacterized protein LOC116915328 [Daphnia magna]	2825	2825	98%	0	98.79%	3985	XP_032776298.2
OUZ56_001155	ubiquitin carboxyl-terminal hydrolase 36 isoform X4 [Daphnia magna]	1691	1691	100%	0	99.88%	813	XP_03779263.2
OUZ56_001158	No significant similarity found							
OUZ56_004077	domesticated amidase effector 2-like [Daphnia carinata]	263	263	54%	2.0E-87	84.25%	146	XP_057376254.1
OUZ56_007467	No significant similarity found							
OUZ56_008941	zinc-finger protein rotund-like isoform X2 [Daphnia pulex]	154	154	70%	2.0E-42	95.83%	1054	XP_46436900.1
OUZ56_009051	39S ribosomal protein L3, mitochondrial isoform X1 [Daphnia magna]	772	772	100%	0	99.73%	374	XP_032779832.2
OUZ56_013429	uncharacterized protein LOC130696589 [Daphnia magna]	1397	1397	100%	0	96.03%	705	XP_057375660.1
OUZ56_013436	NFX1-type zinc finger-containing protein 1 isoform X1 [Daphnia magna]	4774	4774	100%	0	99.18%	2348	XP_045029939.1
OUZ56_019126	pro-resilin-like [Daphnia magna]	570	570	100%	0	98.73%	315	XP_045028693.1
OUZ56_019589	uncharacterized protein LOC116920540 [Daphnia magna]	941	941	100%	0	98.93%	467	XP_032782560.2
OUZ56_019640	Zwei Ig domain protein zig-8 [Daphnia magna]	654	654	100%	0	100%	315	XP_032783218.2
OUZ56_029315	compound eye opsin BCRH2 [Daphnia magna]	803	803	100%	0	100%	386	XP_032792246.1
OUZ56_029317	compound eye opsin BCRH2 [Daphnia magna]	801	801	100%	0	99.74%	385	XP_032792248.1
OUZ56_029343	protein transport protein Sec24C-like isoform [Daphnia magna]	2118	2118	100%	0	99.71%	1032	XP_045034489.1
OUZ56_031840	No significant similarity found							

Figures

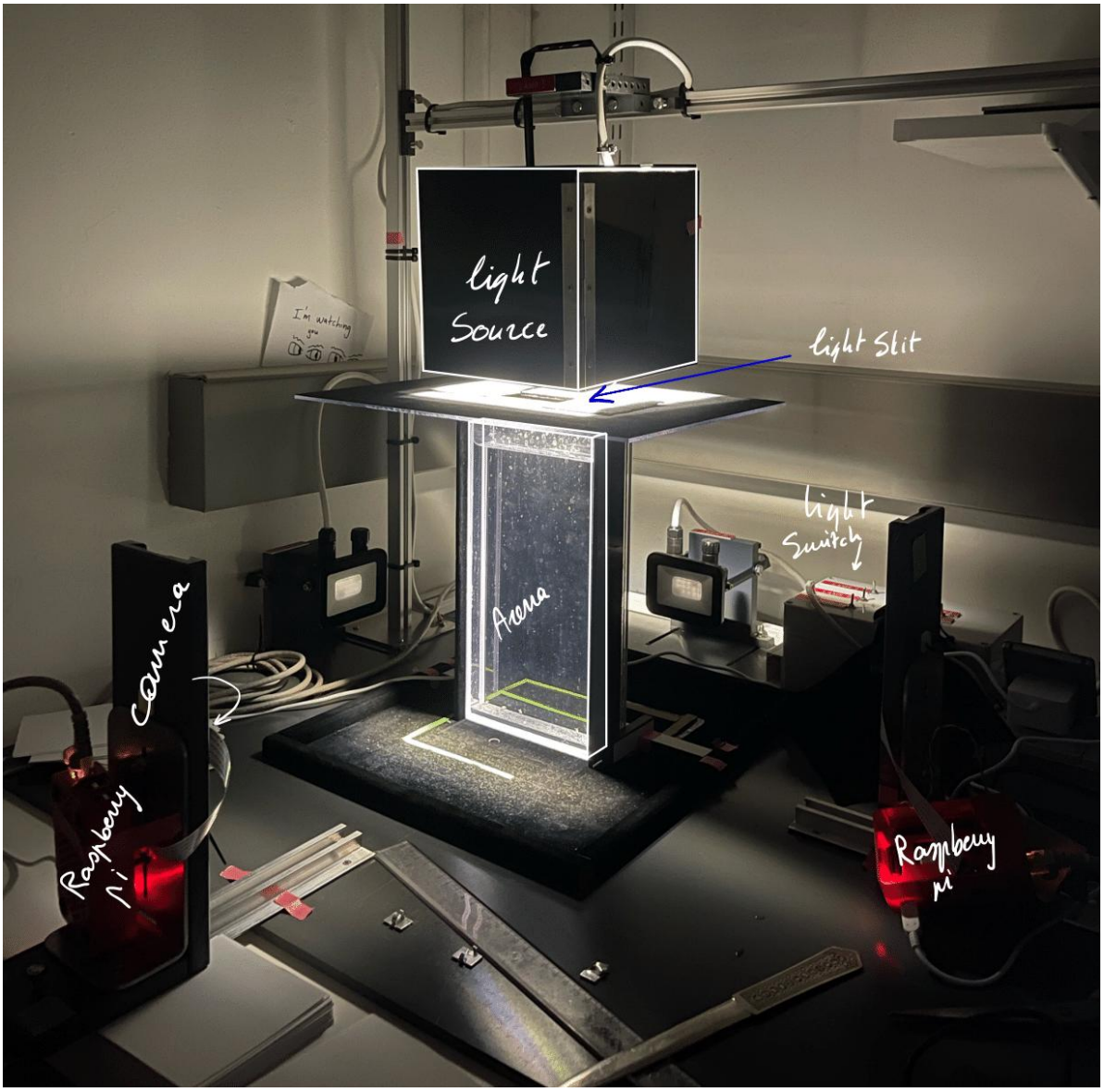


Figure S1: Picture of the phenotypic setup with annotations of the important parts; light source, cameras, Raspberry Pi.

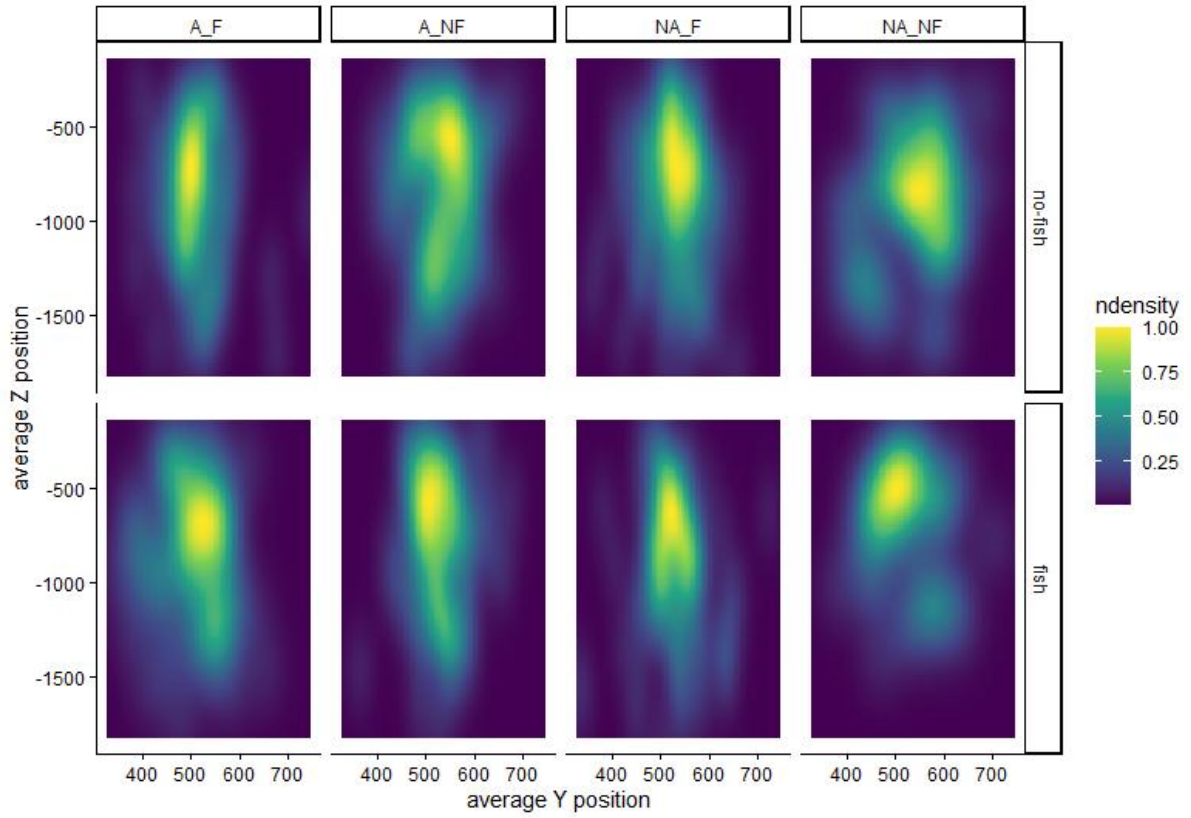


Figure S2: Two-dimensional kernel density distributions of Daphnia positions by population type and condition. Normalised 2D density (ndensity) of mean lateral (Y) and vertical (Z) positions across all tracked individuals, faceted by population type (columns) and condition (rows). Density is normalised per panel to a maximum of 1, allowing visual comparison of distribution patterns between panels.

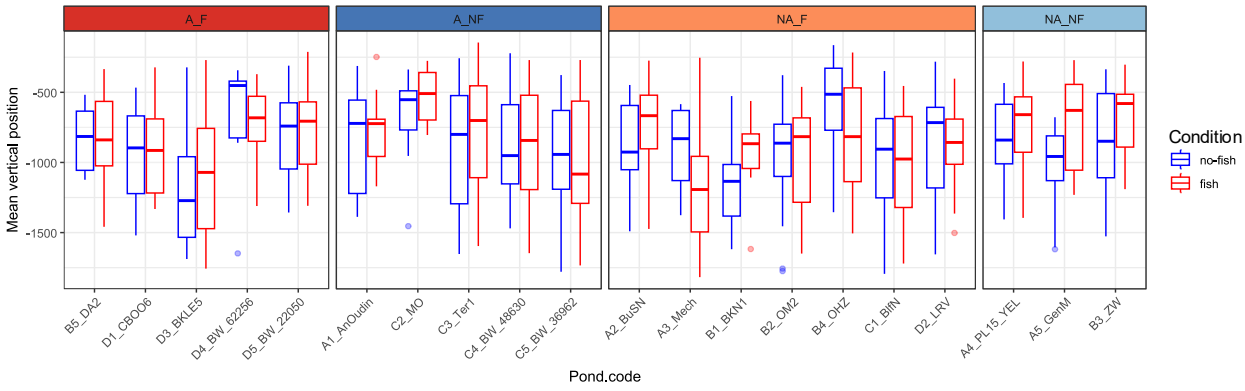


Figure S3: Per-pond distribution of mean vertical position under fish-exposed and control conditions. Boxplots show mean vertical position per pond, grouped by population type. Red: fish kairomone-exposed; blue: control (no-fish).

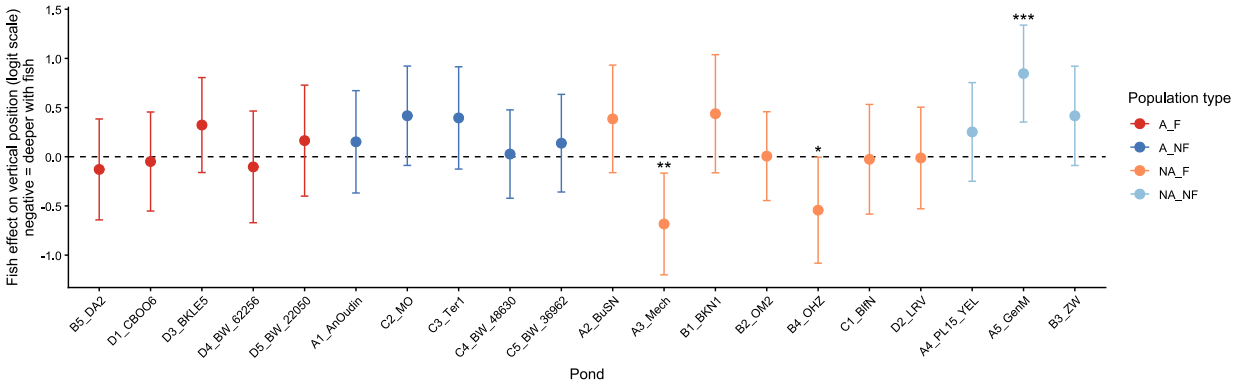


*Figure S4: Per-pond fish kairomone effect on vertical position. Fish kairomone effect sizes (fish - no-fish) on logit-transformed vertical position per pond, derived from post-hoc pairwise comparisons (Table S3). The dashed line indicates no difference from the no-fish baseline. Significance codes: *** p<0.001, ** p<0.01, * p<0.05.*

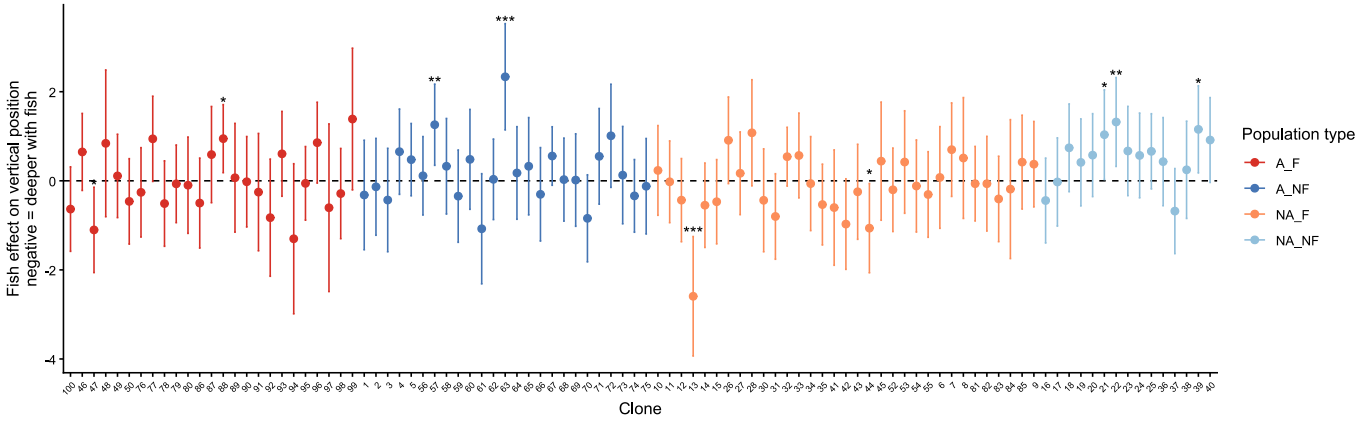


*Figure S5: Per clone fish kairomone effect on vertical position. Fish kairomone effect sizes (fish – no-fish) on logit transformed vertical position per clone, derived from post-hoc pairwise comparisons (Table S5) The dashed line indicates no difference from the no-fish baseline. Significance codes: *** p<0.001, **p<0.01, p<0.05*

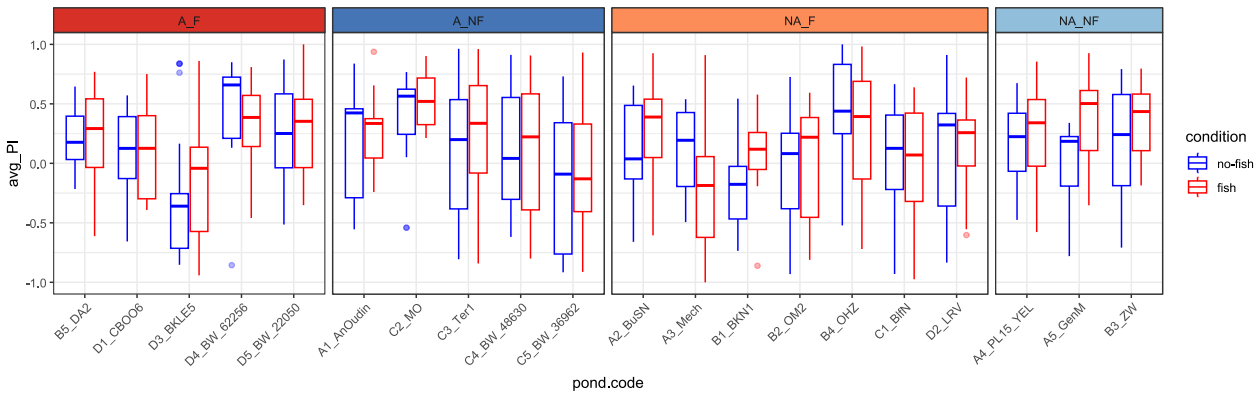


Figure S6: Per-pond distribution of phototactic index under fish-exposed and control conditions. Boxplots show mean phototactic index per pond, grouped by population type. Red: fish kairomone-exposed; blue: control (no-fish)

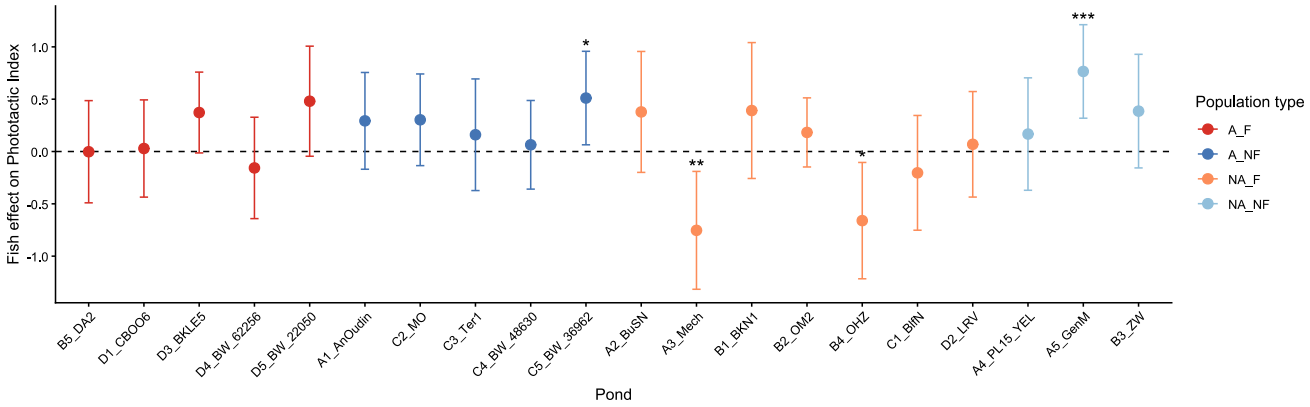


*Figure S7: Per-pond fish kairomone effect on phototactic index. Fish kairomone effect sizes (fish - no-fish) on phototactic index per pond, derived from post-hoc pairwise comparisons (Table S7). The dashed line indicates no difference from the no-fish baseline. Significance codes: *** p<0.001, ** p<0.01, * p<0.05.*

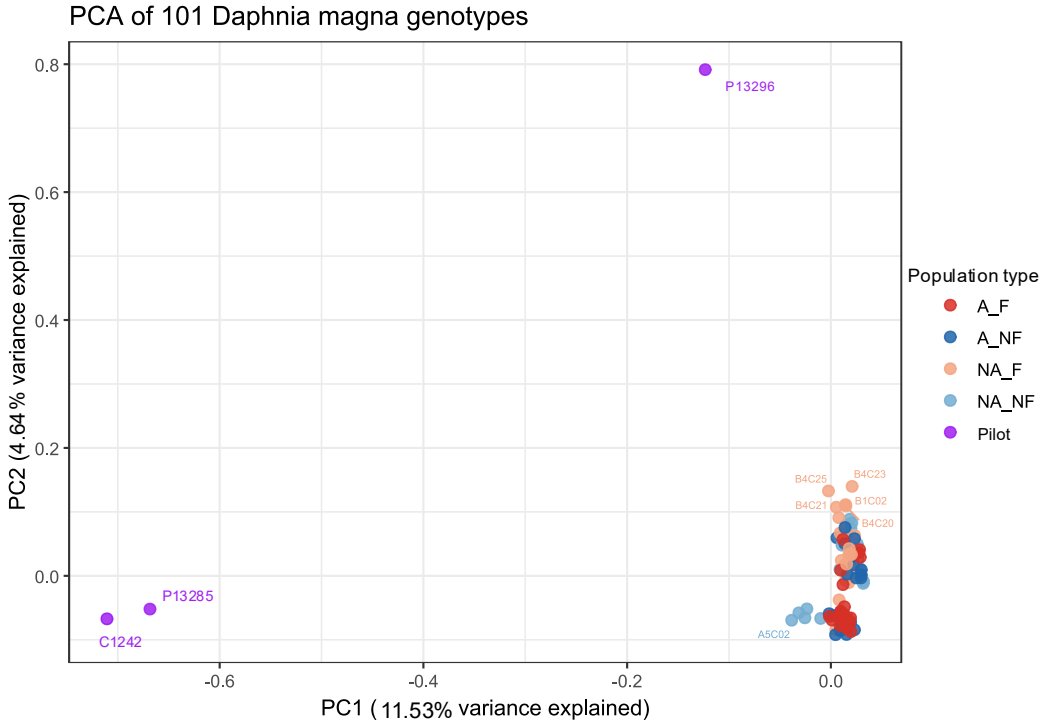


Figure S8: PCA of 101 Daphnia magna genotypes compute from genome-wide SNPs using PLINK v2.0. The three pilot clones (C1242, P_{132},85, P_{132},96; purple) separate from the main genotype cloud on both PC1 and PC2, indicating substantial genetic divergence and justifies exclusion prior to GWAS.

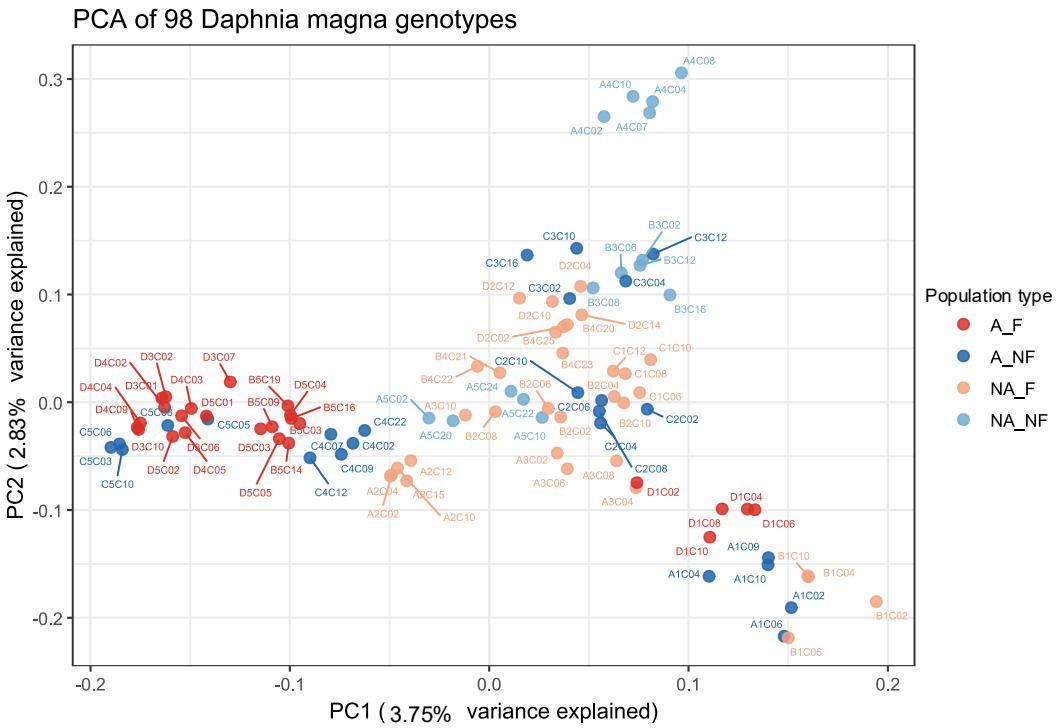


Figure S9: PCA of 98 Daphnia magna genotypes following exclusion of pilot clones (C1242, P_{132},85, P_{132},96), computed from genome-wide SNPs using PLINK v2.0. Colours indicate population type. Partial separation of population types along PC1 and PC2 reflects underlying population structure, which was accounted for in GWAS by inclusion of the top four genomic principal components as covariates.

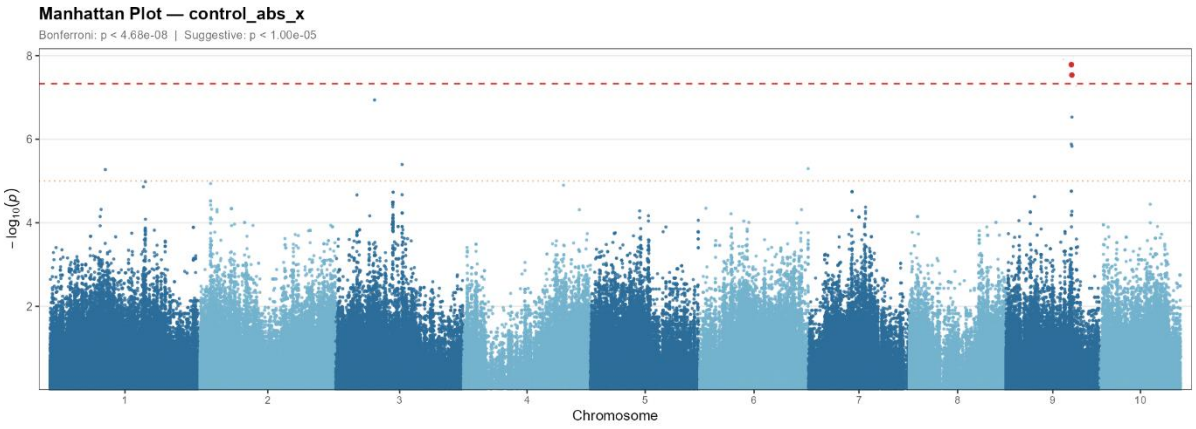


Figure S10: Manhattan plot based on the full 101 genotypes on the vertical position in control condition.

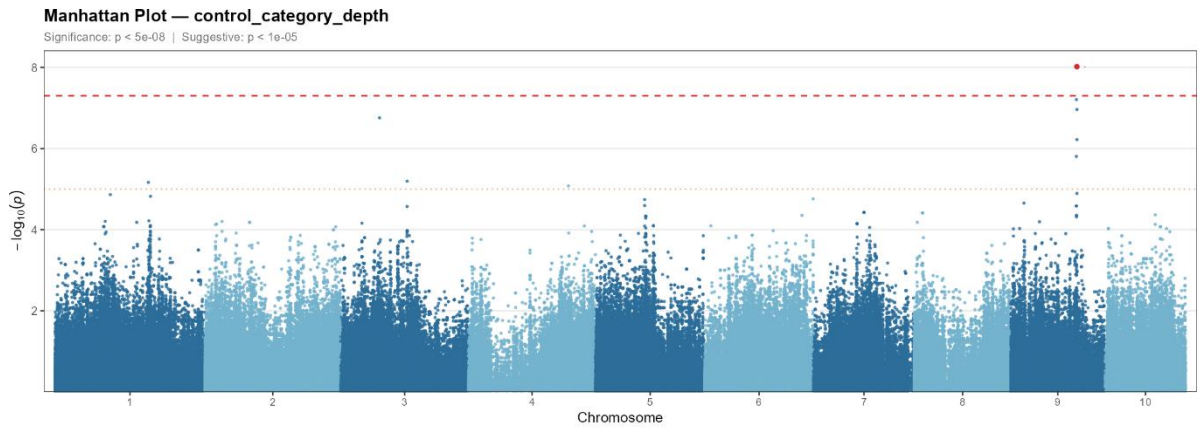


Figure S11: Manhattan plot based on categorical phenotype of the vertical position.

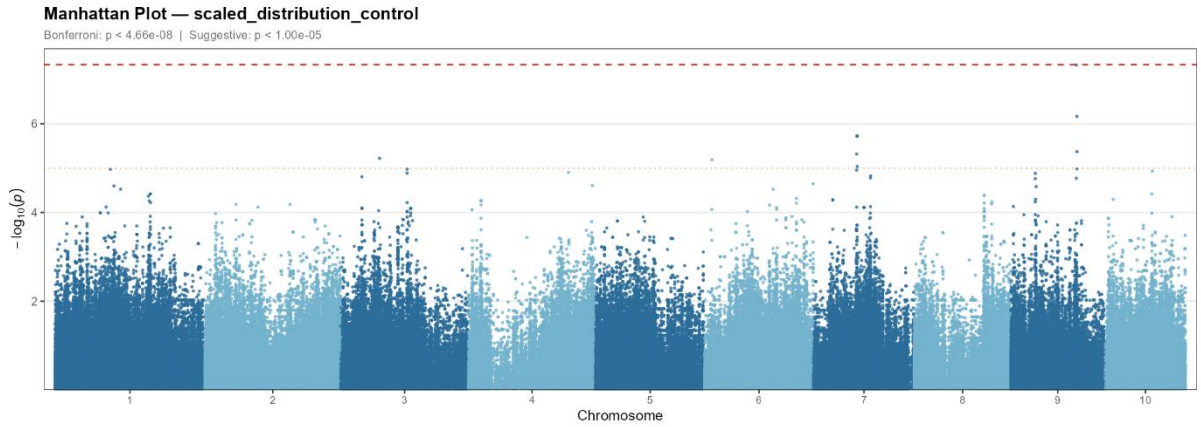


Figure S12: Manhattan plot based on the scaled distribution of vertical position in control condition

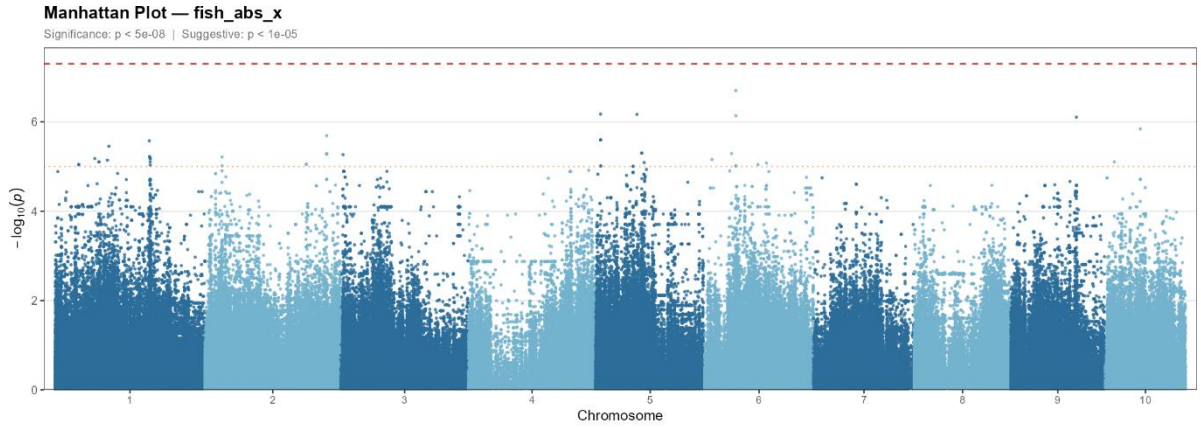


Figure S13: Manhattan plot, based on the vertical position phenotype in the fish exposed phenotype

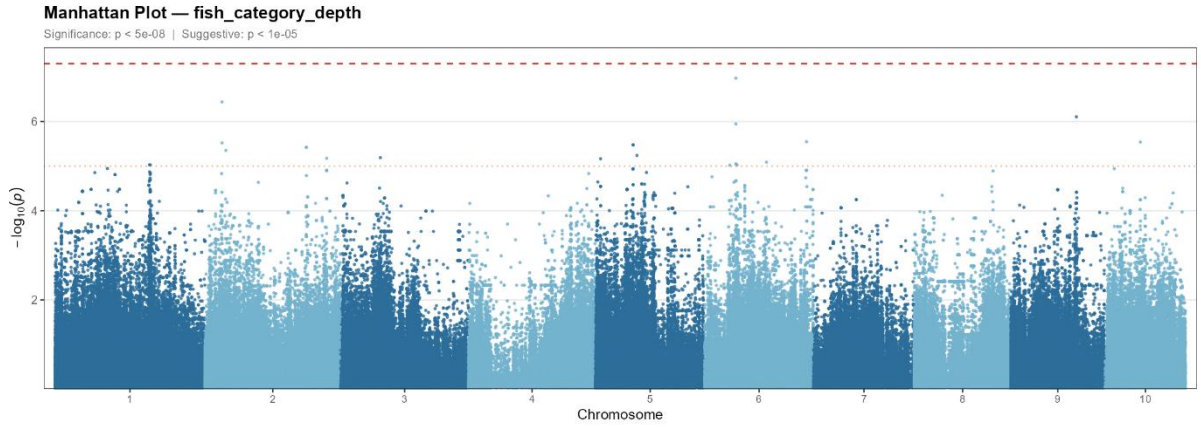


Figure S14: Manhattan plot, based on the categorical depth phenotype in fish exposed condition

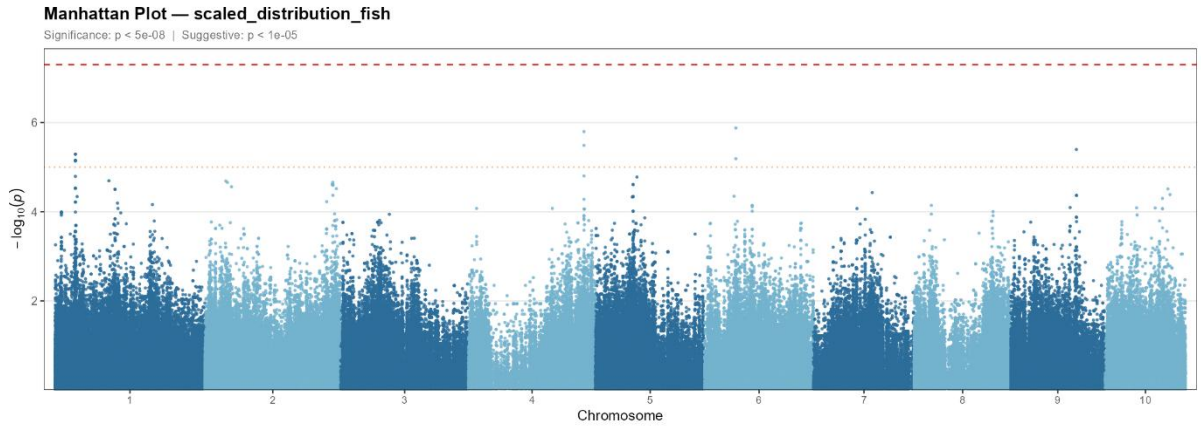


Figure S15: Manhattan plot, based on the scaled distribution phenotype in the fish exposed condition

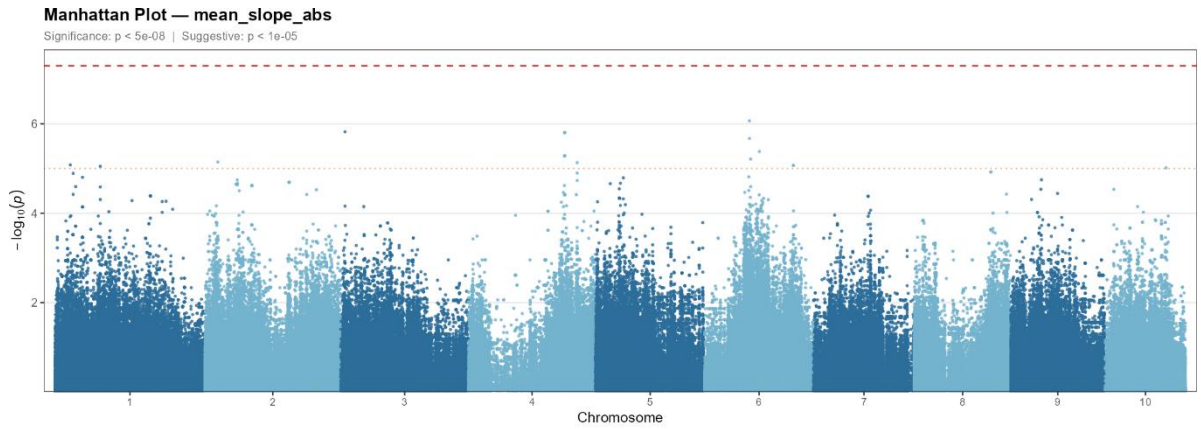


Figure S16: Manhattan plot, based on the mean slope of the reaction norm based on the difference between vertical position in both conditions

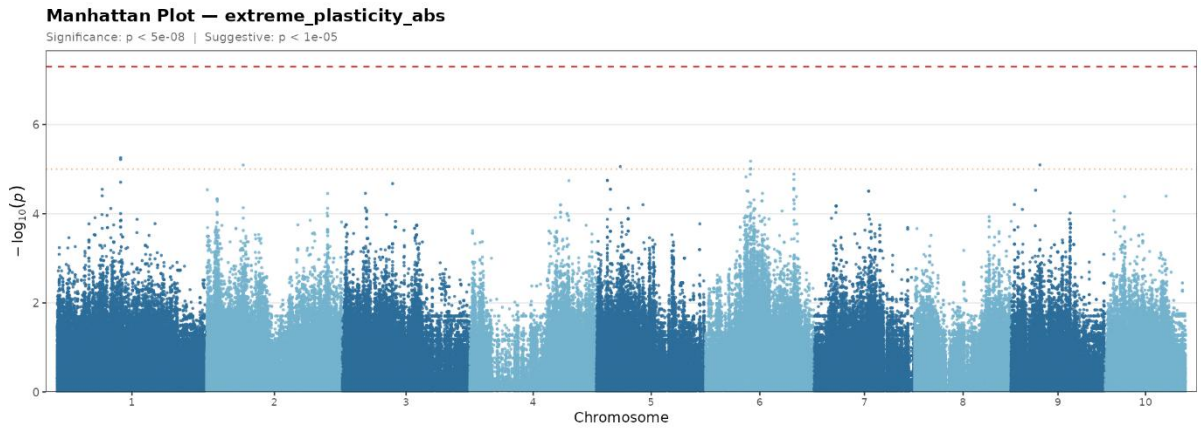


Figure S17: Manhattan plot based on the extreme plasticity phenotype between conditions

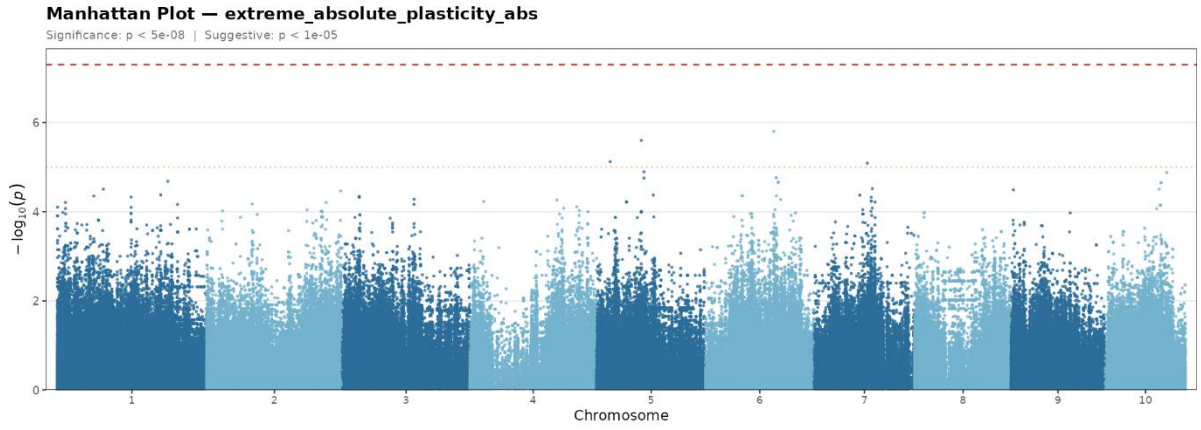


Figure S18: Manhattan plot of the absolute value of the extreme plasticity phenotype

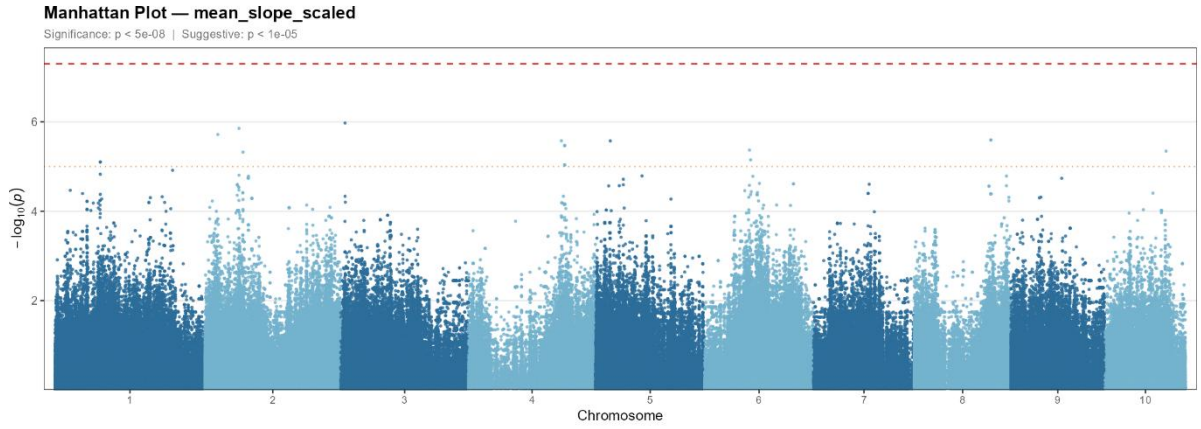


Figure S19: Manhattan plot of the scaled slope of plasticity phenotype

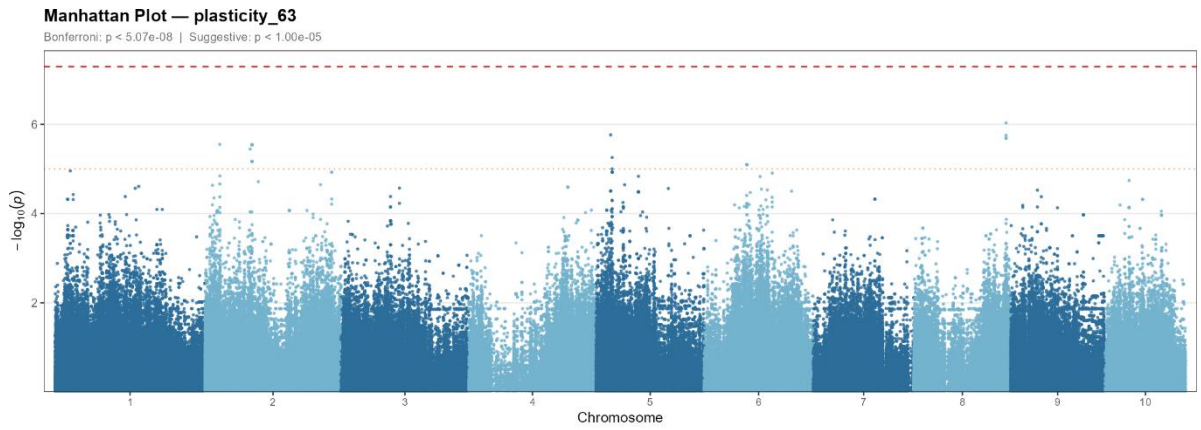


Figure S20: Manhattan plot of the top and bottom 30% responding phenotype

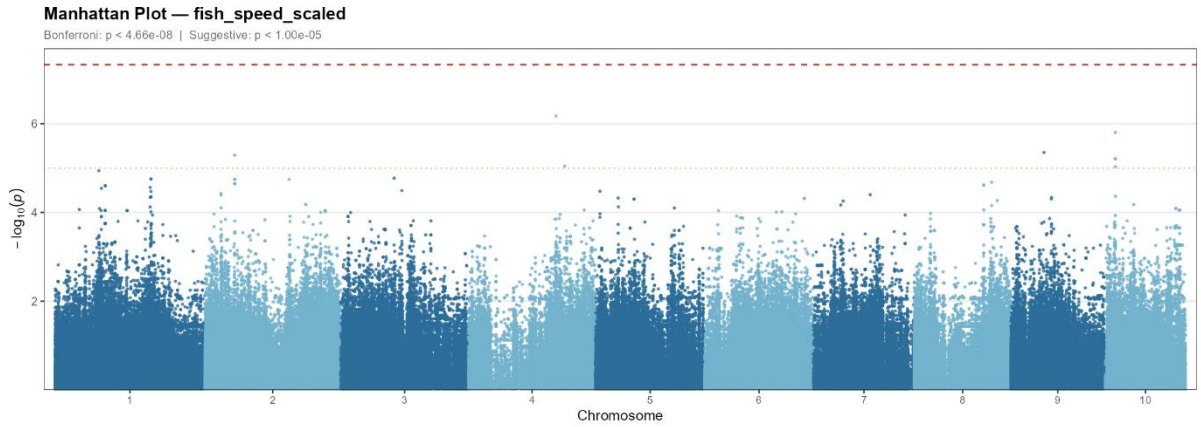


Figure S21: Manhattan plot based on the scaled fish speed

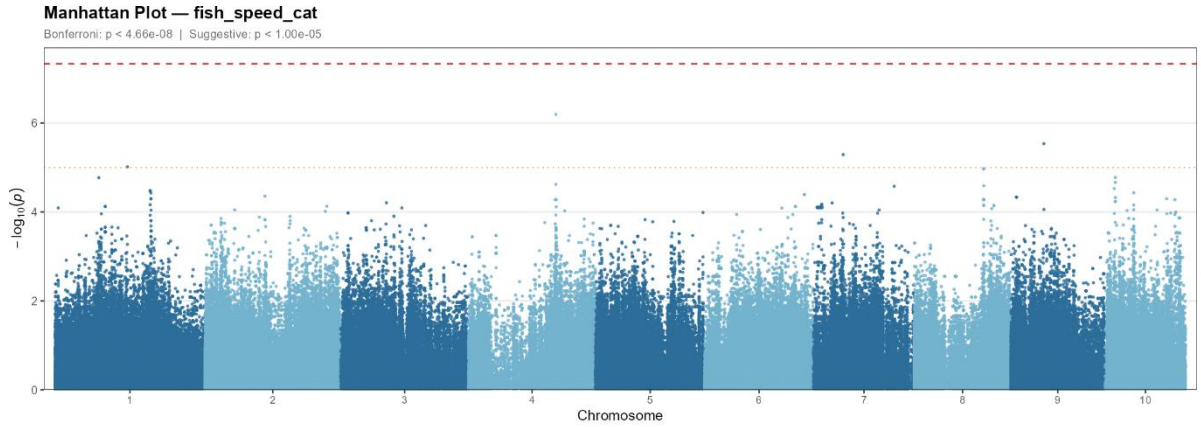


Figure S22: Manhattan plot based on the categorical speed phenotype in fish condition

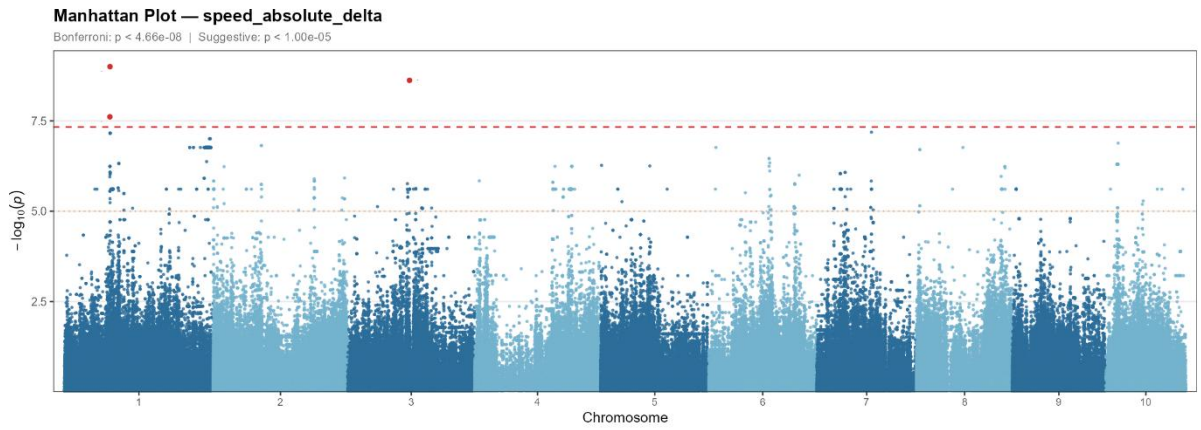


Figure S23: Manhattan plot based on the absolute difference in speed condition

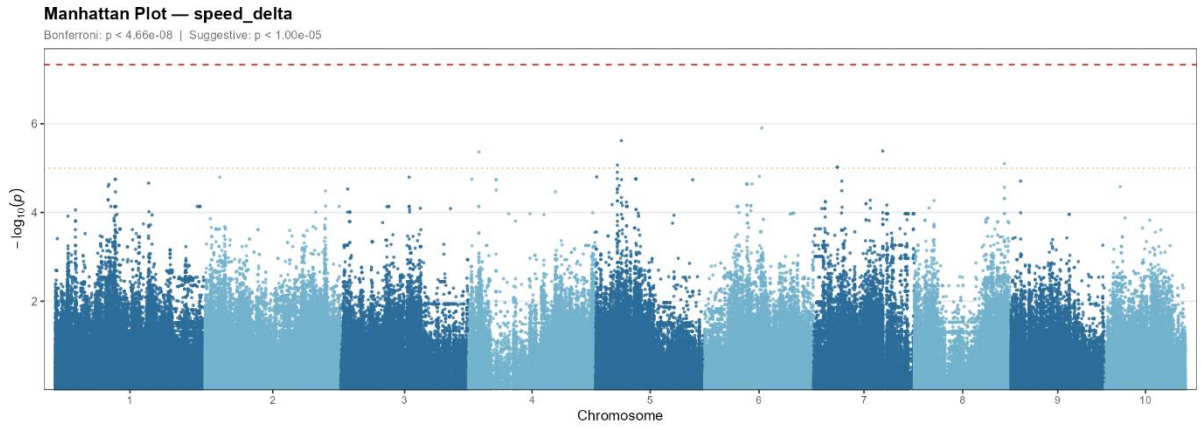


Figure S24: Manhattan plot based on the difference in speed between both conditions

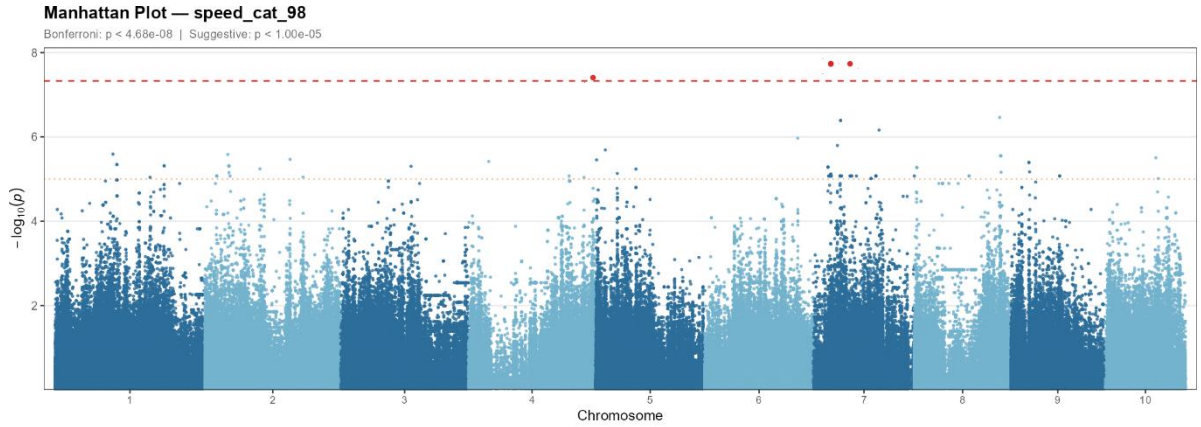


Figure S25: Manhattan plot based on the categorical speed phenotype in the control condition

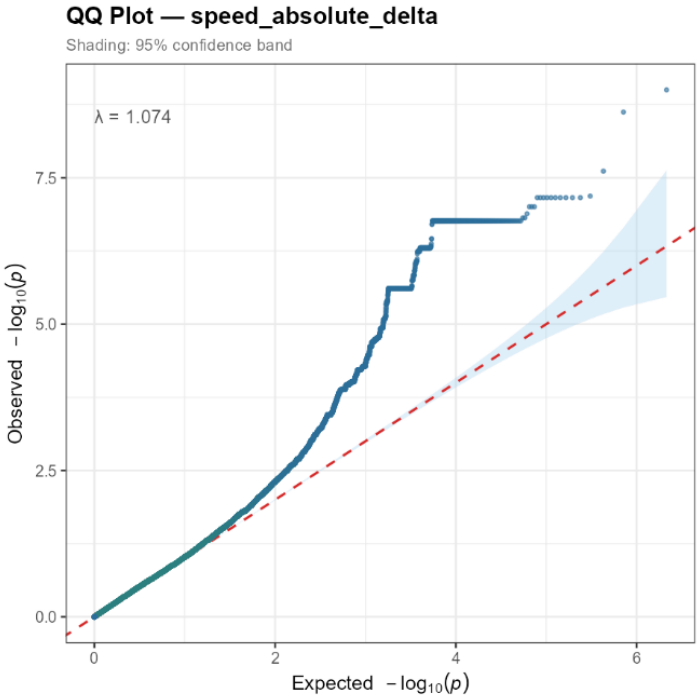


Figure S26: QQ plot of the absolute value of difference in speed between control and fish kairomone exposed conditions

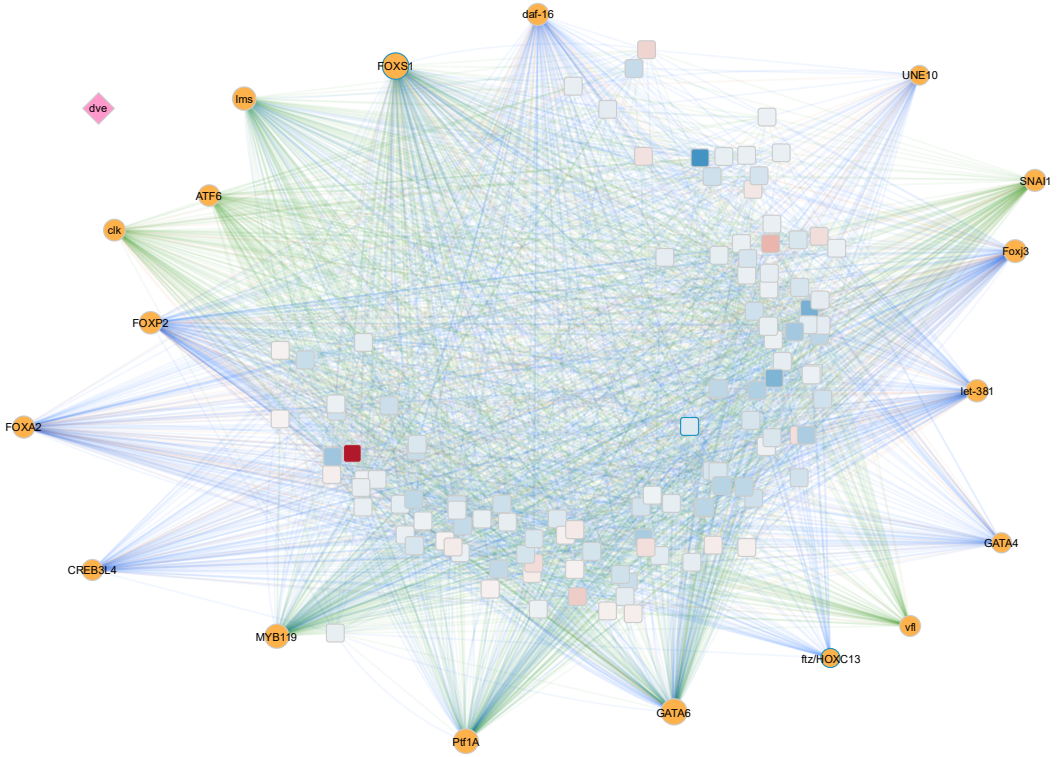


Figure S27: Unfiltered GRN, showing TFs in the outer circle and their downstream genes in the middle. Borders of the nodes are coloured based on their Log2FC, not all TFs in the outer circle are differentially expressed. The nodes in the middle are, and are coloured according to their Log2FC value. The edges connecting the nodes are coloured based on their proximity to the node (promoter:Blue; proximal:Orange, distal;Green). This was used as a base to filter towards the GRN featured in the main text.